Author response to referee comments

We thank the referee for the valuable comments which have greatly helped us improve the manuscript. Please find below our responses (in blue) after the referee comments (in black). The changes in the revised manuscript are written in italic.

Anonymous Referee #1

This article reports the first time the binPMF algorithm has been applied to VOCUS PTR-MS data, as applied to forested environments. There would be a strong interest in this type of broad-base work to try to generalize biogenic emissions, as these can have a profound effect on atmospheric chemistry. While I would say this certainly fits thematically within ACP's scope, right now the paper currently feels unfinished as a research article because while it demonstrates the instrument and algorithm 'working', it currently fails to identify what new understanding this confers to atmospheric science, beyond a running commentary of the authors' interpretations of the factors. I therefore recommend that this paper be published after major revisions. This could take the form of either a research article that is more focused on the atmospheric science arising from the work, or a technical note that explores the technicalities in more detail (I have queries regarding the methodology, see below). While it could in theory present a 'measurement report' based on this work, I feel that this may not be in the spirit of what the authors intended.

Response: We thank Anonymous Referee #1 for the careful review and inputs which helped improving the overall quality of our work. We agree that as a research article, new understanding towards atmospheric science from this work should be highlighted. Therefore, for the "4 Results and discussion" part, we revised the structure of the section to highlight our major scientific findings and add further analysis to gain insights into the atmospheric processes of monoterpenes and sesquiterpenes.

Compared to preexisting studies, this study performed binPMF analysis on Vocus PTR-TOF data and identified both primary emission sources and secondary oxidation processes of atmospheric organic vapors in two forested environments. For the first time, organic precursors, the lightly oxidized products, and the more oxidized products were separated as individual PMF factors. The relative abundances of these factors can be utilized by modelers to evaluate simulation output, improve model performance, and provide new perspectives to understand gas-phase physicochemical processes. Based on the interpretation of the results relating to oxidation processes, further insights were gained regarding monoterpene and sesquiterpene reactions. For example, a strong relative humidity (RH)-dependence was found for the behavior of sesquiterpene lightly oxidized compounds. High concentrations of these compounds only occur at high RH, yet similar behavior was not observed for monoterpene oxidation products. These findings highlight the need for further studies to delve into gas-phase atmospheric processes of monoterpenes and sesquiterpenes.

More details can be found below as response to the referee's first comment.

Comments:

The manuscript currently presents the results very systematically, but it is difficult to see what the reader is supposed to get from these. The authors provide a commentary on their interpretation of the factors, but I am not sure I learned anything new or significant about atmospheric chemistry on reading these. If this is to be presented as a research article, the paper needs to be refocused towards the new scientific insight or a testable hypothesis.

Response: We agree with the reviewer that as a research article, the new scientific insight or hypothesis should be highlighted to make it clear to the readers. Therefore, the structure of the section "4 Results and discussion" was revised as follows:

"4 Results and discussion

4.1 Choice of PMF solution and factor interpretation

4.2 Source identification in the Landes forest

4.3 Source identification in the southern Finnish boreal forest

4.4 Comparison among different factors

4.5 Comparison between the two forests

4.6 Insights into terpene oxidation processes

4.6.1 Monoterpene oxidations

4.6.2 Sesquiterpene oxidations"

In Section 4.4., the identified factors were compared with each other. Based on the similar temporal behavior of Factor L3 (C_6 and C_7 lightly oxidized products) and Factor L7 (C_{13} lightly oxidized products) and our current knowledge of the corresponding compounds, the C_{13} oxidized compounds are speculated to be produced through the dimer formation mechanisms of C_6 and C_7 species. The time series of monoterpene lightly oxidized products and sesquiterpene lightly oxidized products do not follow very well with each other, suggesting probably different atmospheric processes. This is further investigated in Section 4.6.

In Section 4.5, spatial comparison between the two forests were discussed regarding the relative abundances of different identified factors. For the common sources identified in both forests, they show similar mass profiles, indicating that the sources and processes are indeed similar despite the quite different regions the forests are in.

In Section 4.6, based on the separation of terpene oxidation processes with varying oxidation degrees, further insights were gained regarding monoterpene and sesquiterpene oxidations (Figure 14, Figure 15, Figure S16, and Figure S17). A strong relative humidity (RH)-dependence was found for the sesquiterpene lightly oxidized compounds, as well as the correlation between them and the products of [OH] × [sesquiterpenes] or [O_3] × [sesquiterpenes]. However, these RH dependences were not observed for monoterpene lightly oxidized compounds.

Overall, for the first time, the source identification of atmospheric organic vapors measured by Vocus PTR-TOF separated both primary emission sources and secondary oxidation processes with varying oxidation degrees. The relative abundances of organic precursors, the lightly oxidized products, and the more oxidized products can be utilized by modelers to evaluate simulation output, improve model performance, and provide new perspectives to understand gas-phase physicochemical processes. Based on further investigation of monoterpene and sesquiterpene reactions in the atmosphere, a strong RH-dependence was found for the behaviour of sesquiterpene lightly oxidized products but not for that of monoterpene lightly oxidized products.

The corresponding changes can be seen in the revised manuscript as follows:

4.4 Comparison among different factors

The monoterpene factor and sesquiterpene factor correlate very well with each other at both sites (Fig. 11; r^2 = 0.69 in the Landes forest and r^2 = 0.59 at the SMEAR II station). The emissions of monoterpenes and sesquiterpenes are both strongly influenced by temperature. Their signals peak at night with the effect of the shallow boundary layer. In the daytime, the low signals of the monoterpene and sesquiterpene factors are likely a combination of enhanced atmospheric mixing after sunrise and the rapid photochemical consumption of monoterpenes and sesquiterpenes. The signal of monoterpene factor is around 15 times higher than that of sesquiterpene factor at the SMEAR II station while it is around 60 times in the Landes forest. Previous studies found that sesquiterpene emissions from pines, spruces, and birches under normal conditions were 5-15% of total monoterpene emissions by mass (Rinne et al., 2009 and references therein), in line with our observations.

In the Landes forest, a factor of C_6 and C_7 lightly oxidized products (Factor L3) was resolved in the low mass range and a factor representative of C_{13} lightly oxidized products (Factor L7) was identified in the high mass range. Interestingly, these two factors show a close correlation with each other (r^2 = 0.64). The C_6 oxygenated compounds have been observed during the oxidation processes of benzene and C_7 oxygenated compounds from toluene oxidations (Sato et al., 2012; Zaytsev et al., 2019). These compounds can also be directly emitted from biogenic or anthropogenic sources (Conley et al., 2005; Pandya et al., 2006; Rantala et al., 2015). The temporal behaviour of Factor L7 is similar to that of Factor L3, indicating potentially similar formation pathways of these lightly oxygenated compounds. Therefore, the C_{13} oxidized compounds are speculated to be produced through the dimer formation mechanisms of C_6 and C_7 species (Valiev et al., 2019). In addition, $C_{13}H_{20}O_3$ can be direct emissions of methyl jasmonate (Meja), which is a typical green leaf volatile used in plant-plant communications for defensive purposes (Cheong and Choi, 2003). But considering the close correlation between Factor L3 and Factor L7, we conclude that these C13 lightly oxidized compounds are formed from atmospheric oxidation processes, not direct plant emissions.

Monoterpene lightly oxidized products and sesquiterpene lightly oxidized products were resolved as individual factors at both sites (Factor L7 vs. Factor L10 in the Landes forest and Factor S5 vs. Factor S6 at the SMEAR II station). While the diurnal variations of monoterpene lightly oxidized products are similar to those of sesquiterpene lightly oxidized products, their time series do not follow very well with each other, suggesting the probably different formation pathways or different factors influencing the atmospheric processes of monoterpenes and sesquiterpenes. More discussions can be found in Sect. 4.6.

In this study, the source apportionment analysis was performed separately on two subranges of the mass spectra. It can happen that the same factor is identified in both subranges. For example, both Factor L2 and Factor L9 are defined as the plume event during the measurements. The time series of Factor L2 and Factor L9 show a high correlation coefficient of 0.93 and correlate tightly with aromatic compounds, indicating the major influence of anthropogenic sources. As mentioned above, the air masses in the Landes forest were relatively stable during our observations with wind speed below canopy < 1 m s^{-1}. Therefore, the influence of long-range regional transport on the atmosphere in the forest is expected to be minor. We speculate that the plume event is a result of local anthropogenic disturbances favored by the lower boundary layer height at night.

4.5 Comparison between the two forests

To give an overview of the source distributions in the two forest ecosystems, we calculated the mass fraction of each factor based on their average signal intensities. We acknowledge that it is not a perfect method to quantify the contributions of various sources and formation processes. The sensitivities of different VOCs measured by the PTR instruments may vary by a factor of 2-3 (Sekimoto et al., 2017; Yuan et al., 2017). The uncertainties can come from the challenge to convert the signal intensity to atmospheric concentrations because of problematic calibrations, especially given that many unknown molecules exist in the mass spectra. The major bins at m/z 81 Th and 137 Th, which were initially excluded to perform PMF analysis, were counted into their corresponding

factors. For example, the signals of the discarded bins at m/z 81 Th and 137 Th were estimated by multiplying their isotope signals by the corresponding scale number and added to the factor representing monoterpenes. The average mass fractions of various PMF factors in total measured organic vapors are shown in Fig. 12.

While the atmospheric environment and ecosystem processes differ markedly in the Landes forest and the southern Finnish boreal forest, the results of this study reveal similar biogenic sources and oxidation processes in these forest environments. For instance, the biogenic VOCs at the two sites are both dominated by monoterpenes, with the average fractions of 29% in the Landes forest and at the SMEAR II station. These two forests are both characterized by pine trees, with dominant emissions of α-pinene and β-pinene (Riba et al., 1987; Simon et al., 1994; Hellén et al., 2018). According to the PMF results, isoprene and its major oxidation products in these environments (mainly C_4H_6O) contribute 14% and 21% in the two ecosystems, respectively. Factors indicative of sesquiterpenes are identified in the high mass range at both sites. The average contribution of sesquiterpenes (0.5% in the Landes forest and 1.7% at the SMEAR II station) is much smaller than that of monoterpenes and isoprene. Factors of the lightly oxidized products, more oxidized products, and organic nitrates of monoterpenes/sesquiterpenes in total contribute 8% and 12% of the measured organic vapors in the Landes forest and at the SMEAR II station, respectively.

The factor related to $C_4H_8H^+$ ion was resolved at both sites and contributes 10% in the Landes forest and 16% at the SMEAR II station. According to the discussions by Li et al. (2020), the observation of $C_4H_8H^+$ in the Landes forest can be attributed to several sources. For instance, the protonated butene may contribute to the $C_4H_8H^+$ signal, which is emitted by biogenic or anthropogenic sources (Hellén et al., 2006; Zhu et al., 2017). Another possible explanation is that the $C_4H_8H^+$ ion is produced during the fragmentation of many VOCs in the PTR instruments (Pagonis et al., 2019). The green leaf volatiles (GLV) have been found to fragment at m/z 57 Th inside the PTR instruments, which are a group of six-carbon aldehyde, alcohols and their esters released by plants. Furthermore, butanol can easily lose an OH during the PTR source ionization and produce prominent $C_4H_8H^+$ peaks (Spanel and Smith, 1997). Therefore, the condensation particle counters (CPCs) using butanol for aerosol measurements at the site could also be an important source of $C_4H_8H^+$ ions, although the exhaust air from these instruments has been filtered using charcoal denuder. At the SMEAR II station, the bivariate polar plot where the concentrations of air pollutants are shown as a function of WS and WD indicates that high signals of $C_4H_8H^+$ generally occur when the wind comes from the north (Fig. S15). Located in the north of the measurement container is a particle measurement cottage with several CPCs inside using butanol. A previous study at this station also found that $C_4H_8H^+$ signals detected by PTR-TOF mainly come from butanol used by aerosol instruments (Schallhart et al., 2018). Therefore, it is expected that Factor S1 at the SMEAR II station is mainly contributed by butanol fragmentation inside the instrument where butanol comes from nearby aerosol instruments.

Figure 13 presents the comparison of the mass spectra of the common sources identified at both sites, with the x and y axis showing the mass fraction of different bins in the factor profile. The scattering in the plots is mainly caused by mass bins with much lower mass fractions. However, the dominant bins with high mass contributions in the factor profiles generally correlate well and are located close to the 1:1 line. It shows that the mass spectra of the common sources match well in these two forests and the sources and processes are indeed similar despite the quite different regions the forests are in.

4.6 Insights into terpene oxidation processes

Terpenes undergo varying degrees of oxidations in the atmosphere and produce a large variety of organic compounds with different volatilities (Donahue et al., 2012; Ehn et al., 2014). With the sub-range PMF analysis performed in this study, terpene reaction products with varying oxidation degrees are successfully separated. The sources of monoterpene lightly oxidized products, sesquiterpene lightly oxidized products, monoterpene more oxidized compounds, and monoterpene-derived organic nitrates are identified in both forests with distinct characteristics. These factors account for 8-12% of the measured organic vapors in the two forests. It provides a

great opportunity to gain insights into terpene oxidation processes. Because some environmental parameters, for example, measurements of UVB to estimate OH concentration, are not available in the Landes forest, the results from SMEAR II station are presented as follows.

4.6.1 Monoterpene oxidations

The oxidation processes of monoterpenes at the SMEAR II station have been investigated by several previous studies, mostly based on the highly oxidized compounds. Utilizing non-negative matrix factorization analysis on iodide-adduct CIMS data at the SMEAR II station, Lee et al. (2018) found that the gas-phase organic species subgroup of $C_{6\text{-}10}H_yO_{\geq 7}$ showed distinct daytime diel trends. Yan et al. (2016) conducted source apportionment of HOMs at the SMEAR II station and separated various HOM formation pathways, such as monoterpene ozonolysis and monoterpene oxidation initiated by NO_3 radical. In this study, three types of monoterpene reaction products were detected: monoterpene lightly oxidized compounds, monoterpene more oxidized compounds, and monoterpene-derived organic nitrates. The latter two were not clearly separated into different factors at the SMEAR II station due to the similarities in their overall time trends. For example, the time series of $C_{10}H_{15}NO_5H^+$ correlate well with those of $C_{10}H_{16}O_4H^+$ and $C_{10}H_{16}O_5H^+$ ($r^2 > 0.61$).

Consistent with previous observations, monoterpene more oxidized products (i.e., $C_{10}H_{16}O_4$ and $C_{10}H_{14}O_5$) have a broad high distribution throughout the day due to the active photochemical processes during daytime. Monoterpene-derived organic nitrates (i.e., $C_{10}H_{17}NO_4$, $C_{10}H_{15}NO_5$, and $C_9H_{13}NO_6$) are mainly characterized by a distinct morning peak at around 8:00, approximately 2 h after the NO peak. But their intensities are also elevated at night. PMF analysis of NO_3^- CIMS dataset observed similar diurnal variations of terpene organic nitrates factor at a forest site in the southeastern US (Massoli et al., 2018). Compared with β-pinene and most other monoterpenes, the overall organic nitrate yield from α-pinene + NO_3 is rather low (Fry et al., 2014; Kurtén et al., 2017). Laboratory studies found that using iodide-adduct FIGAERO-HR-ToF CIMS, $C_{10}H_{15}NO_6$ is the most abundant organic nitrate in both gas- and particle-phase measurements of α-pinene + NO_3 reactions (Nah et al., 2016). Boyd et al. (2015) mainly detected $C_{10}H_{17}NO_4$, $C_{10}H_{15}NO_5$, $C_{10}H_{17}NO_5$, and $C_{10}H_{15}NO_6$ with iodide-adduct CIMS from the α-pinene + NO_3 system. Using $C_{10}H_{17}NO_5$ and $C_{10}H_{15}NO_6$ as the examples, we checked their correlations with the products of [OH] × [monoterpenes], [O_3] × [monoterpenes], and [NO_3] × [monoterpenes] in different periods of the day (Fig. 14; Fig. S16). Comparatively, $C_{10}H_{17}NO_5$ and $C_{10}H_{15}NO_6$ correlate better with the products of [OH] × [monoterpenes] and [O_3] × [monoterpenes] during daytime (9:00~18:00). However, for the product of [NO_3] × [monoterpenes], its correlation coefficients with $C_{10}H_{17}NO_5$ and $C_{10}H_{15}NO_6$ are a bit higher at night (20:00 to 4:00 of the next day). These results indicate that monoterpene-derived organic nitrates can be mainly formed by the NO_3-initiated oxidations at night, but in daytime by the OH and O_3-initiated oxidations followed by NO termination of the RO_2.

4.6.2 Sesquiterpene oxidations

The lightly oxygenated compounds from sesquiterpene reactions present a big morning peak and elevated signal intensities at night, similar to the diurnal variations of monoterpene lightly oxidized products. Hellén et al. (2018) showed that at the SMEAR II station, O_3 oxidation dominated the first step of sesquiterpene reactions for the whole year. It has also been observed in central Amazonia that sesquiterpenes contributed the highest to total O_3 reactivity although sesquiterpene concentrations were much lower than those of monoterpenes and isoprene (Yee et al., 2018). At the SMEAR II station, emissions of sesquiterpenes are dominated by β-caryophyllene (Hellén et al., 2018). Photooxidation of β-caryophyllene in the chamber experiments resulted in high aerosol yield and is expected to strongly influence SOA formation (Jaoui et al., 2013). Using the mass spectrometric techniques, Jokinen et al. (2016) observed the production of highly oxidized organic compounds from β-caryophyllene ozonolysis, i.e., monomers $C_{15}H_{24}O_{7,9,11}$ and $C_{15}H_{22}O_{9,11}$, and dimers $C_{29}H_{46}O_{12,14,16}$ and $C_{30}H_{46}O_{12,14,16}$. However,

due to the instrumental limitation, only the lightly oxidized products from sesquiterpene reactions were identified in this study.

Interestingly, a strong RH-dependence was observed for the correlations between sesquiterpene lightly oxidized compounds and the product of [OH] × [sesquiterpenes] or [O_3] × [sesquiterpenes]. These products represent the oxidation rates of sesquiterpenes with OH radical and O_3. As shown in Fig. 15, the corresponding correlation coefficients vary significantly with RH. In addition, the signal intensities of sesquiterpene lightly oxidized products also show high dependence on RH. At lower RH (RH<40%), the signal intensities of sesquiterpene lightly oxidized products are relatively low and correlate closely with the product of [OH] × [sesquiterpenes] and [O_3] × [sesquiterpenes]. The high signal intensities of sesquiterpene lightly oxidized products occur when RH>70% but the correlation between sesquiterpene lightly oxidized compounds and the product of [OH] × [sesquiterpenes] or [O_3] × [sesquiterpenes] is more scattered. Such high RH-dependence was not observed for monoterpene lightly oxidized compounds (Fig. S17). These findings have not been observed by previous studies and the reasons behind remain unclear. High-RH conditions typically occur during nights with temperature inversion (Zha et al., 2018), while RH below 40% generally only occurs at the station during sunny days. Future studies are needed to dig deep into the atmospheric processes of sesquiterpenes and monoterpenes.

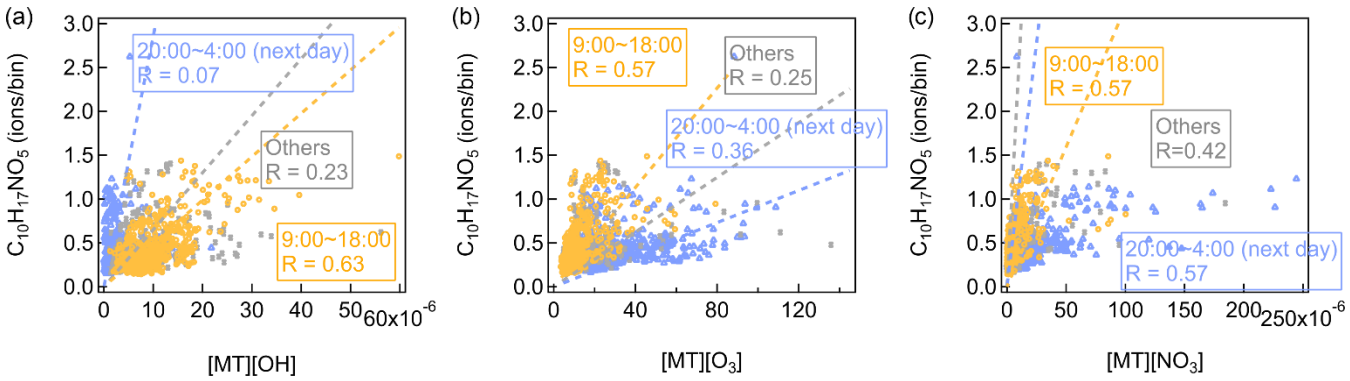

Figure 14. Scatter plots of $C_{10}H_{17}NO_5$ versus the product of (a) [OH] × [monoterpenes], (b) [O_3] × [monoterpenes], and (c) [NO_3] × [monoterpenes]. Different colours represent different periods of the day.

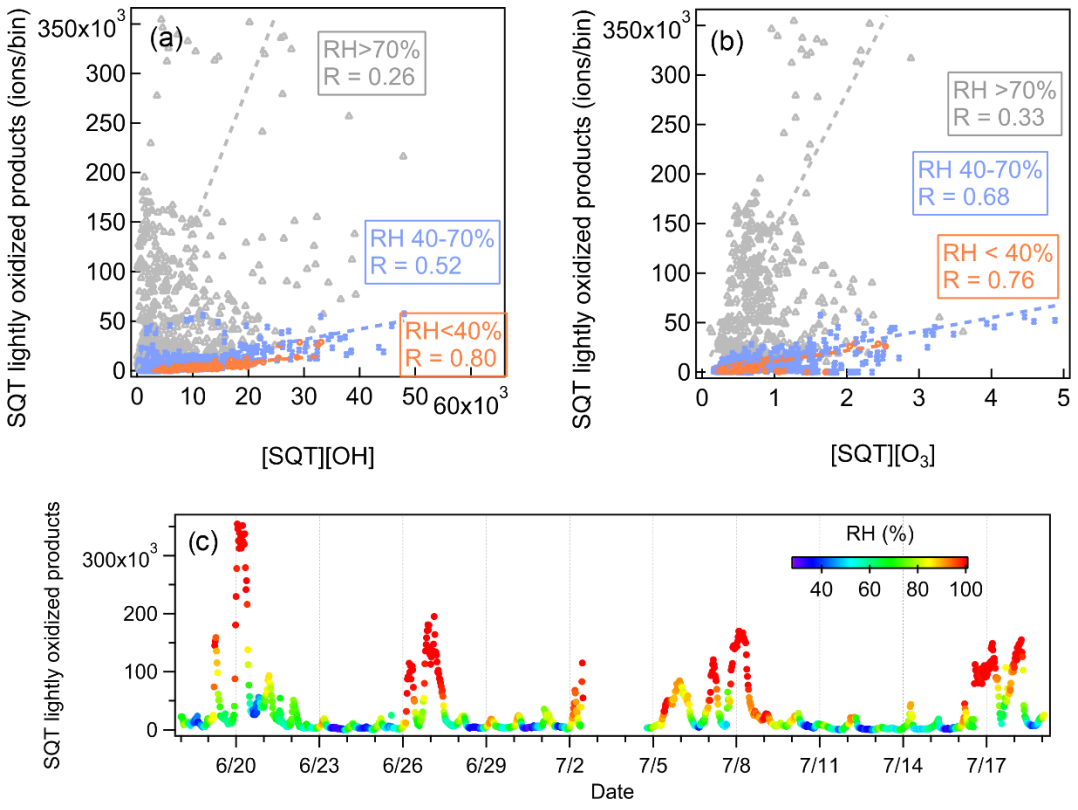

Figure 15. Scatter plots of sesquiterpene lightly oxidized products versus the product of (a) [OH] × [sesquiterpenes], and (b) [O_3] × [sesquiterpenes]. Different colours indicate different ranges of RH. (c) Time series of sesquiterpene lightly oxidized products colored by RH.

A certain amount of work in this paper goes into arriving at factorisations that aren't simply dominated by the big signals. This is probably to be expected because the gas phase VOC ensemble is likely to have many more degrees of freedom than can be accurately represented by the PMF and furthermore, many peaks will have isomers that won't be resolved using PTR. This is done by removing the main monoterpene signal and separating the mass spectrum into different regions. However, this comes across as a little subjective and prevents a direct association between the peaks in the two regions. Did the authors attempt a more conventional approach, such as applying a 'model error' parameter to downweight the larger peaks? More attention should be paid to demonstrating what the effects of not following these procedures in either case, perhaps shown in the supplement.

Response: As the reviewer points out, there are multiple ways in which data can be scaled before factorization, each one giving more or less weight to certain signals in the mass spectra. Earlier studies from our group have explored in detail e.g. scaling according to intensity or mass-to-charge ratio (Fig. 3 and Fig. S7 in Äijälä et al., 2017). The ultimate added value of such labor-intensive approaches is largest when the factorization results are ambiguous or hard to verify. In the current work, we tried a simple approach (removing the main peaks of the largest signals), which will be easy also for others to replicate. This produced factors that made sense both chemically and through their temporal behavior, which lends confidence in the results. The sub-range analysis, which we earlier have shown to be very powerful in separating out less abundant factors (Zhang et al., 2020), also provides a type of "internal verification" when factors with similar temporal and chemical features are resolved

from the two different mass ranges. In the end, there is no single "correct" way to factorize atmospheric data, and the validity of the approach should be referenced to the results, and the conclusion that can be drawn from them.

More specifically concerning this study, the measured signals at *m/z* 81Th and *m/z* 137 Th were much higher than the others. In the Vocus PTR-TOF, *m/z* 81Th mainly comes from the fragmentation of *m/z* 137 Th (monoterpenes) and therefore follows the characteristics of *m/z* 137. With the inclusion of these super high peaks (Figure 1a), the mass profiles of three factors were quite similar and dominated by monoterpenes at *m/z* 137 Th and the major fragment at *m/z* 81 Th. After exclusion of these high peaks, the mass profiles were more distinct and representative of different factors and at the same time, their temporal behaviors were not interfered (Figure 1b). While the parent ions at *m/z* 137 Th and *m/z* 81 were excluded, their corresponding isotopes were retained, effectively downweighting their contributions to the PMF results. The time series of the resolved factors with and without the inclusion of these super high peaks are almost identical. As suggested by the reviewer, the time series and mass profiles of the resolved factors with the inclusion of monoterpene peaks are added in the supplement as Figure S1.

After the exclusion of monoterpene high peaks, if the entire mass spectrum was used for PMF analysis without subranges, factors identified in the high mass range in this study cannot be resolved. As shown in Figure 2, with the entire mass spectrum as PMF input, most identified factors in the low mass range were resolved although there were some mixing of different factors. For example, the factors of C_6 and C_7 lightly oxidized products, a plume event, monoterpenes, unknown source, monoterpene lightly oxidized products, and isoprene and its oxidation products, were clearly seen. However, the PMF analysis cannot separate the factors of sesquiterpenes, sesquiterpene lightly oxidized products, monoterpene more oxidized products, monoterpene-derived organic nitrates, and C_{13} lightly oxidized products. Increasing the number of factors for PMF run did not help.

In this study, with the factorization on subranges of the mass spectra, different factors representing primary emission sources and secondary oxidation processes were identified in both mass ranges. The association between these two ranges were further explored by comparison of their time series, diurnal variations, and correlation analysis (Figure 11 in the manuscript). For example, the factors of a plume event were resolved in both mass ranges and their time series correlated closely with each other. The monoterpene factor in the low mass range showed a good correlation with the sesquiterpene factor in the high mass range. Interestingly, the factor of C_6 and C_7 lightly oxidized products in the low mass range correlated very well with the factor of C_{13} lightly oxidized products in the high mass range, which lead to the speculation that the C_{13} oxygenated compounds are produced through the dimer formation mechanisms of C_6 and C_7 species. In addition, the factor of monoterpene lightly oxidized products showed a poor correlation with the factor of sesquiterpene lightly oxidized products. Without the PMF analysis on subranges of mass spectra, these factors and different processes cannot be separated. Zhang et al. (2020) performed factor analysis on subranges of mass spectra measured by NO_3^- CIMS, and found that the formation of daytime dimer and the monoterpene dimers from the combined products of NO_3 and O_3 oxidations cannot be resolved without the subrange approach.

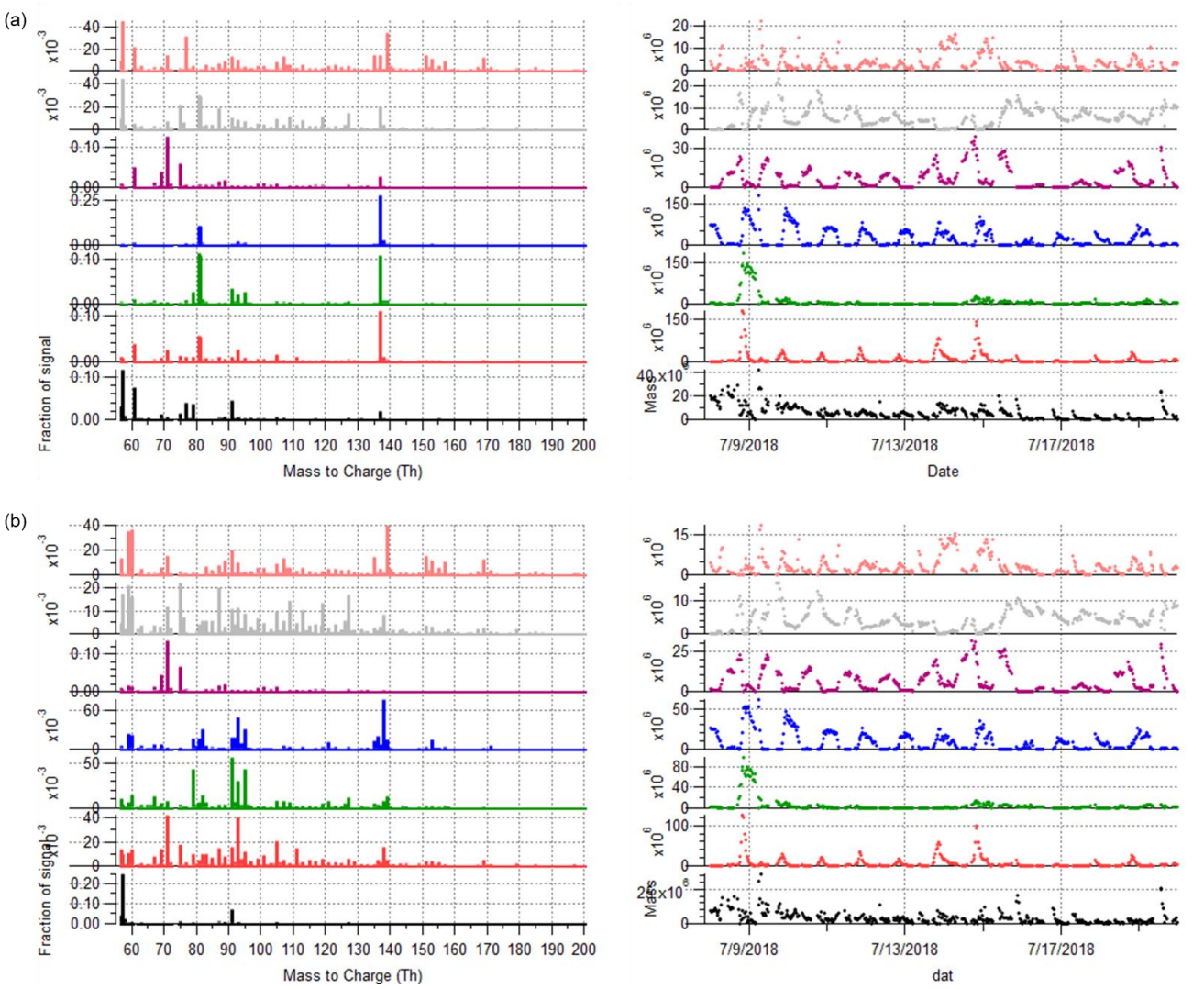

Figure 1. The mass profiles and time series of the seven-factor solution for the low mass range in the Landes forest (a) with and (b) without the inclusion of the signals at *m/z* 81 Th and *m/z* 137 Th.

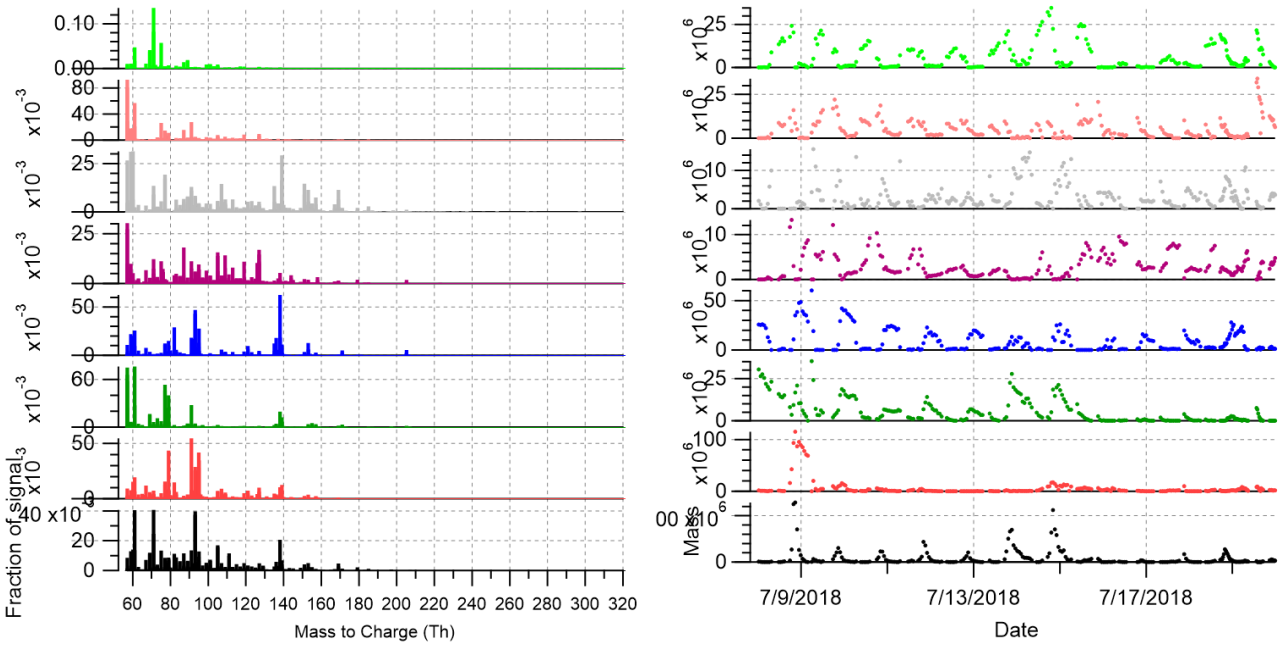

Figure 2. The mass profiles and time series of the eight-factor solution in the Landes forest with the entire mass spectrum as input of PMF analysis. We varied the FPEAK value between -1 and +1 with the step of 0.2. Taking the high mass range of 201-320 Th at the SMEAR IIstation as the example,

One might expect that given the number of degrees of freedom available, there will be a level of rotational ambiguity in the solution sets. This certainly would appear to be the case in figure 11, where all of the factors appear to contain traces of siloxane. Was the amount of rotational freedom available explored?

Response: The rotational freedom of the PMF solutions in this study was explored through use of the FPEAK parameters. For the optimal solutions, we varied the FPEAK value between -1 and +1 with the step of 0.2. For the low mass range of 51-200 Th of the Landes and SMEAR II dataset, the variations in FPEAK value did not influence the mass profile and time series much. For the high mass range of 201-320 Th, we saw the changes especially in the factor profiles by varying FPEAK values. For the Landes measurements, Figure 3 shows the factor profiles of the eight-factor solution with FPEAK = 0, +0.6, and -0.6. The time series of different factors for these FPEAK values are similar. After a detailed evaluation, we found no evidence that solutions with FPEAK value away from zero are preferable. However, for the high mass range of the SMEAR II measurements, as expected by the reviewer, the solutions with positive values of FPEAK work better than that with FPEAK = 0 in terms of the factor profiles. As shown in Fig. 4, by varying FPEAK with positive values, the factor profile of monoterpene more oxidized products (including organic nitrates) contained less traces of siloxanes and showed elevated fractions of the fingerprint peaks. After evaluation, we decided to choose the solution with FPEAK = +0.6 for the high mass range of the SMEAR II dataset.

The corresponding information of rotational ambiguity has been added in the revised manuscript (Lines 230-239): "*The rotational freedom of the PMF solutions was explored through the use of the FPEAK parameters. For each of the optimal solutions, we varied the FPEAK values between -1 and +1 with the step of 0.2. For the low mass ranges of the Landes and SMEAR II dataset, the varying FPEAK values did not change the factor profiles and time series much. For the high mass range of the Landes measurements, we saw variations especially in the factor profiles by varying FPEAK values. But after a detailed evaluation, we found no evidence that solutions with*

FPEAK values away from zero were preferable. However, for the high mass range of the SMEAR II measurements, the solutions with positive values of FPEAK worked better than that with FPEAK = 0 in terms of factor profiles. The factor time series were similar when FPEAK values varied. But for the factor profiles with positive FPEAK values, the factor of monoterpene more oxidized products including organic nitrates contained less traces of siloxanes and showed elevated fractions of the corresponding fingerprint peaks (Fig. S12). After evaluation, we chose the solution with FPEAK = +0.6 for the high mass range of the SMEAR II dataset."

Figure 9, Figure 10, Figure 12, and Figure 13 have been updated accordingly.

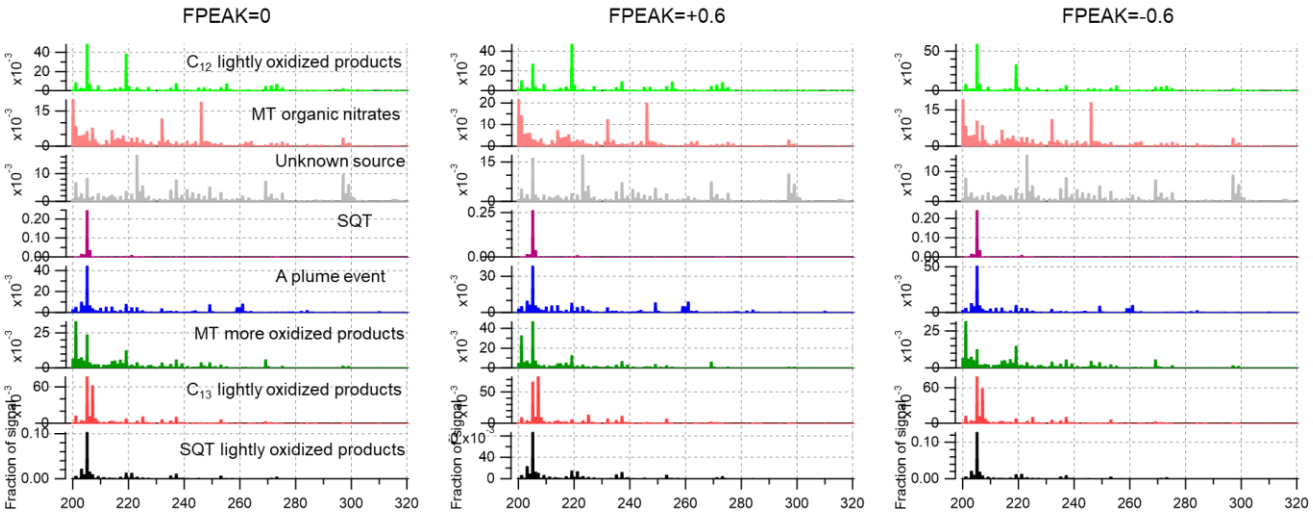

Figure 3. The factor profiles of the eight-factor solution for the high mass range of the Landes measurements with FPEAK = 0, +0.6, and -0.6.

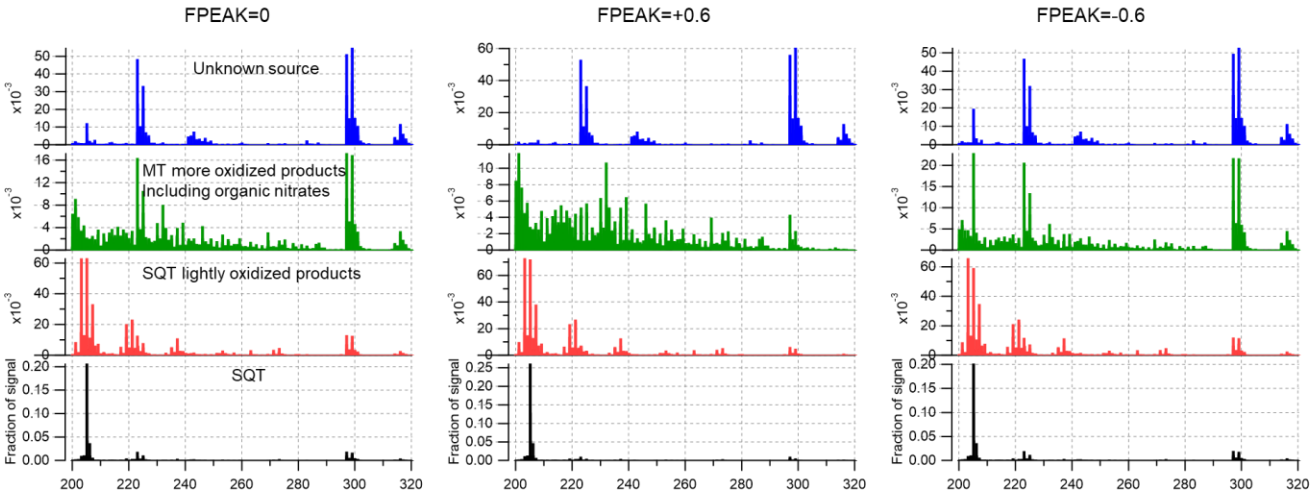

Figure 4. The factor profiles of the four-factor solution for the high mass range of the SMEAR II measurements with FPEAK = 0, +0.6, and -0.6.

The observation that reaction products did not contribute as much to the mass budget is perhaps expected because of their chemical lifetime. However, can the authors be sure the these (presumably more polar) molecules were

being detected with equal efficiency? Have the authors tried comparing with a mechanistic model like the MCM or GECKO-A?

Response: The sensitivities of different VOCs in the PTR instrument are not equal and are linearly related to their proton-transfer reaction rate constants when ion transmission efficiency and fragmentation ions are considered (Sekimoto et al., 2017; Krechmer et al., 2018). According to Sekimoto et al. (2017), the reaction rate constants of different molecules significantly depend on their molecular mass, elemental composition, and functionality. In this study, we acknowledge that it is not a perfect method to quantify the mass fraction of different factors based on their average signal intensities as shown in the pie charts of Figure 12. The related uncertainties are discussed in the manuscript (Lines 419-423): "We acknowledge that it is not a perfect method to quantify the contributions of various sources and formation processes. The sensitivities of different VOCs measured by the PTR instruments may vary by a factor of 2-3 (Sekimoto et al., 2017; Yuan et al., 2017). The uncertainties can come from the challenge to convert the signal intensity to atmospheric concentrations because of problematic calibrations, especially given that many unknown molecules exist in the mass spectra."

In this study, a large mass fraction of the gas-phase organic species were measured and classified including the precursors, the lightly oxidized products, and the more oxidized products, which was not achieved by previous studies. Although it is out of the scope of the current study to perform model simulations, our results provide good data base for potential model study in the future to compare model simulations with our ambient observations, improve model performance, and help scientists better understand the complex atmospheric chemistry. Still, the lack of speciation of e.g. the monoterpenes with the PTR approach remains a challenge for mechanistic modeling, as the oxidation product distributions will vary tremendously depending on the exact VOC distributions in the forests.

Anonymous Referee #2

This paper reports on data collected by a VOCUS PTR-ToF-MS at two forest sites. The VOCUS PTR-ToF is a powerful tool to characterize both biogenic and anthropogenic emissions due to it's high sensitivity and broad range of detectable organic compounds. For the first time, the binned positive matrix factorization (binPMF) algorithm has been applied to VOCUS data. Applying PMF to binned data with subsequent high-resolution peak fitting and identification of peaks found to be relevant is a clever way of data reduction in rich datasets as obtained by modern non-selective CIMS techniques.

The paper is technically sound; the authors describe individual PMF factors in great detail, but, unfortunately, the paper does not go beyond a description of observations, and I agree with Referee #1 that it feels unfinished at this stage. I therefore recommend that this paper be published only after major revisions.

Response: We thank Anonymous Referee #2 for the careful review and inputs which helped improving the overall quality of our work. We agree that as a research article, the paper should go beyond a description of PMF source apportionment and highlight new understanding towards atmospheric science from this work. Therefore, in the revised manuscript, our major findings are highlighted and more insights are gained into monoterpene and sesquiterpene oxidations. Please see more details in our responses to Referee #1.

Comments:

I think that the paper does not identify oxidation processes as stated in the abstract, nor does it provide a more comprehensive understanding of gas-phase organic chemistry.

Response: In this study, a large mass fraction of the gas-phase organic species were measured and classified. In addition to the precursors, their lightly oxidized products and more oxidized products were separated as individual factors. Based on the interpretation of these factors related to oxidation processes, further insights were gained regarding monoterpene and sesquiterpene reactions. In addition, the relative abundances of organic precursors, the lightly oxidized products, and the more oxidized products can be utilized by modelers to evaluate simulation output, improve model performance, and provide new perspectives to understand gas-phase physicochemical processes.

We revised the abstract as follows:

"Atmospheric organic vapors play essential roles in the formation of secondary organic aerosol. Source identification of these vapors is thus fundamental to understand their emission sources and chemical evolution in the atmosphere and their further impact on air quality and climate change. In this study, a Vocus proton-transfer-reaction time-of-flight mass spectrometer (PTR-TOF) was deployed in two forested environments, the Landes forest in southern France and the boreal forest in southern Finland, to measure atmospheric organic vapors, including both volatile organic compounds (VOCs) and their oxidation products. For the first time, we performed binned positive matrix factorization (binPMF) analysis on the complex mass spectra acquired with the Vocus PTR-TOF and identified various emission sources as well as oxidation processes in the atmosphere. Based on separate analysis of low- and high-mass ranges, fifteen PMF factors in the Landes forest and nine PMF factors in the Finnish boreal forest were resolved, showing a high similarity between the two sites. Particularly, terpenes and various terpene reaction products were separated into individual PMF factors with varying oxidation degrees, such as lightly oxidized compounds from both monoterpene and sesquiterpene oxidations, monoterpene-derived organic nitrates, and monoterpene more oxidized compounds. Factors representing monoterpenes dominated the biogenic VOCs in both forests, with less contributions from the isoprene factors and sesquiterpene factors. Factors of the lightly oxidized products, more oxidized products, and organic nitrates of monoterpenes/sesquiterpenes accounted for 8-12% of the measured gas-phase organic vapors in the two forests. Based on the interpretation of the results relating to oxidation processes, further insights were gained regarding monoterpene and sesquiterpene reactions. For example, a strong relative humidity (RH)-dependence was found for the behavior of sesquiterpene

lightly oxidized compounds. High concentrations of these compounds only occur at high RH, yet similar behavior was not observed for monoterpene oxidation products. These findings highlight the need for further studies to delve into gas-phase atmospheric processes of monoterpenes and sesquiterpenes."

The authors divided the mass spectra into two regions: 51 to 200 Th and 201 to 320 Th. Furthermore, they excluded two masses with high signal intensities (m81 and m137) from the PMF analysis, since these peaks were dominating the mass profiles. As far as I understand, both actions are necessary due to the fact that ambient concentrations of organic species and oxidaion products vary by many orders of magnitude, and the PMF method cannot resolve small signals. Maybe it's worth coming up with either a peak-by-peak normalization method prior to PMF analysis or feed the algorithm with logarithmized signal intensities. Please see this comment being made out of curiosity rather than critical.

Response: As the reviewer points out, there are multiple ways in which data can be scaled before factorization, each one giving more or less weight to certain signals in the mass spectra. Earlier studies from our group have explored in detail e.g. scaling according to intensity or mass-to-charge ratio (Fig. 3 and Fig. S7 in Äijälä et al., 2017). The ultimate added value of such labor-intensive approaches is largest when the factorization results are ambiguous or hard to verify. In the current work, we tried a simple approach (removing the main peaks of the largest signals), which will be easy also for others to replicate. This produced factors that made sense both chemically and through their temporal behavior, which lends confidence in the results. The sub-range analysis, which we earlier have shown to be very powerful in separating out less abundant factors (Zhang et al., 2020), also provides a type of "internal verification" when factors with similar temporal and chemical features are resolved from the two different mass ranges. In the end, there is no single "correct" way to factorize atmospheric data, and the validity of the approach should be referenced to the results, and the conclusion that can be drawn from them.

Specific comments: Figures 4,7,9 and 12: the y-axis' unit is 'ions/bin' - I think that should be changed into something like 'ions/factor'.

Response: These figures show the time series of different factors. The unit corresponds to the binned signal intensities measured by the mass spectrometer and should be "ions/bin".

line 62 and 307: replace "complicated" with "complex"

Response: Replaced.

line 182: please specifiy what 'high' means.

Response: As shown in Figure S2, for some bins, the scaled residual can as high as ±200. In the revised manuscript (Line 196), it is specified as "*For some bins the residuals are still high (the scaled residuals as high as ±200).*"

line 293: "much higher intensities" - please rephrase

Response: Done.

References

Äijälä, M., Heikkinen, L., Fröhlich, R., Canonaco, F., Prévôt, A. S. H., Junninen, H., Petäjä, T., Kulmala, M., Worsnop, D., and Ehn, M.: Resolving anthropogenic aerosol pollution types – deconvolution and exploratory classification of pollution events, Atmos. Chem. Phys., 17, 3165–3197, https://doi.org/10.5194/acp-17-3165-2017, 2017.

Zhang, Y., Peräkylä, O., Yan, C., Heikkinen, L., Äijälä, M., Daellenbach, K. R., Zha, Q., Riva, M., Garmash, O., Junninen, H., Paatero, P., Worsnop, D., and Ehn, M.: Insights into atmospheric oxidation processes by performing factor analyses on subranges of mass spectra, Atmos. Chem. Phys., 20, 5945–5961, https://doi.org/10.5194/acp-20-5945-2020, 2020.

~~Source identification of a~~Atmospheric organic vapors in two European pine forests measured by a ~~: Results from~~ Vocus PTR-TOF ~~observations~~: insights into monoterpene and sesquiterpene oxidation processes

Haiyan Li[1], Manjula R. Canagaratna[2], Matthieu Riva[3], Pekka Rantala[1], Yanjun Zhang[1], Steven Thomas[1], Liine Heikkinen[1], Pierre-Marie Flaud[4,5], Eric Villenave[4,5], Emilie Perraudin[4,5], Douglas Worsnop[2], Markku Kulmala[1], Mikael Ehn[1], Federico Bianchi[1]

[1] Institute for Atmospheric and Earth System Research/Physics, Faculty of Science, University of Helsinki, Helsinki, 00014, Finland
[2] Aerodyne Research Inc., Billerica, Massachusetts 01821, USA
[3] Univ. Lyon, Université Claude Bernard Lyon 1, CNRS, IRCELYON, 69626, Villeurbanne, France
[4] University of Bordeaux, EPOC, UMR 5805 CNRS, 33405 Talence Cedex, France
[5] CNRS, EPOC, UMR 5805 CNRS, 33405 Talence Cedex, France

Correspondence: Haiyan Li (haiyan.li@helsinki.fi)

Abstract.

Atmospheric organic vapors play essential roles in the formation of secondary organic aerosol. Source identification of these vapors is thus fundamental to understand their emission sources and chemical evolution in the atmosphere and their further impact on air quality and climate change. In this study, a Vocus proton-transfer-reaction time-of-flight mass spectrometer (PTR-TOF) was deployed in two forested environments, the Landes forest in southern France and the boreal forest in southern Finland, to measure atmospheric organic vapors, including both volatile organic compounds (VOCs) and their oxidation products. For the first time, we performed binned positive matrix factorization (binPMF) analysis on the complex mass spectra acquired with the Vocus PTR-TOF and identified various emission sources as well as oxidation processes in the atmosphere. Based on separate analysis of low- and high-mass ranges, fifteen PMF factors in the Landes forest and nine PMF factors in the Finnish boreal forest were resolved, showing a high similarity between the two sites. Particularly, terpenes and various terpene reaction products were separated into individual PMF factors with varying oxidation degrees, such as lightly oxidized compounds from both monoterpene and sesquiterpene oxidations, monoterpene-derived organic nitrates, and monoterpene more oxidized compounds. Factors representing monoterpenes dominated the biogenic VOCs in both forests, with less contributions from the isoprene factors and sesquiterpene factors. Factors of the lightly oxidized products, more oxidized products, and organic nitrates of monoterpenes/sesquiterpenes accounted for 8-12% of the measured gas-phase organic vapors in the two forests. Based on the interpretation of the results relating to oxidation processes, further insights were gained regarding monoterpene and sesquiterpene reactions. For example, a strong relative humidity (RH)-dependence was found for the behavior of sesquiterpene lightly oxidized compounds. High concentrations of these compounds only occur at high RH,

yet similar behavior was not observed for monoterpene oxidation products. These findings highlight the need for further studies to delve into gas-phase atmospheric processes of monoterpenes and sesquiterpenes. ~~These factors display similar mass profiles and diurnal variations between the two sites, revealing similar terpene reaction pathways in these forests. With the distinct characteristics of VOCs and oxygenated VOCs measured by the Vocus PTR-TOF, this study identified various primary emission sources and secondary oxidation processes of atmospheric organic vapors in the European pine forests, providing a more comprehensive understanding of gas-phase atmospheric chemistry.~~

1 Introduction

Volatile organic compounds (VOCs) and their oxidation products are important contributors to atmospheric secondary organic aerosol (SOA) (Hallquist et al., 2009; Ehn et al., 2014) and new particle formation (Bianchi et al., 2016; Kirkby et al., 2016). Therefore, the identification of these organic vapors and their sources is fundamental for understanding the effects of atmospheric aerosols on climate change and air quality (Schell et al., 2001; Maria et al., 2004). Large amounts of VOCs with varying physicochemical properties are emitted from both biogenic and anthropogenic sources (Friedrich et al., 1999; Kesselmeier et al., 1999), and their oxidation processes in the atmosphere can lead to the formation of thousands of structurally distinct products containing multiple functional groups (Hallquist et al., 2009; Wennberg et al., 2018). Due to the enormous challenge in characterizing these organic vapors at molecular level, knowledge of their sources or formation pathways has remained lacking.

Globally, SOA production from biogenic sources is much larger than that from anthropogenic sources (Tsigaridis and Kanakidou, 2003). As a group of highly reactive gases, typically with one or more C = C double bounds, terpenes make up a major fraction of biogenic VOCs, including isoprene, monoterpenes, and sesquiterpenes (Guenther et al., 1995). In the atmosphere, they react with various oxidants, i.e., hydroxyl radical (OH), ozone (O_3), and nitrate radical (NO_3), and produce a large variety of oxygenated molecules. Isoprene is the most emitted biogenic VOC on the global scale but has a relatively small SOA yield (Ahlberg et al., 2017; McFiggans et al., 2019). Monoterpenes are important sources of SOA (Ehn et al., 2014; Zhang et al., 2018) and their oxidation processes have been found to play important roles in new particle formation (Kirkby et al., 2016; Simon et al., 2020). High ambient concentrations of monoterpenes have been observed in numerous pine forests (Hakola et al., 2012; Noe et al., 2012; Bourtsoukidis et al., 2014). While the concentrations of sesquiterpenes are generally much smaller than those of isoprene and monoterpenes (Sakulyanontvittaya et al., 2008; Sindelarova et al., 2014), sesquiterpenes could contribute significantly to SOA formation because of their reactivity and high aerosol yields (Calogirou et al., 1999; Khan et al., 2017). Previous studies found that sesquiterpenes contributed to the O_3 and OH reactivity in forest environments (Kim et al., 2011; Hellén et al., 2018). The recently developed Vocus proton-transfer-reaction time-of-flight mass spectrometry (PTR-TOF) enables the real-time detection of both VOCs and their oxidation products. With a new chemical ionization source called Vocus, the instrument significantly improves its detection efficiency of product ions compared with conventional PTR instruments (Krechmer et al., 2018). Based on a laboratory comparison of different chemical

ionization techniques, Riva et al. (2019) revealed that Vocus PTR-TOF is sensitive to a large range of oxygenated VOCs. With the deployment of a Vocus PTR-TOF in the French Landes forest, Li et al. (2020) observed various terpenes and terpene oxidation products, including a range of organic nitrates.

With the benefit of the state-of-the-art capabilities of Vocus PTR-TOF to detect hundreds to thousands of molecules, a great challenge arises to analyze the ~~complicated~~ complex dataset where emission sources and atmospheric physical and chemical processes are mixed together. The characteristic analysis based solely on individually identified compounds cannot give the full picture of the measurements. Factor analytical techniques, e.g., positive matrix factorization (PMF), have been utilized to extract information from mass spectrometer data by resolving co-varying signals with common sources or atmospheric processes into a single factor (Paatero and Tapper, 1994). For example, PMF analysis has been widely applied by the research community using aerosol mass spectrometer to identify multiple primary organic aerosol sources and SOA aging processes (Lanz et al., 2007; Ulbrich et al., 2009; Zhang et al., 2011). Yan et al. (2016) successfully applied PMF to unit-mass-resolution (UMR) nitrate ion-based chemical ionization mass spectrometer (NO_3^- CIMS) data to differentiate mainly monoterpene highly oxygenated organic molecules (HOMs) formed from different formation pathways in the boreal forest. The application of PMF to high-resolution (HR) NO_3^- CIMS data by Massoli et al. (2018) identified more HOM factors at an isoprene-dominated forest site in Alabama, USA. Recently, the mass spectral binning combined with PMF (binPMF) was proposed as a novel and simple method for analyzing high-resolution mass spectra datasets (Zhang et al., 2019a). This approach divides the full mass spectra into small bins as input data to PMF, thus avoiding the time-consuming and complicated peak identification. Zhang et al. (2019b) further applied binPMF to sub-ranges of ambient NO_3^- CIMS mass spectra and separated more meaningful factors related to chemical processes yielding HOMs.

In this work, we present the first factor analysis on Vocus PTR-TOF datasets to identify and apportion the contribution of different sources and formation pathways to atmospheric organic vapors. The measurements were conducted in two forest ecosystems in Europe, the French Landes forest and the boreal forest in southern Finland. Due to orders of magnitude differences in the signal intensities of ions between lower mass range and higher mass range, we divided the mass spectra into two sub-ranges (50–200 Th and 201–320 Th) and performed binPMF analysis on these ranges separately. While the UMR analysis loses all possible HR details and the HR peak identification introduces high uncertainties due to the complexity of overlapping peaks, the binPMF method includes as much of the HR information as possible in a robust way. The resolved factors were linked to possible sources or chemistry processes by examining their mass profiles, time series, diurnal cycles, and correlation with molecular markers. ~~Spatial comparisons were discussed for the common sources apportioned in both forests.~~ Comparison were discussed among different factors and also between the two forests for the common sources apportioned. Based on the interpretation of the resolved factors, further insights were provided regarding the atmospheric processes of monoterpenes and sesquiterpenes.

2 Materials and methods

2.1 Site description and measurement period

The measurement data were obtained during summertime in two forest environments in Europe, the Landes forest in southwestern France and the boreal forest research station SMEAR (Station for Measuring Forest Ecosystem-Atmosphere Relations) II in southern Finland. The field campaign in the Landes forest was conducted from 8 to 20 July 2018 as part of the Characterization of Emissions and Reactivity of Volatile Organic Compounds in the Landes forest (CERVOLAND) campaign. An overview of the Vocus PTR-TOF measurements in the Landes forest has been presented earlier by Li et al. (2020). The ambient observations at the SMEAR II station were performed during 18 June – 18 July 2019.

The Landes forest (44º29'N, 0º57'W) is the largest man-made pine forest in Europe, mainly filled with maritime pine trees (*Pinus pinaster Aiton*). The sampling site is situated at the European Integrated Carbon Observation System (ICOS) station at Bilos. The nearest urban area of the Bordeaux metropole is around 40 km to the northwest. A more detailed description of the measurement site can be found elsewhere (Kammer et al., 2018; Bsaibes et al., 2020; Li et al., 2020). Ambient meteorological parameters, including temperature, relative humidity (RH), wind speed and direction, solar radiation, and pressure, and mixing ratios of nitrogen oxides (NO and NO_2) and O_3 were continuously monitored at the station throughout the campaign.

The SMEAR II station (61º51'N, 24º17'E) is located in a boreal mixed-coniferous forest in Hyytiälä, southern Finland (Hari and Kulmala, 2005). The site is dominated by a rather homogeneous Scots pine (*Pinus sylvestris L.*) stand and represents a rural background measurement station. The nearest large city Tampere, located about 60 km to the southwest, has approximately 200 000 inhabitants. The station is equipped with extensive facilities to measure forest ecosystem-atmosphere interactions. Ambient meteorological parameters (i.e., global radiation, UVA, UVB, temperature, RH, pressure, and wind speed and direction), mixing ratios of various trace gases (i.e., carbon dioxide, carbon monoxide, sulfur dioxide, NO_x, and O_3), and particle concentration and size distribution, are continuously measured at the station.

2.2 Instrumentation

A Vocus PTR-TOF was deployed in both forest ecosystems to characterize atmospheric organic vapors. Equipped with a new chemical ionization source with a low-pressure reagent-ion source and focusing ion-molecule reactor (FIMR), the Vocus PTR-TOF is able to measure organic vapors with a wide range of volatilities (Krechmer et al., 2018; Riva et al., 2019; Li et al., 2020). A quadrupole radio frequency (RF) field inside the FIMR focuses ions to the central axis and improves the detection efficiency of product ions. Compared with conventional PTR instruments, the sensitivity and detection efficiency of Vocus PTR-TOF are significantly improved (detection limit < 1 pptv). With a high water mixing ratio (10% v/v–20% v/v) in the FIMR, the instrument shows no humidity dependence for sensitivity. More instrumental details have been provided elsewhere (Krechmer et al., 2018; Li et al., 2020).

During both campaigns, we operated the Vocus ionization source at a pressure of 1.5 mbar. Sample air was drawn in through a ~1-m-long PTFE tubing (10 mm o.d., 8 mm i.d.). A sample air flow of 4.5 L min^{-1} was used to reduce inlet wall

losses and sampling delay. Around 100–150 ccm of this flow was sampled into the Vocus and the remainder was directed to the exhaust. The mass resolving power of the long TOF mass analyzer was 12 000 – 13 000 m Δm^{-1} during our measurements. Data were recorded with a time resolution of 5 s. During the campaign in the Landes forest, background checks were automatically performed every hour using ultra-high-purity nitrogen (UHP N_2). The instrument was calibrated twice a day using a mixture of terpenes (α-/β-pinene+limonene; *p*-cymene). For measurements at the SMEAR II station, background measurements by injection of zero air using a built-in active carbon filter and quantitative calibrations with a multi-component standard cylinder were automatically conducted every three hours. All the *m/z* ratios mentioned in this work include the contribution from the charger ion (H^+, mass of 1 Th) unless stated otherwise.

2.3 binPMF data preparation and analysis

As described by Zhang et al. (2019a), binPMF divides the mass spectra into small bins and then takes advantage of PMF analysis to separate different sources or formation processes. The binPMF allows utilization of the high-resolution information of the complex mass spectra without the time-consuming and potentially error-prone steps of peak identification and peak fitting before the factorization. Selected peaks of interest can be analyzed after binPMF, based on the output factors. PMF assumes that factor profiles are constant and unique, and the measured signal of a chemical component is a linear combination of different factors. This approach does not require a priori information about the factors. The detailed working principle of PMF has been provided in numerous previous studies (Paatero and Tapper, 1994; Zhang et al., 2011; Yan et al., 2016).

To prepare the data and error matrices for PMF input, the Vocus PTR-TOF data were processed using the software package "Tofware" (v3.2.0; Tofwerk), which runs in the Igor Pro environment (WaveMetrics, OR, USA). The detailed data processing routines have been presented elsewhere (Stark et al., 2015). Signals were averaged over 30 min for data processing. Unlike traditional UMR or HR fitting of the mass spectra, in binPMF analysis, the mass spectra were divided into small bins after mass calibration. Due to the greater mass resolving power of the TOF mass analyzer compared with former binPMF studies (Zhang et al., 2019a, 2019b), a bin width of 0.01 Th was applied in this study. At a nominal mass *N*, signals between *N*-0.15 and *N*+0.35 Th were included for binning. The error matrix was calculated to include uncertainty from counting statistics following Poisson distribution and instrument electronic noise, as described by Yan et al. (2016) and Zhang et al. (2019a). The electric noise was estimated as the median of the standard deviation of binned noise signals between two nominal masses, with noise range between *N*+0.4 and *N*+0.6 Th.

Figure 1 shows the average mass spectra of the measurements in the Landes forest as an example. Since the signal intensity of larger molecules is generally much lower than that of low-mass molecules, we divided the mass spectra into two sub-ranges, the low mass range (51–200 Th) and the high mass range (201–320 Th). Factor analysis was separately performed on these two sub-ranges using an Igor-based open-source PMF Evaluation Tool (PET; http://cires1.colorado.edu/jimenez-group/wiki/index.php/PMF-AMS_Analysis_Guide#PMF_Evaluation_Tool_Software). We ran the PMF up to ten factors for both sub-ranges. For the low mass range of 51–200 Th, the signals at *m/z* 81 Th ($C_6H_8H^+$, monoterpene fragment) and 137 Th ($C_{10}H_{16}H^+$, monoterpenes) were markedly higher than the others. With the inclusion of these ions, the mass profiles of several

factors were quite similar and dominated by these peaks (Fig. S1). ~~In the initial PMF results, the mass profiles of all resolved factors were dominated by these ions.~~ Therefore, the major mass bins of these ions were excluded for further PMF analysis, but their corresponding isotopes were retained, effectively downweighting their contributions to the PMF result. However, to quantify the relative contribution of different factors, the signals of these removed mass bins were counted back into their corresponding factors. More details can be found in Sect. 4.4.

2.4 Estimation of OH and NO_3 radicals

The OH concentration was calculated by scaling the measured UVB radiation intensity with the empirically derived factors from Petäjä et al. (2009) and Kontkanen et al. (2016):

$$[OH]_{proxy} = \left(\frac{8.4 \times 10^{-7}}{8.6 \times 10^{-10}} UVB^{0.32}\right)^{1.92}$$

Measurements of NO_3 concentration is challenging. The concentration of NO_3 radical was calculated by assuming a steady state between its production from O_3 and NO_2 and its removal by oxidation reactions and losses in the atmosphere. Details can be found in Allan et al. (2000) and Peräkylä et al. (2014).

3 Dataset overview

Figure 2 shows the temporal behaviors of temperature, global radiation, concentrations of O_3 and NO_x, and concentrations of isoprene and monoterpenes in the Landes forest and at the SMEAR II station. In the Landes forest, the weather was mainly sunny during the observation period (global radiation > 400 W m^{-2}), indicating strong photochemical activity. The air mass in the forest was largely influenced by local sources, with wind speeds below canopy lower than 1 m s^{-1} over the whole campaign. The O_3 concentration fluctuated dramatically between day and night, with the average daytime concentration peaking up to 50 ppb and the average nighttime level falling below 2 ppb (Li et al., 2020). The low O_3 concentration at night was probably to some extent caused by its titration by monoterpenes (Fig. 2a; Kammer et al., 2018, 2020). The Landes forest is known for strong monoterpene emissions (Simon et al., 1994). During our measurements, the average mixing ratios of isoprene and monoterpenes were 0.6 ppb and 6.0 ppb, respectively. More details about this dataset can be found in Li et al. (2020). All data in the Landes forest are reported in local time and all data at the SMEAR II station in Finnish winter time (both equal UTC time + 2).

During the measurements at the SMEAR II station, 84% (26 out of 31) of the days had strong photochemistry (global radiation > 400 W m^{-2}), with the rest being cloudy days. The diurnal variation in O_3 concentration was not as dramatic as that in the Landes forest. In the daytime, the O_3 concentration sometimes reached up to 50 ppb. At night, the O_3 level still largely remained high, above 20 ppb, in contrast to the observations in the Landes forest. A possible explanation is less nighttime O_3 consumption by terpenes at the SMEAR II station. On average, the mixing ratios of isoprene and monoterpenes were 0.2 ppb and 0.8 ppb, respectively, during the measurements, much lower than those in the Landes forest.

4 Results and discussion

4.1 Choice of PMF solution and factor interpretation

To interpret the PMF results, the most critical decision is to choose the best number of factors. More factors introduce more degrees of freedom to explain variations in the data, but too many factors may cause splitting of real factors and lead to mathematical artifacts without physical meaning (Ulbrich et al., 2009). The factor interpretation results in this work are summarized in Table 1. In the factor name, L means the Landes forest and S means the SMEAR II station.

For the low mass range of the Landes forest dataset, the Q/Q_{exp} varied from 15.5 to 6.0 for two to ten factors (Q is the total sum of the squares of the scaled residuals for PMF solutions). The larger Q/Q_{exp} indicates underestimation of the errors or high residuals for some bins that cannot be simply modeled by the solution (Ulbrich et al., 2009). After seven factors, increasing the factor number does not significantly decrease the Q/Q_{exp}. The optimal solution of seven factors was chosen after a detailed evaluation following the procedures proposed by Ulbrich et al. (2009) and Zhang et al. (2011). Figure S2~~1~~ shows the distribution of scaled residuals as a function of *m/z*. For some bins the residuals are still high (the scaled residuals as high as ±200). The seven factors include Factor L1 closely related to the $C_4H_8H^+$ ion, Factor L2 attributed to a plume event occurring on a single night during the campaign, Factor L3 mainly containing lightly oxidized compounds with six or seven carbon atoms ("C_6" or "C_7"), Factor L4 representing monoterpenes, Factor L5 indicative of isoprene and its oxidation products, Factor L6 identified as unknown source with large contributions from unknown peaks, and Factor L7 dominated by monoterpene lightly oxidized compounds. The direct comparison of the mass spectra, time series, and diurnal cycles of six-factor and eight-factor solutions are shown in Fig. S3~~2~~ and Fig. S4~~3~~. In the six-factor case, the $C_4H_8H^+$ ion-related factor cannot be separated. With eight-factor results, the factor representing isoprene and its oxidation products is split into two components with similar time series. For the high mass range of the Landes forest dataset, the Q/Q_{exp} decreased from 2.5 to 0.9 for two to ten factors. After evaluation, we choose the eight-factor solution to explain the data. The Q/Q_{exp} value of the eight-factor solution was 1.1 and the decreasing trend in Q/Q_{exp} obviously slowed down after eight factors. The distribution of scaled residuals as a function of *m/z* for the eight-factor solution is shown in Fig. S5~~4~~. The eight factors are interpreted as Factor L8 dominated by lightly oxygenated compounds containing 13 carbon atoms ("C_{13}"), Factor L9 attributed to a plume event occurring on a single night during the campaign, Factor L10 mainly related to sesquiterpene lightly oxidized compounds, Factor L11 representing more oxidized products mainly from monoterpene oxidations, Factor L12 indicating sesquiterpenes, Factor L13 largely composed of monoterpene-derived organic nitrates, Factor L14 mainly containing oxidized compounds with twelve, fourteen or sixteen carbon atoms ("C_{12}", "C_{14}" or "C_{16}")and Factor L15 as unknown source largely contributed by siloxane compounds. Figure S6~~5~~ and Figure S7~~6~~ display the mass spectra, time series, and daily variations of seven-factor and nine-factor solutions. In the seven-factor case, monoterpene more oxidized products and monoterpene-derived organic nitrates are mixed together into a single factor. However, in the nine-factor solution, the unknown factor mainly composed of siloxane compounds is split into two factors with similar mass profiles and similar diurnal trends.

For the SMEAR II dataset, the optimal solutions of five-factor and four-factor are chosen for the low and high mass ranges, respectively. The Q/Q_{exp} varied from 7.2 to 2.5 for two to ten factors in the low mass range and from 2.0 to 1.0 for two to ten factors in the high mass range. The five factors for the low mass range are identified as Factor S1 - $C_4H_8H^+$ ion-related, Factor S2 - monoterpenes, Factor S3 - lightly oxidized compounds with six to nine carbon atoms, Factor S4 - isoprene and its oxidation products, and Factor S5 - monoterpene lightly oxidized compounds. The mass spectra, time series, and diurnal profiles of the four-factor and six-factor solutions for the low mass range are presented in Fig. S8~~7~~ and Fig. S9~~8~~. For the four-factor solution, monoterpene lightly oxidized products are not separated as a single factor and mixed into the others. In the six-factor case, the factor indicative of monoterpene lightly oxidized products is split into two factors. The four factors for the high mass range include Factor S6 - sesquiterpene lightly oxidized products, Factor S7 - sesquiterpenes, Factor S8 - more oxidized compounds, and Factor S9 - unknown source. The direct comparison of the mass spectra, time series, and diurnal variations of three-factor and five-factor solutions are shown in Fig. S10~~9~~ and Fig. S11~~0~~. The three-factor solution does not identify a factor representing sesquiterpenes. In the five-factor case, the factor of unknown source mainly contributed by siloxane compounds is split into two factors with similar mass profiles.

The rotational freedom of the PMF solutions was explored through the use of the FPEAK parameters. For each of the optimal solutions, we varied the FPEAK values between -1 and +1 with the step of 0.2. For the low mass ranges of the Landes and SMEAR II dataset, the varying FPEAK values did not change the factor profiles and time series much. For the high mass range of the Landes measurements, we saw variations especially in the factor profiles by varying FPEAK values. But after a detailed evaluation, we found no evidence that solutions with FPEAK values away from zero were preferable. However, for the high mass range of the SMEAR II measurements, the solutions with positive values of FPEAK worked better than that with FPEAK = 0 in terms of factor profiles. The factor time series were similar when FPEAK values varied. But for the factor profiles with positive FPEAK values, the factor of monoterpene more oxidized products including organic nitrates contained less traces of siloxanes and showed elevated fractions of the corresponding fingerprint peaks (Fig. S12). After evaluation, we chose the solution with FPEAK = +0.6 for the high mass range of the SMEAR II dataset.

4.2 Source identification in the Landes forest

Figure 3 and Figure 4 illustrate the factor profiles, time series, and diurnal variations of the seven factors resolved in the low mass range. For the high mass range, t~~T~~he mass spectra of the five factors ~~identified in the high mass range~~ are shown in Fig. 5~~6~~, and their time series and daily variations in Fig. 6~~7~~. ~~Figure 5 includes the correlations of these five factors with fingerprint molecules.~~The high-resolution peak fitting was further performed on the mass profile to identify the fingerprint peaks in the factors. Fingerprint peaks are defined largely based on their distribution in the factors rather than their absolute intensity in the mass profile. The correlation map of each factor with various compounds is shown in Fig. S13~~5~~.

4.2.1 Low mass range (51–200 Th)

~~Figure 3 and Figure 4 illustrate the factor profiles, time series, and diurnal variations of the seven factors resolved in the low mass range. The high-resolution peak fitting was further performed on the mass profile to identify the fingerprint peaks in the factors. Fingerprint peaks are defined largely based on their distribution in the factors rather than their absolute intensity in the mass profile. The correlation map of each factor with various compounds is shown in Fig. 5.~~

Factor L1: $C_4H_8H^+$ ion-related

Factor L1 shows irregular diurnal variations with spiky peaks in the time series (Fig. 4b). The major bins that are largely distributed into this factor are $C_4H_8H^+$ and $C_4H_{10}O_2H^+$. Factor L1 closely correlates with these fingerprint peaks. Considering the high signal intensity of $C_4H_8H^+$ ion and its large contribution to this factor, we name Factor L1 as $C_4H_8H^+$ ion-related. ~~According to the discussions by Li et al. (2020), the observation of $C_4H_8H^+$ in the Landes forest can be attributed to several sources. For instance, the protonated butene may contribute to the $C_4H_8H^+$ signal, which is emitted by biogenic or anthropogenic sources (Hellén et al., 2006; Zhu et al., 2017). Another possible explanation is that the $C_4H_8H^+$ ion is produced during the fragmentation of many VOCs in the PTR instruments (Pagonis et al., 2019). The green leaf volatiles (GLV) have been found to fragment at *m/z* 57 Th inside the PTR instruments, which are a group of six-carbon aldehyde, alcohols and their esters released by plants. Furthermore, butanol can easily lose an OH during the PTR source ionization and produce prominent $C_4H_8H^+$ peaks (Spanel and Smith, 1997). Therefore, the condensation particle counters (CPCs) using butanol for aerosol measurements at the site could also be an important source of $C_4H_8H^+$ ions, although the exhaust air from these instruments has been filtered using charcoal denuder.~~

Factor L2: A plume event

Factor L2 is identified as a plume event occurring on a single night during the campaign. As shown in Fig. 4a, the time series of this factor are characterized by much higher intensities at midnight of 9 July 2018 than over the other days. Fingerprint peaks in this factor are aromatic compounds such as $C_6H_6H^+$, $C_7H_6H^+$, and $C_6H_6OH^+$. Factor L2 is well correlated with benzene and phenol (r^2 = 0.88; Fig. S13~~5~~)~~, indicating the major influence of anthropogenic sources. As mentioned above, the air masses in the forest were relatively stable during our observations with wind speed below canopy < 1 m s^{-1}. Therefore, the influence of long-range regional transport on the atmosphere in the forest is expected to be minor. We speculate that Factor L2 is a result of local anthropogenic disturbances favored by the lower boundary layer height at night.~~

Factor L3: C_6 and C_7 lightly oxidized products

The diurnal cycle of Factor L3 exhibits a small morning peak at 9:00 and significantly elevated intensities during nighttime, peaking at around 22:00 (Fig. 4b). As illustrated in the mass profile of Factor L3, this factor is mainly composed of lightly oxidized compounds containing six or seven carbon atoms such as $C_6H_{10}OH^+$, $C_7H_{10}OH^+$, $C_6H_{10}O_2H^+$, and $C_7H_{12}O_2H^+$. ~~The C_6 oxygenated compounds have been observed during the oxidation processes of benzene and C_7 oxygenated compounds from toluene oxidations (Sato et al., 2012; Zaytsev et al., 2019). These compounds can also be directly emitted from biogenic~~

~~or anthropogenic sources (Conley et al., 2005; Pandya et al., 2006; Rantala et al., 2015). Factor L3 shows tight correlations with $C_7H_{10}OH^+$ and $C_6H_{10}O_2H^+$ (r^2 > 0.92; Fig. 5).~~

Factor L4: monoterpenes

The mass profile of Factor L4 is dramatically characterized by a monoterpene peak ($^{13}CC_9H_{16}H^+$) and its major fragments (i.e., $^{13}CC_5H_8H^+$ and $C_7H_8H^+$) inside the instrument. As shown in Fig. 4b, the diurnal variation of this factor follows a similar pattern to that of monoterpenes (Li et al., 2020). The signal intensity of the factor starts to increase at 20:00, peaks at midnight, and then drops to around the detection limit during daytime. Monoterpene emissions are mainly influenced by temperature (Hakola et al., 2006; Kaser et al., 2013). Therefore, with the continuous emissions of monoterpenes and the shallow boundary layer at night, the signal intensities of monoterpenes are observed to be elevated. ~~The lower signal of Factor L4 in the daytime is likely a combination of enhanced atmospheric mixing after sunrise and the rapid photochemical consumption of monoterpenes.~~ The signal of $C_{10}H_{16}OH^+$ is also mostly resolved into this factor. $C_{10}H_{16}O$ could be primary emissions of oxygenated monoterpenes or monoterpene oxidation products (Kallio et al., 2006; McKinney et al., 2011). Previous ambient observation has demonstrated that the atmospheric behavior of $C_{10}H_{16}O$ has high similarity to that of monoterpenes (Li et al., 2020).

Factor L5: isoprene and its oxidation products

The marker peaks in Factor L5 are highly dominated by isoprene and its major oxidation products in the atmosphere, i.e., $C_5H_8H^+$ and $C_4H_6OH^+$ (Wennberg et al., 2018). Isoprene emissions strongly depend on light intensity (Monson and Fall, 1989; Kaser et al., 2013) and generally show high concentrations in the day. Similarly, the daily variations of Factor L5 display maximum signal during daytime and minima at night.

Factor L6: unknown source

Factor L6 is characterized by increased signals in the afternoon. The major peaks in its factor profile are $C_6H_4O_2H^+$, $C_6H_6O_3H^+$, and numerous unidentified peaks with negative mass defect. As this factor is clearly separated as a single source with high signals during our observations and the molecule markers remain unidentified, we name this factor as an unknown source.

Factor L7: monoterpene lightly oxidized products

Fingerprint peaks in this factor are monoterpene oxidation products with oxygen number from one to three, such as $C_9H_{14}OH^+$, $C_{10}H_{14}OH^+$, $C_{10}H_{16}O_2H^+$, and $C_{10}H_{16}O_3H^+$. This factor displays clear morning and evening peaks, similar to the behavior of these lightly oxidized compounds (Li et al., 2020). ~~By calculating the reaction rates of monoterpenes with OH and O_3, Li et al. (2020) demonstrated that both OH- and O_3-initiated oxidation processes contribute to the formation of these compounds in the Landes forest.~~

4.2.2 High mass range (201–320 Th)

~~The mass spectra of the five factors identified in the high mass range are shown in Fig. 6, and their time series and daily variations in Fig. 7. Figure 5 includes the correlations of these five factors with fingerprint molecules.~~

Factor L8: C_{13} lightly oxidized products

The mass profile of Factor L8 is characterized by high peaks of lightly oxidized compounds containing 13 carbon atoms, like $C_{13}H_{18}O_2H^+$ and $C_{13}H_{20}O_3H^+$. Similar to C_6 and C_7 lightly oxidized compounds, this factor shows a morning peak at 9:00 and an evening peak at around midnight (Fig. 6~~7~~b). ~~The time series of this factor correlate well with those of Factor L3 and Factor L7 (r^2 = 0.64 and 0.40; Fig. S11), indicating potentially similar formation mechanisms of these lightly oxygenated compounds. Therefore, the C_{13} oxidized compounds are speculated to be produced through the dimer formation mechanisms of C_6 and C_7 peroxy radicals (Valiev et al., 2019). In addition, $C_{13}H_{20}O_3$ can be direct emissions of methyl jasmonate (Meja), which is a typical green leaf volatile used in plant-plant communications for defensive purposes (Cheong and Choi, 2003). But with similar temporal behaviors to Factor L3 and Factor L7, we conclude that these C_{13} lightly oxidized compounds are formed from atmospheric oxidation processes, not direct plant emissions.~~

Factor L9: A plume event

~~Similar to Factor L2,~~ Factor L9 is characterized with much high~~e~~r intensities on a single night (9 July 2018) during the campaign (Fig. 6~~7~~a). Fingerprint peaks in the mass profile of Factor L9 are numerous unidentified ions. The time series of Factor L9 correlate tightly with ~~those of Factor L2 (r^2 = 0.93) and~~ aromatic compounds C_6H_6 and C_6H_6O (r^2 = 0.75). ~~Therefore, we define Factor L9 as a similar plume event to Factor L2 resolved in the high mass range.~~

Factor L10: sesquiterpene lightly oxidized products

The fingerprint peaks identified in this factor are $C_{15}H_{22}OH^+$, $C_{15}H_{24}OH^+$, $C_{15}H_{22}O_2H^+$, $C_{15}H_{24}O_2H^+$, and $C_{15}H_{24}O_3H^+$, which are typical reaction products from sesquiterpene oxidations (Fu et al., 2009; Yee et al., 2018). The signal intensity of this factor is generally high during nighttime, but shows another morning peak at 8:00. In addition to the production from sesquiterpene oxidation processes, $C_{15}H_{22}O$ and $C_{15}H_{24}O$ can be oxygenated sesquiterpene alcohols and aldehydes directly emitted from vegetation (Kännaste et al., 2014).

Factor L11: monoterpene more oxidized products

The mass spectrum of this factor is mainly characterized by more oxidized compounds from monoterpene oxidations such as $C_{10}H_{16}O_4H^+$, $C_{10}H_{14}O_5H^+$, $C_{10}H_{16}O_5H^+$, and $C_{10}H_{16}O_6H^+$. As shown in Fig. S13~~5~~, the time series of Factor L11 show good correlations with these compounds. Compared with monoterpene lightly oxidized compounds, the diurnal cycle of this factor shows a broad daytime distribution peaking between 14:00 and 20:00, caused by strong and ~~complicated~~ complex photochemical reactions during the day.

Factor L12: sesquiterpenes

The mass spectra of Factor L12 are clearly dominated by a big single peak of $C_{15}H_{24}H^+$, indicating the influence of sesquiterpenes. Sesquiterpene emissions from plants are found to exhibit a strong dependence on temperature (Duhl et al., 2008). Therefore, similar to the diurnal cycle of Factor L4, this factor shows prominently enhanced signals during nighttime. ~~As shown in Fig. S11, Factor L12 and Factor L4 correlate quite well with each other (r^2 = 0.69).~~

Factor L13: monoterpene-derived organic nitrates

The signal intensity of this factor starts to increase in the early morning (around 7:00) and presents a distinct morning peak at 9:00. In addition, a much smaller evening peak is observed at 21:00. The daily variations of this factor are quite similar to those of monoterpene-derived organic nitrates measured in the Landes forest (Li et al., 2020). Consistently, the major peaks in the factor profile are $C_{10}H_{15}NO_4H^+$, $C_{10}H_{15}NO_5H^+$, $C_9H_{13}NO_6H^+$, and $C_{10}H_{15}NO_6H^+$, indicating the dominant contribution of organic nitrates formed from monoterpene oxidation processes. ~~According to the calculation of the reaction rates of monoterpenes with OH radical, O_3, and NO_3 radical, the big morning peak came from O_3- and OH initiated monoterpene oxidations in the presence of NO_x, while for the small evening peak the additional contribution of NO_3 radical induced monoterpene oxidations should be included (Li et al., 2020). $C_{10}H_{17}NO_4$, $C_{10}H_{15}NO_5$, $C_{10}H_{17}NO_5$, and $C_{10}H_{15}NO_6$ have been found to be major gas-phase organic nitrates from α-pinene and/or β-pinene + NO_3 oxidation systems (Wängberg et al., 1997; Perraud et al., 2010; Boyd et al., 2015).~~

Factor L14: C_{12}, C_{14} or C_{16} lightly oxidized compounds

The mass profile of Factor L14 is characterized with distinct peaks of C_{12}, C_{14} or C_{16} lightly oxidized compounds, i.e., $C_{12}H_{26}O_3H^+$, $C_{14}H_{26}O_2H^+$, $C_{16}H_{30}O_2H^+$, and $C_{16}H_{30}O_3H^+$. The time series of Factor L14 correlate very well with those of $C_{12}H_{26}O_3$ (r^2 = 0.83), characterized with enhanced signals during daytime and low intensities at night (Fig. 6~~7~~b). $C_{12}H_{26}O_3$ has been found during the photooxidation of dodecane (Zhang et al., 2014).

Factor L15: unknown source

The mass profile of Factor L15 is predominantly characterized by high cyclic volatile methyl siloxanes (VMSs) peaks and some unidentified peaks (Fig. 5~~6~~). The major cyclic VMSs are protonated D3 siloxane, D4 siloxane, and their H_3O^+ cluster ions, which have been widely used in cosmetics and personal care products (Buser et al., 2013; Yucuis et al., 2013). The diurnal cycle of this factor shows a bit higher intensity during daytime but also big background signals at night. A similar factor has also been identified at the SMEAR II station. More detailed discussions can be found in Sect. 4.3.2.

4.3 Source identification in the southern Finnish boreal forest

The factor profiles, time series, and diurnal cycles of the five-factor solution for the low mass range are presented in Fig. 7~~8~~ and Fig. 8~~9~~. ~~Figure 10 illustrates the correlation of the five factors with various molecules.~~Figure 9~~11~~ and Figure 10~~2~~ present the mass spectra, time series, and daily variations of the four factors identified in the higher mass range at the SMEAR II station. The correlation coefficients among each factor and various fingerprint compounds can be found in Fig. S14~~0~~.

4.3.1 Low mass range (51–200 Th)

~~The factor profiles, time series, and diurnal cycles of the five-factor solution for the low mass range are presented in Fig. 8 and Fig. 9. Figure 10 illustrates the correlation of the five factors with various molecules.~~

Factor S1: $C_4H_8H^+$ ion-related

Similar to the source identification in the Landes forest, a factor related to $C_4H_8H^+$ ion is clearly resolved at the SMEAR II station. The major peaks in this factor are $C_4H_8H^+$, $C_4H_{12}O_2H^+$, and $C_4H_{14}O_3H^+$. ~~As discussed in Section 4.2.1, several~~

~~sources could contribute to the detection of $C_4H_8H^+$ ion. However, at this site, the bivariate polar plot where the concentrations of air pollutants are shown as a function of WS and WD indicates that high signals of $C_4H_8H^+$ generally occur when the wind comes from the north (Fig. S12). Located in the north of the measurement container is a particle measurement cottage with several CPCs inside using butanol. A previous study at this station also found that $C_4H_8H^+$ signals detected by PTR-TOF mainly come from butanol used by aerosol instruments (Schallhart et al., 2018). Therefore, it is expected that Factor S1 at the SMEAR II station is mainly contributed by butanol fragmentation inside the instrument where butanol comes from nearby aerosol instruments.~~

Factor S2: monoterpenes

A factor representing monoterpenes is also identified at the SMEAR II station, with fingerprint peaks of $^{13}CC_5H_8H^+$, $C_7H_{10}H^+$, and $^{13}CC_9H_{16}H^+$. Monoterpenes undergo some degree of fragmentation within PTR instruments, and $C_6H_8H^+$ and $C_7H_{10}H^+$ have been observed to be the major fragments of monoterpenes (Tani et al., 2003; Tani, 2013; Kari et al., 2018). The signal intensity of monoterpenes at the SMEAR II station is much lower than that in the Landes forest.

Factor S3: C_6-C_9 lightly oxygenated compounds

The mass profile of Factor S3 is characterized by lightly oxygenated compounds with carbon atoms varying from six to nine (C_6-C_9) such as $C_6H_{10}OH^+$, $C_6H_{12}OH^+$, $C_7H_{10}OH^+$, $C_8H_{14}OH^+$, and $C_9H_{18}OH^+$. The signal intensity of this factor shows high peaks at night and low appearance during daytime. ~~As discussed in Section 4.2.1, T~~these lightly oxygenated molecules can be directly emitted from anthropogenic and biogenic sources or come from oxidation processes of various VOC precursors (Conley et al., 2005; Pandya et al., 2006; Rantala et al., 2015; Hartikainen et al., 2018). For instance, $C_7H_{10}O$ has been found from direct soil emissions (Abis et al., 2020) or oxidation processes of 1,2,4-trimethyl benzene (Mehra et al., 2020). Therefore, we expect the molecules in this factor to be either directly emitted or as oxidation products of forest emissions.

Factor S4: isoprene and its oxidation products

At the SMEAR II station, a factor largely composed of isoprene and its oxidation products is also resolved. The outstanding peaks in the factor profile are $C_5H_8H^+$, $C_4H_6OH^+$, $C_4H_8O_2H^+$, and $C_5H_8O_2H^+$. The signal intensity of this factor is around ten times lower than that of Factor L5 measured in the Landes forest. Similar to previous isoprene observations at the sampling site (Hakola et al., 2012), this factor shows a broad daytime peak and low signals at night.

Factor S5: monoterpene lightly oxidized products

Similar to Factor L7 identified in the Landes forest, this factor is characterized by major peaks of monoterpene lightly oxidized compounds, as shown in Fig. 7~~8~~. The signal intensity of this factor starts to increase at 20:00 and presents an obvious morning peak at 7:00.

4.3.2 High mass range (201-320 Th)

~~Figure 11 and Figure 12 present the mass spectra, time series, and daily variations of the four factors identified in the higher mass range at the SMEAR II station. The correlation coefficients among each factor and various fingerprint compounds can be found in Fig. 10.~~

Factor S6: sesquiterpene lightly oxidized products

This factor is identified as sesquiterpene lightly oxidized compounds with high peaks of $C_{14}H_{22}OH^+$, $C_{14}H_{24}OH^+$, $C_{15}H_{22}OH^+$, and $C_{15}H_{24}OH^+$, similar to Factor L10 in the Landes forest. The time series of this factor show strong correlations with the lightly oxidized products of sesquiterpenes (Fig. S14~~0~~; $r^2 > 0.88$).

Factor S7: sesquiterpenes

Similar to Factor L12 in the Landes forest, this factor is characterized by the big peak of $C_{15}H_{24}H^+$, demonstrating the dominance of sesquiterpenes in the factor. Figure S14~~0~~ shows that this factor closely correlates with monoterpenes and sesquiterpenes, with r^2 being 0.73 and 0.85, respectively. Compared with the identification of Factor L12, representing sesquiterpenes in the Landes forest, the signal intensity of this factor at the SMEAR II station is approximately three times lower. Including the lower signals of monoterpenes and isoprene, the results indicate weaker biogenic VOC emissions in the Hyytiälä boreal forest than in the Landes forest.

Factor S8: monoterpene more oxidized products including organic nitrates

Factor S8 is mainly composed of more oxidized compounds, particularly from monoterpene oxidation processes, including monoterpene-derived organic nitrates. The major peaks are shown in Fig. 9~~11~~. Mixed with monoterpene-derived organic nitrates, this factor of more oxidized compounds displays a small morning peak at 8:00 and generally high signals during daytime (Fig. 10~~2~~). ~~Utilizing non-negative matrix factorization analysis on iodide-adduct CIMS data at the SMEAR II station, Lee et al. (2018) found that the gas-phase organic species subgroup of $C_{6-10}H_yO_{\geq 7}$ showed distinct daytime diel trends. Yan et al. (2016) conducted source apportionment of HOMs at the SMEAR II station and separated various HOM formation pathways, such as monoterpene ozonolysis and monoterpene oxidation initiated by NO_3 radical. Unfortunately, due to the similar time series of monoterpene more oxidized compounds and monoterpene derived organic nitrates, these different formation mechanisms cannot be separated in this study. For example, the time series of $C_{10}H_{15}NO_5H^+$ correlate well with those of $C_{10}H_{16}O_4H^+$ and $C_{10}H_{16}O_5H^+$ ($r^2 \geq 0.61$).~~

Factor S9: unknown source

The marker peaks of Factor S9 are mainly high cyclic volatile methyl siloxanes (VMSs) and unidentified compounds (Fig. 9~~11~~), i.e., protonated D3 siloxane, D4 siloxane, and their H_3O^+ cluster ions. In addition to cosmetics and personal care products, siloxanes can also be emitted by silicone oils (Schweigkofler et al., 1999), which have been widely used in instrument pumps (Gonvers et al., 1985). In this study, the temporal behaviors of Factor S9 are contributed by high background signals and present a very regular diurnal cycle with higher signal intensities during daytime and lower ones at night, which basically follow the variations in ambient temperature. Therefore, we speculate that Factor S9 is mainly caused by emissions from silicone oil pumps used by several instruments in the container, and these emissions are influenced by daily temperature changes.

4.4 Comparison among different factors

The monoterpene factor and sesquiterpene factor correlate very well with each other at both sites (Fig. 11; r^2 = 0.69 in the Landes forest and r^2 = 0.59 at the SMEAR II station). The emissions of monoterpenes and sesquiterpenes are both strongly influenced by temperature. Their signals peak at night with the effect of the shallow boundary layer. In the daytime, the low signals of the monoterpene and sesquiterpene factors are likely a combination of enhanced atmospheric mixing after sunrise and the rapid photochemical consumption of monoterpenes and sesquiterpenes. The signal of monoterpene factor is around 15 times higher than that of sesquiterpene factor at the SMEAR II station while it is around 60 times in the Landes forest. Previous studies found that sesquiterpene emissions from pines, spruces, and birches under normal conditions were 5-15% of total monoterpene emissions by mass (Rinne et al., 2009 and references therein), in line with our observations.

In the Landes forest, a factor of C_6 and C_7 lightly oxidized products (Factor L3) was resolved in the low mass range and a factor representative of C_{13} lightly oxidized products (Factor L7) was identified in the high mass range. Interestingly, these two factors show a close correlation with each other (r^2 = 0.64). The C_6 oxygenated compounds have been observed during the oxidation processes of benzene and C_7 oxygenated compounds from toluene oxidations (Sato et al., 2012; Zaytsev et al., 2019). These compounds can also be directly emitted from biogenic or anthropogenic sources (Conley et al., 2005; Pandya et al., 2006; Rantala et al., 2015). The temporal behaviour of Factor L7 is similar to that of Factor L3, indicating potentially similar formation pathways of these lightly oxygenated compounds. Therefore, the C_{13} oxidized compounds are speculated to be produced through the dimer formation mechanisms of C_6 and C_7 species (Valiev et al., 2019). In addition, $C_{13}H_{20}O_3$ can be direct emissions of methyl jasmonate (Meja), which is a typical green leaf volatile used in plant-plant communications for defensive purposes (Cheong and Choi, 2003). But considering the close correlation between Factor L3 and Factor L7, we conclude that these C13 lightly oxidized compounds are formed from atmospheric oxidation processes, not direct plant emissions.

Monoterpene lightly oxidized products and sesquiterpene lightly oxidized products were resolved as individual factors at both sites (Factor L7 vs. Factor L10 in the Landes forest and Factor S5 vs. Factor S6 at the SMEAR II station). While the diurnal variations of monoterpene lightly oxidized products are similar to those of sesquiterpene lightly oxidized products, their time series do not follow very well with each other, suggesting the probably different formation pathways or different factors influencing the atmospheric processes of monoterpenes and sesquiterpenes. More discussions can be found in Sect. 4.6.

In this study, the source apportionment analysis was performed separately on two subranges of the mass spectra. It can happen that the same factor is identified in both subranges. For example, both Factor L2 and Factor L9 are defined as the plume event during the measurements. The time series of Factor L2 and Factor L9 show a high correlation coefficient of 0.93 and correlate tightly with aromatic compounds, indicating the major influence of anthropogenic sources. As mentioned above, the air masses in the Landes forest were relatively stable during our observations with wind speed below canopy < 1 m s^{-1}.

Therefore, the influence of long-range regional transport on the atmosphere in the forest is expected to be minor. We speculate that the plume event is a result of local anthropogenic disturbances favored by the lower boundary layer height at night.

4.54 Comparison between the two forests

To give an overview of the source distributions in the two forest ecosystems, we calculated the mass fraction of each factor based on their average signal intensities. We acknowledge that it is not a perfect method to quantify the contributions of various sources and formation processes. The sensitivities of different VOCs measured by the PTR instruments may vary by a factor of 2-3 (Sekimoto et al., 2017; Yuan et al., 2017). The uncertainties can come from the challenge to convert the signal intensity to atmospheric concentrations because of problematic calibrations, especially given that many unknown molecules exist in the mass spectra. The major bins at *m/z* 81 Th and 137 Th, which were initially excluded to perform PMF analysis, were counted into their corresponding factors. For example, the signals of the discarded bins at *m/z* 81 Th and 137 Th were estimated by multiplying their isotope signals by the corresponding scale number and added to the factor representing monoterpenes. The average mass fractions of various PMF factors in total measured organic vapors are shown in Fig. 123.

While the atmospheric environment and ecosystem processes differ markedly in the Landes forest and the southern Finnish boreal forest, the results of this study reveal similar biogenic sources and oxidation processes in these forest environments. For instance, the biogenic VOCs at the two sites are both dominated by monoterpenes, with the average fractions of 29% in the Landes forest and at the SMEAR II station. These two forests are both characterized by pine trees, with dominant emissions of α-pinene and β-pinene (Riba et al., 1987; Simon et al., 1994; Hellén et al., 2018). According to the PMF results, isoprene and its major oxidation products in these environments (mainly C_4H_6O) contribute 14% and 21% in the two ecosystems, respectively. Factors indicative of sesquiterpenes are identified in the high mass range at both sites. The average contribution of sesquiterpenes (0.5% in the Landes forest and 1.7% at the SMEAR II station) is much smaller than that of monoterpenes and isoprene. Factors of the lightly oxidized products, more oxidized products, and organic nitrates of monoterpenes/sesquiterpenes in total contribute 8% and 12% of the measured organic vapors in the Landes forest and at the SMEAR II station, respectively.

The factor related to $C_4H_8H^+$ ion was resolved at both sites and contributes 10% in the Landes forest and 16% at the SMEAR II station. According to the discussions by Li et al. (2020), the observation of $C_4H_8H^+$ in the Landes forest can be attributed to several sources. For instance, the protonated butene may contribute to the $C_4H_8H^+$ signal, which is emitted by biogenic or anthropogenic sources (Hellén et al., 2006; Zhu et al., 2017). Another possible explanation is that the $C_4H_8H^+$ ion is produced during the fragmentation of many VOCs in the PTR instruments (Pagonis et al., 2019). The green leaf volatiles (GLV) have been found to fragment at *m/z* 57 Th inside the PTR instruments, which are a group of six-carbon aldehyde, alcohols and their esters released by plants. Furthermore, butanol can easily lose an OH during the PTR source ionization and produce prominent $C_4H_8H^+$ peaks (Spanel and Smith, 1997). Therefore, the condensation particle counters (CPCs) using butanol for aerosol measurements at the site could also be an important source of $C_4H_8H^+$ ions, although the exhaust air from these instruments has been filtered using charcoal denuder. At the SMEAR II station, the bivariate polar plot where the

concentrations of air pollutants are shown as a function of WS and WD indicates that high signals of $C_4H_8H^+$ generally occur when the wind comes from the north (Fig. S15). Located in the north of the measurement container is a particle measurement cottage with several CPCs inside using butanol. A previous study at this station also found that $C_4H_8H^+$ signals detected by PTR-TOF mainly come from butanol used by aerosol instruments (Schallhart et al., 2018). Therefore, it is expected that Factor S1 at the SMEAR II station is mainly contributed by butanol fragmentation inside the instrument where butanol comes from nearby aerosol instruments.

Figure 13 presents the comparison of the mass spectra of the common sources identified at both sites, with the *x* and *y* axis showing the mass fraction of different bins in the factor profile. The scattering in the plots is mainly caused by mass bins with much lower mass fractions. However, the dominant bins with high mass contributions in the factor profiles generally correlate well and are located close to the 1:1 line. It shows that the mass spectra of the common sources match well in these two forests and the sources and processes are indeed similar despite the quite different regions the forests are in. ~~Figure 14 presents the comparison between the factor profiles of common sources identified at both sites, where the fractions of different bins in the mass spectra of the factors are plotted. As shown in Fig. 14c, d, and f, the mass spectra of the factors indicative of monoterpenes, isoprene and its oxidation products, and sesquiterpenes, match quite well between the two forests, particularly for the dominant mass bins in the factor profile.~~

4.6 Insights into terpene oxidation processes

Terpenes undergo varying degrees of oxidations in the atmosphere and produce a large variety of organic compounds with different volatilities (Donahue et al., 2012; Ehn et al., 2014). With the sub-range PMF analysis performed in this study, terpene reaction products with varying oxidation degrees are successfully separated. The sources of monoterpene lightly oxidized products, sesquiterpene lightly oxidized products, monoterpene more oxidized compounds, and monoterpene-derived organic nitrates are identified in both forests with distinct characteristics. These factors account for 8-12% of the measured organic vapors in the two forests. It provides a great opportunity to gain insights into terpene oxidation processes. Because some environmental parameters, for example, measurements of UVB to estimate OH concentration, are not available in the Landes forest, the results from SMEAR II station are presented as follows.

4.6.1 Monoterpene oxidations

The oxidation processes of monoterpenes at the SMEAR II station have been investigated by several previous studies, mostly based on the highly oxidized compounds. Utilizing non-negative matrix factorization analysis on iodide-adduct CIMS data at the SMEAR II station, Lee et al. (2018) found that the gas-phase organic species subgroup of $C_{6\text{-}10}H_yO_{\geq 7}$ showed distinct daytime diel trends. Yan et al. (2016) conducted source apportionment of HOMs at the SMEAR II station and separated various HOM formation pathways, such as monoterpene ozonolysis and monoterpene oxidation initiated by NO_3 radical. In this study, three types of monoterpene reaction products were detected: monoterpene lightly oxidized compounds, monoterpene more oxidized compounds, and monoterpene-derived organic nitrates. The latter two were not clearly separated into different factors

at the SMEAR II station due to the similarities in their overall time trends. ~~Unfortunately, due to the similar time series of monoterpene more oxidized compounds and monoterpene derived organic nitrates, these different formation mechanisms cannot be separated in this study.~~ For example, the time series of $C_{10}H_{15}NO_5H^+$ correlate well with those of $C_{10}H_{16}O_4H^+$ and $C_{10}H_{16}O_5H^+$ ($r^2 > 0.61$).

Consistent with previous observations, monoterpene more oxidized products (i.e., $C_{10}H_{16}O_4$ and $C_{10}H_{14}O_5$) have a broad high distribution throughout the day due to the active photochemical processes during daytime. Monoterpene-derived organic nitrates (i.e., $C_{10}H_{17}NO_4$, $C_{10}H_{15}NO_5$, and $C_9H_{13}NO_6$) are mainly characterized by a distinct morning peak at around 8:00, approximately 2 h after the NO peak. But their intensities are also elevated at night. PMF analysis of NO_3^- CIMS dataset observed similar diurnal variations of terpene organic nitrates factor at a forest site in the southeastern US (Massoli et al., 2018). Compared with β-pinene and most other monoterpenes, the overall organic nitrate yield from α-pinene + NO_3 is rather low (Fry et al., 2014; Kurtén et al., 2017). Laboratory studies found that using iodide-adduct FIGAERO-HR-ToF CIMS, $C_{10}H_{15}NO_6$ is the most abundant organic nitrate in both gas- and particle-phase measurements of α-pinene + NO_3 reactions (Nah et al., 2016). Boyd et al. (2015) mainly detected $C_{10}H_{17}NO_4$, $C_{10}H_{15}NO_5$, $C_{10}H_{17}NO_5$, and $C_{10}H_{15}NO_6$ with iodide-adduct CIMS from the α-pinene + NO_3 system. Using $C_{10}H_{17}NO_5$ and $C_{10}H_{15}NO_6$ as the examples, we checked their correlations with the products of [OH] × [monoterpenes], [O_3] × [monoterpenes], and [NO_3] × [monoterpenes] in different periods of the day (Fig. 14; Fig. S16). Comparatively, $C_{10}H_{17}NO_5$ and $C_{10}H_{15}NO_6$ correlate better with the products of [OH] × [monoterpenes] and [O_3] × [monoterpenes] during daytime (9:00~18:00). However, for the product of [NO_3] × [monoterpenes], its correlation coefficients with $C_{10}H_{17}NO_5$ and $C_{10}H_{15}NO_6$ are a bit higher at night (20:00 to 4:00 of the next day). These results indicate that monoterpene-derived organic nitrates can be mainly formed by the NO_3-initiated oxidations at night, but in daytime by the OH and O_3-initiated oxidations followed by NO termination of the RO_2.

4.6.2 Sesquiterpene oxidations

The lightly oxygenated compounds from sesquiterpene reactions present a big morning peak and elevated signal intensities at night, similar to the diurnal variations of monoterpene lightly oxidized products. Hellén et al. (2018) showed that at the SMEAR II station, O_3 oxidation dominated the first step of sesquiterpene reactions for the whole year. It has also been observed in central Amazonia that sesquiterpenes contributed the highest to total O_3 reactivity although sesquiterpene concentrations were much lower than those of monoterpenes and isoprene (Yee et al., 2018). At the SMEAR II station, emissions of sesquiterpenes are dominated by β-caryophyllene (Hellén et al., 2018). Photooxidation of β-caryophyllene in the chamber experiments resulted in high aerosol yield and is expected to strongly influence SOA formation (Jaoui et al., 2013). Using the mass spectrometric techniques, Jokinen et al. (2016) observed the production of highly oxidized organic compounds from β-caryophyllene ozonolysis, i.e., monomers $C_{15}H_{24}O_{7,9,11}$ and $C_{15}H_{22}O_{9,11}$, and dimers $C_{29}H_{46}O_{12,14,16}$ and $C_{30}H_{46}O_{12,14,16}$. However, due to the instrumental limitation, only the lightly oxidized products from sesquiterpene reactions were identified in this study.

Interestingly, a strong RH-dependence was observed for the correlations between sesquiterpene lightly oxidized compounds and the product of [OH] × [sesquiterpenes] or [O_3] × [sesquiterpenes]. These products represent the oxidation rates of sesquiterpenes with OH radical and O_3. As shown in Fig. 15, the corresponding correlation coefficients vary significantly with RH. In addition, the signal intensities of sesquiterpene lightly oxidized products also show high dependence on RH. At lower RH (RH<40%), the signal intensities of sesquiterpene lightly oxidized products are relatively low and correlate closely with the product of [OH] × [sesquiterpenes] and [O_3] × [sesquiterpenes]. The high signal intensities of sesquiterpene lightly oxidized products occur when RH>70% but the correlation between sesquiterpene lightly oxidized compounds and the product of [OH] × [sesquiterpenes] or [O_3] × [sesquiterpenes] is more scattered. Such high RH-dependence was not observed for monoterpene lightly oxidized compounds (Fig. S17). These findings have not been observed by previous studies and the reasons behind remain unclear. High-RH conditions typically occur during nights with temperature inversion (Zha et al., 2018), while RH below 40% generally only occurs at the station during sunny days. Future studies are needed to dig deep into the atmospheric processes of sesquiterpenes and monoterpenes.

~~For the lightly oxygenated compounds from monoterpene or sesquiterpene reactions, they present similar temporal behaviors at the two sites, with a small morning peak and increased signal intensities at night. The mass spectra of these factors show high similarities in the two forests (Fig. 14e and g). Monoterpene-derived organic nitrates are mainly characterized by a distinct morning peak at 9:00. With the active photochemical processes during daytime, more oxidized reaction products have a broad high distribution throughout the day. At the SMEAR II station, more oxidized compounds are mixed together with monoterpene organic nitrates and resolved into a single factor. Therefore, the mass spectra comparison between the two forests are more scattered for the factors of monoterpene-derived organic nitrates and more-oxidized compounds. Overall, these common sources and their similar characteristics indicate the similar atmospheric chemical processes in the two forest ecosystems.~~

5 Concluding remarks

In this study, we conducted Vocus PTR-TOF measurements in two forest environments and performed binPMF analysis on these complex mass spectra. In addition to VOC species, Vocus PTR-TOF is able to measure large amounts of oxygenated VOCs with enhanced detection efficiency. According to the results in this work, factor analysis on Vocus PTR-TOF mass spectra separated VOC precursors and their reaction products with varying oxidation degrees into different factors. These factors showed distinct characteristics in the atmosphere. Comparatively, the conventional PTR instruments or gas chromatograph-mass spectrometry (GC-MS) largely detect VOC precursors of low-mass molecules (Dewulf et al., 2002; de Gouw et al., 2007). Previous source apportionment studies on these datasets mainly identified primary biogenic and anthropogenic emission sources (Vlasenko et al., 2009; Patokoski et al., 2014; Baudic et al., 2016; Debevec et al., 2017; Sarkar et al., 2017; Wang et al., 2020). Recently, factorization methods have been applied on NO_3^- CIMS dataset to identify various atmospheric formation pathways of HOMs (Yan et al., 2016; Massoli et al., 2018; Zhang et al., 2019b). Here, for the first time,

source apportionment of Vocus PTR-TOF data identified various primary emission sources and secondary formation pathways of atmospheric organic vapors, highlighting the novelty of Vocus PTR-TOF in measuring both VOCs and oxygenated VOCs ~~and providing new perspectives to understand gas-phase chemical processes~~. The relative abundances of organic precursors, the lightly oxidized products, and the more oxidized products can be utilized by modellers to evaluate simulation output, improve model performance, and provide new perspectives to understand gas-phase physicochemical processes.

Compared with VOC species, VOC reaction products are generally present in much smaller amounts in the atmosphere. Therefore, utilizing a sub-range PMF analysis, or other similarly weighting method, is particularly important for Vocus PTR-TOF observations, where several orders of magnitude differences are expected between VOC precursors and their oxidation products. Compared with the low mass range, the average contributions of the high mass range in total signals are significantly smaller, 2% and 9%, in the Landes forest and at the SMEAR II station, respectively. However, the identified ~~sources~~ factors in the high mass range, such as sesquiterpenes, sesquiterpene lightly oxidized products, monoterpene-derived organic nitrates, and more oxidized compounds, can provide crucial insights into atmospheric physicochemical processes. For example, we found that the correlations between sesquiterpene lightly oxidized compounds and the products of [OH] × [sesquiterpenes] or [O_3] × [sesquiterpenes] show strong dependences on RH. High signal intensities of sesquiterpene lightly oxidized compounds only occur at high-RH conditions. Such high RH-dependence was not observed for monoterpene lightly oxidized compounds.

To summarize, this study successfully performed binPMF analysis on sub-ranges of mass spectrometry dataset acquired with a Vocus PTR-TOF in two European forest ecosystems, the Landes forest and a southern Finnish boreal forest. Both primary emission sources and secondary oxidation processes ~~Similar sources and formation pathways~~ of organic vapors were identified in the two environments, particularly for terpenes and their reaction products with varying oxidation degrees (including organic nitrates). Factors of the lightly oxidized products, more oxidized products, and organic nitrates of monoterpenes/sesquiterpenes accounted for 8-12% of the measured gas-phase organic vapors in the two forests. Further interpretations show a strong RH-dependence for the behaviour of sesquiterpene lightly oxidized products but not for that of monoterpene lightly oxidized products, for which the reasons behind need more investigations in the future.

~~With the broad coverage of various organic vapors measured by Vocus PTR-TOF, this study provides a more comprehensive picture of gas-phase source identifications in the European forest ecosystems, covering both primary emissions and secondary oxidation processes.~~

Data Availability. The time series of the measured trace gases, meteorological parameters, and the concentrations of isoprene and monoterpenes in the Landes forest and at the SMEAR II station are available from https://doi.org/10.5281/zenodo.3946644 (Li, 2020).

Author contributions. HL and ME conceived the study. HL, MR, ST, LH, PMF, EV, and EP conducted the field measurements. HL carried out the data analysis. MC, YZ, ME, and FB participated in the discussions on data analysis. HL wrote the paper with inputs from all coauthors.

Competing interests. Manjula R. Canagaratna and Douglas Worsnop both work for Aerodyne Research Inc.

Acknowledgements. This work was supported by the H2020 European Research Council (grant nos. ATM-GP (742206), COALA (638703), and CHAPAs (850614)) and the Academy of Finland (grant nos. 317380 and 320094). We thank the SMEAR II station staff for their help during field measurements in Hyytiälä. The authors also would like to thank the PRIME-QUAL program for financial support (ADEME, convention#1662C0024) and the French National Research Agency (ANR) in the frame of the "Investments for the Future" program, within the Cluster of Excellence COTE (ANR-10-LABX-45) of the University of Bordeaux for financial support. Harald Stark and Donna T. Sueper from Aerodyne Research Inc. are acknowledged for helpful discussions.

References

Abis, L., Loubet, B., Ciuraru, R., Lafouge, F., Houot, S., Nowak, V., Tripied, J., Dequiedt, S., Maron, P. A., and Sadet-Bourgeteau, S.: Reduced microbial diversity induces larger volatile organic compound emissions from soils, Scientific Reports, 10, 6104, 10.1038/s41598-020-63091-8, 2020.

Ahlberg, E., Falk, J., Eriksson, A., Holst, T., Brune, W. H., Kristensson, A., Roldin, P., and Svenningsson, B.: Secondary organic aerosol from VOC mixtures in an oxidation flow reactor, Atmos Environ, 161, 210-220, https://doi.org/10.1016/j.atmosenv.2017.05.005, 2017.

Allan, B. J., McFiggans, G., Plane, J. M. C., Coe, H., and McFadyen, G. G.: The nitrate radical in the remote marine boundary layer, J. Geophys. Res.-Atmos., 105, 24191–24204, https://doi.org/10.1029/2000JD900314, 2000.

Aschmann, S. M., Arey, J., and Atkinson, R.: OH radical formation from the gas-phase reactions of O3 with a series of terpenes, Atmos Environ, 36, 4347-4355, https://doi.org/10.1016/S1352-2310(02)00355-2, 2002.

Baudic, A., Gros, V., Sauvage, S., Locoge, N., Sanchez, O., Sarda-Estève, R., Kalogridis, C., Petit, J.-E., Bonnaire, N., Baisnée, D., Favez, O., Albinet, A., Sciare, J., and Bonsang, B.: Seasonal variability and source apportionment of volatile organic

compounds (VOCs) in the Paris megacity (France), Atmos. Chem. Phys., 16, 11961–11989, https://doi.org/10.5194/acp-16-11961-2016, 2016.

Bianchi, F., Tröstl, J., Junninen, H., Frege, C., Henne, S., Hoyle, C. R., Molteni, U., Herrmann, E., Adamov, A., Bukowiecki, N., Chen, X., Duplissy, J., Gysel, M., Hutterli, M., Kangasluoma, J., Kontkanen, J., Kürten, A., Manninen, H. E., Münch, S., Peräkylä, O., Petäjä, T., Rondo, L., Williamson, C., Weingartner, E., Curtius, J., Worsnop, D. R., Kulmala, M., Dommen, J., and Baltensperger, U.: New particle formation in the free troposphere: A question of chemistry and timing, Science, 352, 1109-1112, 10.1126/science.aad5456, 2016.

Bourtsoukidis, E., Williams, J., Kesselmeier, J., Jacobi, S., and Bonn, B.: From emissions to ambient mixing ratios: online seasonal field measurements of volatile organic compounds over a Norway spruce-dominated forest in central Germany, Atmos. Chem. Phys., 14, 6495–6510, https://doi.org/10.5194/acp-14-6495-2014, 2014.

Boyd, C. M., Sanchez, J., Xu, L., Eugene, A. J., Nah, T., Tuet, W. Y., Guzman, M. I., and Ng, N. L.: Secondary organic aerosol formation from the β-pinene+NO3 system: effect of humidity and peroxy radical fate, Atmos. Chem. Phys., 15, 7497–7522, https://doi.org/10.5194/acp-15-7497-2015, 2015.

Bsaibes, S., Al Ajami, M., Mermet, K., Truong, F., Batut, S., Hecquet, C., Dusanter, S., Léornadis, T., Sauvage, S., Kammer, J., Flaud, P.-M., Perraudin, E., Villenave, E., Locoge, N., Gros, V., and Schoemaecker, C.: Variability of hydroxyl radical (OH) reactivity in the Landes maritime pine forest: results from the LANDEX campaign 2017, Atmos. Chem. Phys., 20, 1277–1300, https://doi.org/10.5194/acp-20-1277-2020, 2020.

Buser, A. M., Kierkegaard, A., Bogdal, C., MacLeod, M., Scheringer, M., and Hungerbühler, K.: Concentrations in Ambient Air and Emissions of Cyclic Volatile Methylsiloxanes in Zurich, Switzerland, Environmental Science & Technology, 47, 7045-7051, 10.1021/es3046586, 2013.

Calogirou, A., Kotzias, D., and Kettrup, A.: Product analysis of the gas-phase reaction of β-caryophyllene with ozone, Atmos Environ, 31, 283-285, https://doi.org/10.1016/1352-2310(96)00190-2, 1997.

Calogirou, A., Larsen, B. R., and Kotzias, D.: Gas-phase terpene oxidation products: a review, Atmos Environ, 33, 1423-1439, https://doi.org/10.1016/S1352-2310(98)00277-5, 1999.

Cheong, J.-J. and Choi, Y. D.: Methyl jasmonate as a vital substance in plants, Trends Genet., 19, 409–413, doi:10.1016/S0168-9525(03)00138-0, 2003.

Conley, F. L., Thomas, R. L., and Wilson, B. L.: Measurement of Volatile Organic Compounds in the Urban Atmosphere of Harris County, Texas, Journal of Environmental Science and Health, Part A, 40, 1689-1699, 10.1081/ESE-200067996, 2005.

de Gouw, J., and Warneke, C.: Measurements of volatile organic compounds in the earth's atmosphere using proton-transfer-reaction mass spectrometry, Mass Spectrometry Reviews, 26, 223-257, 10.1002/mas.20119, 2007.

Debevec, C., Sauvage, S., Gros, V., Sciare, J., Pikridas, M., Stavroulas, I., Salameh, T., Leonardis, T., Gaudion, V., Depelchin, L., Fronval, I., Sarda-Esteve, R., Baisnée, D., Bonsang, B., Savvides, C., Vrekoussis, M., and Locoge, N.: Origin and

variability in volatile organic compounds observed at an Eastern Mediterranean background site (Cyprus), Atmos. Chem. Phys., 17, 11355–11388, https://doi.org/10.5194/acp-17-11355-2017, 2017.

Dewulf, J., Van Langenhove, H., and Wittmann, G.: Analysis of volatile organic compounds using gas chromatography, TrAC Trends in Analytical Chemistry, 21, 637-646, https://doi.org/10.1016/S0165-9936(02)00804-X, 2002.

Donahue, N. M., Kroll, J. H., Pandis, S. N., and Robinson, A. L.: A two-dimensional volatility basis set – Part 2: Diagnostics of organic-aerosol evolution, Atmos. Chem. Phys., 12, 615–634, https://doi.org/10.5194/acp-12-615-2012, 2012.

Duhl, T. R., Helmig, D., and Guenther, A.: Sesquiterpene emissions from vegetation: a review, Biogeosciences, 5, 761–777, https://doi.org/10.5194/bg-5-761-2008, 2008.

Ehn, M., Thornton, J. A., Kleist, E., Sipilä, M., Junninen, H., Pullinen, I., Springer, M., Rubach, F., Tillmann, R., Lee, B., Lopez-Hilfiker, F., Andres, S., Acir, I.-H., Rissanen, M., Jokinen, T., Schobesberger, S., Kangasluoma, J., Kontkanen, J., Nieminen, T., Kurtén, T., Nielsen, L. B., Jørgensen, S., Kjaergaard, H. G., Canagaratna, M., Maso, M. D., Berndt, T., Petäjä, T., Wahner, A., Kerminen, V.-M., Kulmala, M., Worsnop, D. R., Wildt, J., and Mentel, T. F.: A large source of low-volatility secondary organic aerosol, Nature, 506, 476-479, 10.1038/nature13032, 2014.

Friedrich, R., and Obermeier, A.: Chapter 1 - Anthropogenic Emissions of Volatile Organic Compounds, in: Reactive Hydrocarbons in the Atmosphere, edited by: Hewitt, C. N., Academic Press, San Diego, 1-39, 1999.

Fry, J. L., Draper, D. C., Barsanti, K. C., Smith, J. N., Ortega, J., Winkler, P. M., Lawler, M. J., Brown, S. S., Edwards, P. M., Cohen, R. C., and Lee, L.: Secondary Organic Aerosol Formation and Organic Nitrate Yield from NO3 Oxidation of Biogenic Hydrocarbons, Environmental Science & Technology, 48, 11944-11953, 10.1021/es502204x, 2014.

Fu, P., Kawamura, K., Chen, J., and Barrie, L. A.: Isoprene, Monoterpene, and Sesquiterpene Oxidation Products in the High Arctic Aerosols during Late Winter to Early Summer, Environmental Science & Technology, 43, 4022-4028, 10.1021/es803669a, 2009.

Gonvers, M.: A New Silicone Oil Pump, American Journal of Ophthalmology, 99, 210, https://doi.org/10.1016/0002-9394(85)90236-3, 1985.

Guenther, A., Hewitt, C. N., Erickson, D., Fall, R., Geron, C., Graedel, T., Harley, P., Klinger, L., Lerdau, M., McKay, W. A., Pierce, T., Scholes, B., Steinbrecher, R., Tallamraju, R., Taylor, J., and Zimmerman, P.: A global model of natural volatile organic compound emissions, J. Geophys. Res.-Atmos., 100, 8873–8892, https://doi.org/10.1029/94JD02950, 1995.

Hakola, H., Tarvainen, V., Bäck, J., Ranta, H., Bonn, B., Rinne, J., and Kulmala, M.: Seasonal variation of mono- and sesquiterpene emission rates of Scots pine, Biogeosciences, 3, 93–101, https://doi.org/10.5194/bg-3-93-2006, 2006.

Hakola, H., Hellén, H., Hemmilä, M., Rinne, J., and Kulmala, M.: In situ measurements of volatile organic compounds in a boreal forest, Atmos. Chem. Phys., 12, 11665–11678, https://doi.org/10.5194/acp-12-11665-2012, 2012.

Hallquist, M., Wenger, J. C., Baltensperger, U., Rudich, Y., Simpson, D., Claeys, M., Dommen, J., Donahue, N. M., George, C., Goldstein, A. H., Hamilton, J. F., Herrmann, H., Hoffmann, T., Iinuma, Y., Jang, M., Jenkin, M. E., Jimenez, J. L., Kiendler-Scharr, A., Maenhaut, W., McFiggans, G., Mentel, Th. F., Monod, A., Prévôt, A. S. H., Seinfeld, J. H., Surratt,

J. D., Szmigielski, R., and Wildt, J.: The formation, properties and impact of secondary organic aerosol: current and emerging issues, Atmos. Chem. Phys., 9, 5155–5236, https://doi.org/10.5194/acp-9-5155-2009, 2009.

Hari, P. and Kulmala, M.: Station for measuring ecosystem-atmosphere relations, Boreal Environ. Res., 10, 315–322, 2005.

Hartikainen, A., Yli-Pirilä, P., Tiitta, P., Leskinen, A., Kortelainen, M., Orasche, J., Schnelle-Kreis, J., Lehtinen, K. E. J., Zimmermann, R., Jokiniemi, J., and Sippula, O.: Volatile Organic Compounds from Logwood Combustion: Emissions and Transformation under Dark and Photochemical Aging Conditions in a Smog Chamber, Environmental Science & Technology, 52, 4979-4988, 10.1021/acs.est.7b06269, 2018.

Hellén, H., Hakola, H., Pystynen, K.-H., Rinne, J., and Haapanala, S.: C2-C10 hydrocarbon emissions from a boreal wetland and forest floor, Biogeosciences, 3, 167–174, https://doi.org/10.5194/bg-3-167-2006, 2006.

Hellén, H., Praplan, A. P., Tykkä, T., Ylivinkka, I., Vakkari, V., Bäck, J., Petäjä, T., Kulmala, M., and Hakola, H.: Long-term measurements of volatile organic compounds highlight the importance of sesquiterpenes for the atmospheric chemistry of a boreal forest, Atmos. Chem. Phys., 18, 13839-13863, 10.5194/acp-18-13839-2018, 2018.

Jaoui, M., Kleindienst, T. E., Docherty, K. S., Lewandowski, M., and Offenberg, J. H.: Secondary organic aerosol formation from the oxidation of a series of sesquiterpenes: α-cedrene, β-caryophyllene, α-humulene and α-farnesene with O3, OH and NO3 radicals, Environmental Chemistry, 10, 178-193, 2013.

Jokinen, T., Kausiala, O., Garmash, O., Peräkylä, O., Junninen, H., Schobesberger, S., Yan, C., Sipilä, M., and Rissanen, M. P.: Production of highly oxidized organic compounds from ozonolysis of β-caryophyllene: laboratory and field measurements, Boreal Environ. Res., 21, 262–273, 2016.

Kallio, M., Jussila, M., Rissanen, T., Anttila, P., Hartonen, K., Reissell, A., Vreuls, R., Adahchour, M., and Hyötyläinen, T.: Comprehensive two-dimensional gas chromatography coupled to time-of-flight mass spectrometry in the identification of organic compounds in atmospheric aerosols from coniferous forest, Journal of Chromatography A, 1125, 234-243, https://doi.org/10.1016/j.chroma.2006.05.050, 2006.

Kännaste, A., Copolovici, L., and Niinemets, Ü.: Gas Chromatography–Mass Spectrometry Method for Determination of Biogenic Volatile Organic Compounds Emitted by Plants, in: Plant Isoprenoids: Methods and Protocols, edited by: Rodríguez-Concepción, M., Springer New York, New York, NY, 161-169, 2014.

Kammer, J., Perraudin, E., Flaud, P. M., Lamaud, E., Bonnefond, J. M., and Villenave, E.: Observation of nighttime new particle formation over the French Landes forest, Sci. Total Environ., 621, 1084–1092, https://doi.org/10.1016/j.scitotenv.2017.10.118, 2018.

Kammer, J., Flaud, P. M., Chazeaubeny, A., Ciuraru, R., Le Menach, K., Geneste, E., Budzinski, H., Bonnefond, J. M., Lamaud, E., Perraudin, E., and Villenave, E.: Biogenic volatile organic compounds (BVOCs) reactivity related to new particle formation (NPF) over the Landes forest, Atmospheric Research, 237, 104869, https://doi.org/10.1016/j.atmosres.2020.104869, 2020.

Kari, E., Miettinen, P., Yli-Pirilä, P., Virtanen, A., and Faiola, C. L.: PTR-ToF-MS product ion distributions and humidity-dependence of biogenic volatile organic compounds, International Journal of Mass Spectrometry, 430, 87-97, https://doi.org/10.1016/j.ijms.2018.05.003, 2018.

Kaser, L., Karl, T., Guenther, A., Graus, M., Schnitzhofer, R., Turnipseed, A., Fischer, L., Harley, P., Madronich, M., Gochis, D., Keutsch, F. N., and Hansel, A.: Undisturbed and disturbed above canopy ponderosa pine emissions: PTR-TOF-MS measurements and MEGAN 2.1 model results, Atmos. Chem. Phys., 13, 11935–11947, https://doi.org/10.5194/acp-13-11935-2013, 2013.

Kesselmeier, J., and Staudt, M.: Biogenic Volatile Organic Compounds (VOC): An Overview on Emission, Physiology and Ecology, J Atmos Chem, 33, 23-88, 10.1023/A:1006127516791, 1999.

Khan, M. A. H., Jenkin, M. E., Foulds, A., Derwent, R. G., Percival, C. J., and Shallcross, D. E.: A modeling study of secondary organic aerosol formation from sesquiterpenes using the STOCHEM global chemistry and transport model, Journal of Geophysical Research: Atmospheres, 122, 4426-4439, 10.1002/2016JD026415, 2017.

Kim, S., Guenther, A., Karl, T., and Greenberg, J.: Contributions of primary and secondary biogenic VOC tototal OH reactivity during the CABINEX (Community Atmosphere-Biosphere INteractions Experiments)-09 field campaign, Atmos. Chem. Phys., 11, 8613–8623, https://doi.org/10.5194/acp-11-8613-2011, 2011.

Kirkby, J., Duplissy, J., Sengupta, K., Frege, C., Gordon, H., Williamson, C., Heinritzi, M., Simon, M., Yan, C., Almeida, J., Tröstl, J., Nieminen, T., Ortega, I. K., Wagner, R., Adamov, A., Amorim, A., Bernhammer, A.-K., Bianchi, F., Breitenlechner, M., Brilke, S., Chen, X., Craven, J., Dias, A., Ehrhart, S., Flagan, R. C., Franchin, A., Fuchs, C., Guida, R., Hakala, J., Hoyle, C. R., Jokinen, T., Junninen, H., Kangasluoma, J., Kim, J., Krapf, M., Kürten, A., Laaksonen, A., Lehtipalo, K., Makhmutov, V., Mathot, S., Molteni, U., Onnela, A., Peräkylä, O., Piel, F., Petäjä, T., Praplan, A. P., Pringle, K., Rap, A., Richards, N. A. D., Riipinen, I., Rissanen, M. P., Rondo, L., Sarnela, N., Schobesberger, S., Scott, C. E., Seinfeld, J. H., Sipilä, M., Steiner, G., Stozhkov, Y., Stratmann, F., Tomé, A., Virtanen, A., Vogel, A. L., Wagner, A. C., Wagner, P. E., Weingartner, E., Wimmer, D., Winkler, P. M., Ye, P., Zhang, X., Hansel, A., Dommen, J., Donahue, N. M., Worsnop, D. R., Baltensperger, U., Kulmala, M., Carslaw, K. S., and Curtius, J.: Ion-induced nucleation of pure biogenic particles, Nature, 533, 521-526, 10.1038/nature17953, 2016.

Kontkanen, J., Paasonen, P., Aalto, J., Bäck, J., Rantala, P., Petäjä, T., and Kulmala, M.: Simple proxies for estimating the concentrations of monoterpenes and their oxidation products at a boreal forest site, Atmos. Chem. Phys., 16, 13291–13307, https://doi.org/10.5194/acp-16-13291-2016, 2016.

Krechmer, J., Lopez-Hilfiker, F., Koss, A., Hutterli, M., Stoermer, C., Deming, B., Kimmel, J., Warneke, C., Holzinger, R., Jayne, J., Worsnop, D., Fuhrer, K., Gonin, M., and de Gouw, J.: Evaluation of a New Reagent-Ion Source and Focusing Ion–Molecule Reactor for Use in Proton-Transfer-Reaction Mass Spectrometry, Analytical Chemistry, 90, 12011-12018, 10.1021/acs.analchem.8b02641, 2018.

Kurtén, T., Møller, K. H., Nguyen, T. B., Schwantes, R. H., Misztal, P. K., Su, L., Wennberg, P. O., Fry, J. L., and Kjaergaard, H. G.: Alkoxy Radical Bond Scissions Explain the Anomalously Low Secondary Organic Aerosol and Organonitrate

Yields From α-Pinene + NO3, The Journal of Physical Chemistry Letters, 8, 2826-2834, 10.1021/acs.jpclett.7b01038, 2017.

Kundu, S., Fisseha, R., Putman, A. L., Rahn, T. A., and Mazzoleni, L. R.: Molecular formula composition of β-caryophyllene ozonolysis SOA formed in humid and dry conditions, Atmos Environ, 154, 70-81, https://doi.org/10.1016/j.atmosenv.2016.12.031, 2017.

Lanz, V. A., Alfarra, M. R., Baltensperger, U., Buchmann, B., Hueglin, C., and Prévôt, A. S. H.: Source apportionment of submicron organic aerosols at an urban site by factor analytical modelling of aerosol mass spectra, Atmos. Chem. Phys., 7, 1503–1522, https://doi.org/10.5194/acp-7-1503-2007, 2007.

Lee, B. H., Lopez-Hilfiker, F. D., D'Ambro, E. L., Zhou, P., Boy, M., Petäjä, T., Hao, L., Virtanen, A., and Thornton, J. A.: Semi-volatile and highly oxygenated gaseous and particulate organic compounds observed above a boreal forest canopy, Atmos. Chem. Phys., 18, 11547–11562, https://doi.org/10.5194/acp-18-11547-2018, 2018.

Li, H., Riva, M., Rantala, P., Heikkinen, L., Daellenbach, K., Krechmer, J. E., Flaud, P.-M., Worsnop, D., Kulmala, M., Villenave, E., Perraudin, E., Ehn, M., and Bianchi, F.: Terpenes and their oxidation products in the French Landes forest: insights from Vocus PTR-TOF measurements, Atmos. Chem. Phys., 20, 1941–1959, https://doi.org/10.5194/acp-20-1941-2020, 2020.

Li, H.: Data for "Source identification of atmospheric organic vapors in two European pine forests: Results from Vocus PTR-TOF observations", http://doi.org/10.5281/zenodo.3946644, 2020.

Li, X., Chee, S., Hao, J., Abbatt, J. P. D., Jiang, J., and Smith, J. N.: Relative humidity effect on the formation of highly oxidized molecules and new particles during monoterpene oxidation, Atmos. Chem. Phys., 19, 1555–1570, https://doi.org/10.5194/acp-19-1555-2019, 2019.

Maria, S. F., Russell, L. M., Gilles, M. K., and Myneni, S. C. B.: Organic Aerosol Growth Mechanisms and Their Climate-Forcing Implications, Science, 306, 1921-1924, 10.1126/science.1103491, 2004.

Massoli, P., Stark, H., Canagaratna, M. R., Krechmer, J. E., Xu, L., Ng, N. L., Mauldin, R. L., Yan, C., Kimmel, J., Misztal, P. K., Jimenez, J. L., Jayne, J. T., and Worsnop, D. R.: Ambient Measurements of Highly Oxidized Gas-Phase Molecules during the Southern Oxidant and Aerosol Study (SOAS) 2013, ACS Earth and Space Chemistry, 2, 653-672, 10.1021/acsearthspacechem.8b00028, 2018.

McFiggans, G., Mentel, T. F., Wildt, J., Pullinen, I., Kang, S., Kleist, E., Schmitt, S., Springer, M., Tillmann, R., Wu, C., Zhao, D., Hallquist, M., Faxon, C., Le Breton, M., Hallquist, Å. M., Simpson, D., Bergström, R., Jenkin, M. E., Ehn, M., Thornton, J. A., Alfarra, M. R., Bannan, T. J., Percival, C. J., Priestley, M., Topping, D., and Kiendler-Scharr, A.: Secondary organic aerosol reduced by mixture of atmospheric vapours, Nature, 565, 587-593, 10.1038/s41586-018-0871-y, 2019.

McKinney, K. A., Lee, B. H., Vasta, A., Pho, T. V., and Munger, J. W.: Emissions of isoprenoids and oxygenated biogenic volatile organic compounds from a New England mixed forest, Atmos. Chem. Phys., 11, 4807–4831, https://doi.org/10.5194/acp-11-4807-2011, 2011.

Mehra, A., Wang, Y., Krechmer, J. E., Lambe, A., Majluf, F., Morris, M. A., Priestley, M., Bannan, T. J., Bryant, D. J., Pereira, K. L., Hamilton, J. F., Rickard, A. R., Newland, M. J., Stark, H., Croteau, P., Jayne, J. T., Worsnop, D. R., Canagaratna, M. R., Wang, L., and Coe, H.: Evaluation of the Chemical Composition of Gas and Particle Phase Products of Aromatic Oxidation, Atmos. Chem. Phys. Discuss., https://doi.org/10.5194/acp-2020-161, in review, 2020.

Monson, R. K. and Fall, R.: Isoprene Emission from Aspen Leaves, Influence of Environment and Relation to Photosynthesis and Photorespiration, J. Plant. Physiol., 90, 267–274, https://doi.org/10.1104/pp.90.1.267, 1989.

Nah, T., Sanchez, J., Boyd, C. M., and Ng, N. L.: Photochemical Aging of α-pinene and β-pinene Secondary Organic Aerosol formed from Nitrate Radical Oxidation, Environmental Science & Technology, 50, 222-231, 10.1021/acs.est.5b04594, 2016.

Noe, S. M., Hüve, K., Niinemets, Ü., and Copolovici, L.: Seasonal variation in vertical volatile compounds air concentrations within a remote hemiboreal mixed forest, Atmos. Chem. Phys., 12, 3909–3926, https://doi.org/10.5194/acp-12-3909-2012, 2012.

Paatero, P., and Tapper, U.: Positive matrix factorization: A non-negative factor model with optimal utilization of error estimates of data values, Environmetrics, 5, 111-126, 10.1002/env.3170050203, 1994.

Pagonis, D., Sekimoto, K., and de Gouw, J.: A Library of Proton-Transfer Reactions of H3O+ Ions Used for Trace Gas Detection, Journal of The American Society for Mass Spectrometry, 30, 1330-1335, 10.1007/s13361-019-02209-3, 2019.

Pandya, G. H., Gavane, A. G., Bhanarkar, A. D., and Kondawar, V. K.: Concentrations of volatile organic compounds (VOCs) at an oil refinery, International Journal of Environmental Studies, 63, 337-351, 10.1080/00207230500241918, 2006.

Patokoski, J., Ruuskanen, T. M., Hellén, H., Taipale, R., Grönholm, T., Kajos, M. K., Petäjä, T., Hakola, H., Kulmala, M., and Rinne, J.: Winter to spring transition and diurnal variation of VOCs in Finland at an urban background site and a rural site, Boreal Environ. Res., 19, 79–103, 2014.

Peräkylä, O., Vogt, M., Tikkanen, O.-P., Laurila, T., Kajos, M. K., Rantala, P. A., Patokoski, J., Aalto, J., Yli-Juuti, T., Ehn, M., Sipilä, M., Paasonen, P., Rissanen, M., Nieminen, T., Taipale, R., Keronen, P., Lappalainen, H. K., Ruuskanen, T. M., Rinne, J., Kerminen, V.-M., Kulmala, M., Bäck, J., and Petäjä, T.: Monoterpenes' oxidation capacity and rate over a boreal forest: temporal variation and connection to growth of newly formed particles, Boreal Environ. Res., 19, 293–310, 2014.

Perraud, V., Bruns, E. A., Ezell, M. J., Johnson, S. N., Greaves, J., and Finlayson-Pitts, B. J.: Identification of Organic Nitrates in the NO3 Radical Initiated Oxidation of α-Pinene by Atmospheric Pressure Chemical Ionization Mass Spectrometry, Environmental Science & Technology, 44, 5887-5893, 10.1021/es1005658, 2010.

Petäjä, T., Mauldin, III, R. L., Kosciuch, E., McGrath, J., Nieminen, T., Paasonen, P., Boy, M., Adamov, A., Kotiaho, T., and Kulmala, M.: Sulfuric acid and OH concentrations in a boreal forest site, Atmos. Chem. Phys., 9, 7435–7448, https://doi.org/10.5194/acp-9-7435-2009, 2009.

Rantala, P., Aalto, J., Taipale, R., Ruuskanen, T. M., and Rinne, J.: Annual cycle of volatile organic compound exchange between a boreal pine forest and the atmosphere, Biogeosciences, 12, 5753–5770, https://doi.org/10.5194/bg-12-5753-2015, 2015.

Riba, M. L., Tathy, J. P., Tsiropoulos, N., Monsarrat, B., and Torres, L.: Diurnal variation in the concentration of α- and β-pinene in the landes forest (France), Atmospheric Environment (1967), 21, 191-193, https://doi.org/10.1016/0004-6981(87)90285-X, 1987.

Rinne, J., Back, J., and Hakola, H.: Biogenic volatile organic compound emissions from the Eurasian taiga: current knowledge and future directions, Boreal Environ. Res., 14, 807–826, 2009.

Riva, M., Rantala, P., Krechmer, J. E., Peräkylä, O., Zhang, Y., Heikkinen, L., Garmash, O., Yan, C., Kulmala, M., Worsnop, D., and Ehn, M.: Evaluating the performance of five different chemical ionization techniques for detecting gaseous oxygenated organic species, Atmos. Meas. Tech., 12, 2403–2421, https://doi.org/10.5194/amt-12-2403-2019, 2019.

Sakulyanontvittaya, T., Duhl, T., Wiedinmyer, C., Helmig, D., Matsunaga, S., Potosnak, M., Milford, J., and Guenther, A.: Monoterpene and Sesquiterpene Emission Estimates for the United States, Environmental Science & Technology, 42, 1623-1629, 10.1021/es702274e, 2008.

Sarkar, C., Sinha, V., Sinha, B., Panday, A. K., Rupakheti, M., and Lawrence, M. G.: Source apportionment of NMVOCs in the Kathmandu Valley during the SusKat-ABC international field campaign using positive matrix factorization, Atmos. Chem. Phys., 17, 8129–8156, https://doi.org/10.5194/acp-17-8129-2017, 2017.

Sato, K., Takami, A., Kato, Y., Seta, T., Fujitani, Y., Hikida, T., Shimono, A., and Imamura, T.: AMS and LC/MS analyses of SOA from the photooxidation of benzene and 1,3,5-trimethylbenzene in the presence of NOx: effects of chemical structure on SOA aging, Atmos. Chem. Phys., 12, 4667–4682, https://doi.org/10.5194/acp-12-4667-2012, 2012.

Schallhart, S., Rantala, P., Kajos, M. K., Aalto, J., Mammarella, I., Ruuskanen, T. M., and Kulmala, M.: Temporal variation of VOC fluxes measured with PTR-TOF above a boreal forest, Atmos Chem Phys, 18, 815-832, 2018.

Schell, B., Ackermann, I. J., Hass, H., Binkowski, F. S., and Ebel, A.: Modeling the formation of secondary organic aerosol within a comprehensive air quality model system, Journal of Geophysical Research: Atmospheres, 106, 28275-28293, 10.1029/2001JD000384, 2001.

Schweigkofler, M., and Niessner, R.: Determination of Siloxanes and VOC in Landfill Gas and Sewage Gas by Canister Sampling and GC-MS/AES Analysis, Environmental Science & Technology, 33, 3680-3685, 10.1021/es9902569, 1999.

Sekimoto, K., Li, S.-M., Yuan, B., Koss, A., Coggon, M., Warneke, C., and de Gouw, J.: Calculation of the sensitivity of proton-transfer-reaction mass spectrometry (PTR-MS) for organic trace gases using molecular properties, International Journal of Mass Spectrometry, 421, 71-94, https://doi.org/10.1016/j.ijms.2017.04.006, 2017.

Simon, V., Clement, B., Riba, M.-L., and Torres, L.: The Landes experiment: Monoterpenes emitted from the maritime pine, J. Geophys. Res., 99, 16501–16510, https://doi.org/10.1029/94JD00785, 1994.

Simon, M., Dada, L., Heinritzi, M., Scholz, W., Stolzenburg, D., Fischer, L., Wagner, A. C., Kürten, A., Rörup, B., He, X.-C., Almeida, J., Baalbaki, R., Baccarini, A., Bauer, P. S., Beck, L., Bergen, A., Bianchi, F., Bräkling, S., Brilke, S., Caudillo,

L., Chen, D., Chu, B., Dias, A., Draper, D. C., Duplissy, J., El Haddad, I., Finkenzeller, H., Frege, C., Gonzalez-Carracedo, L., Gordon, H., Granzin, M., Hakala, J., Hofbauer, V., Hoyle, C. R., Kim, C., Kong, W., Lamkaddam, H., Lee, C. P., Lehtipalo, K., Leiminger, M., Mai, H., Manninen, H. E., Marie, G., Marten, R., Mentler, B., Molteni, U., Nichman, L., Nie, W., Ojdanic, A., Onnela, A., Partoll, E., Petäjä, T., Pfeifer, J., Philippov, M., Quéléver, L. L. J., Ranjithkumar, A., Rissanen, M., Schallhart, S., Schobesberger, S., Schuchmann, S., Shen, J., Sipilä, M., Steiner, G., Stozhkov, Y., Tauber, C., Tham, Y. J., Tomé, A. R., Vazquez-Pufleau, M., Vogel, A., Wagner, R., Wang, M., Wang, D. S., Wang, Y., Weber, S. K., Wu, Y., Xiao, M., Yan, C., Ye, P., Ye, Q., Zauner-Wieczorek, M., Zhou, X., Baltensperger, U., Dommen, J., Flagan, R. C., Hansel, A., Kulmala, M., Volkamer, R., Winkler, P. M., Worsnop, D. R., Donahue, N. M., Kirkby, J., and Curtius, J.: Molecular understanding of new-particle formation from alpha-pinene between −50 °C and 25 °C, Atmos. Chem. Phys. Discuss., https://doi.org/10.5194/acp-2019-1058, in review, 2020.

Sindelarova, K., Granier, C., Bouarar, I., Guenther, A., Tilmes, S., Stavrakou, T., Müller, J.-F., Kuhn, U., Stefani, P., and Knorr, W.: Global data set of biogenic VOC emissions calculated by the MEGAN model over the last 30 years, Atmos. Chem. Phys., 14, 9317–9341, https://doi.org/10.5194/acp-14-9317-2014, 2014.

Spanel, P., and Smith, D.: SIFT studies of the reactions of H3O+, NO+ and O2+ with a series of alcohols, International Journal of Mass Spectrometry and Ion Processes, 167-168, 375-388, https://doi.org/10.1016/S0168-1176(97)00085-2, 1997.

Stark, H., Yatavelli, R. L. N., Thompson, S. L., Kimmel, J. R., Cubison, M. J., Chhabra, P. S., Canagaratna, M. R., Jayne, J. T., Worsnop, D. R., and Jimenez, J. L.: Methods to extract molecular and bulk chemical information from series of complex mass spectra with limited mass resolution, Int. J. Mass Spectrom., 389, 26–38, https://doi.org/10.1016/j.ijms.2015.08.011, 2015.

Tani, A., Hayward, S., and Hewitt, C. N.: Measurement of monoterpenes and related compounds by proton transfer reaction-mass spectrometry (PTR-MS), International Journal of Mass Spectrometry, 223-224, 561-578, https://doi.org/10.1016/S1387-3806(02)00880-1, 2003.

Tani, A.: Fragmentation and Reaction Rate Constants of Terpenoids Determined by Proton Transfer Reaction-mass Spectrometry, Environmental Control in Biology, 51, 23-29, 10.2525/ecb.51.23, 2013.

Tillmann, R., Hallquist, M., Jonsson, Å. M., Kiendler-Scharr, A., Saathoff, H., Iinuma, Y., and Mentel, Th. F.: Influence of relative humidity and temperature on the production of pinonaldehyde and OH radicals from the ozonolysis of α-pinene, Atmos. Chem. Phys., 10, 7057–7072, https://doi.org/10.5194/acp-10-7057-2010, 2010.

Tsigaridis, K. and Kanakidou, M.: Global modelling of secondary organic aerosol in the troposphere: a sensitivity analysis, Atmos. Chem. Phys., 3, 1849–1869, https://doi.org/10.5194/acp-3-1849-2003, 2003.

Ulbrich, I. M., Canagaratna, M. R., Zhang, Q., Worsnop, D. R., and Jimenez, J. L.: Interpretation of organic components from Positive Matrix Factorization of aerosol mass spectrometric data, Atmos. Chem. Phys., 9, 2891–2918, https://doi.org/10.5194/acp-9-2891-2009, 2009.

Valiev, R. R., Hasan, G., Salo, V.-T., Kubečka, J., and Kurten, T.: Intersystem Crossings Drive Atmospheric Gas-Phase Dimer Formation, The Journal of Physical Chemistry A, 123, 6596-6604, 10.1021/acs.jpca.9b02559, 2019.

Vlasenko, A., Slowik, J. G., Bottenheim, J. W., Brickell, P. C., Chang, R. Y. W., Macdonald, A. M., Shantz, N. C., Sjostedt, S. J., Wiebe, H. A., Leaitch, W. R., and Abbatt, J. P. D.: Measurements of VOCs by proton transfer reaction mass spectrometry at a rural Ontario site: Sources and correlation to aerosol composition, Journal of Geophysical Research: Atmospheres, 114, 10.1029/2009JD012025, 2009.

Wang, L., Slowik, J. G., Tripathi, N., Bhattu, D., Rai, P., Kumar, V., Vats, P., Satish, R., Baltensperger, U., Ganguly, D., Rastogi, N., Sahu, L. K., Tripathi, S. N., and Prévôt, A. S. H.: Source characterization of volatile organic compounds measured by PTR-ToF-MS in Delhi, India, Atmos. Chem. Phys. Discuss., https://doi.org/10.5194/acp-2020-11, in review, 2020.

Wängberg, I., Barnes, I., and Becker, K. H.: Product and Mechanistic Study of the Reaction of NO3 Radicals with α-Pinene, Environmental Science & Technology, 31, 2130-2135, 10.1021/es960958n, 1997.

Wennberg, P. O., Bates, K. H., Crounse, J. D., Dodson, L. G., McVay, R. C., Mertens, L. A., Nguyen, T. B., Praske, E., Schwantes, R. H., Smarte, M. D., St Clair, J. M., Teng, A. P., Zhang, X., and Seinfeld, J. H.: Gas-Phase Reactions of Isoprene and Its Major Oxidation Products, Chem Rev, 118, 3337-3390, 2018.

Winterhalter, R., Herrmann, F., Kanawati, B., Nguyen, T. L., Peeters, J., Vereecken, L., and Moortgat, G. K.: The gas-phase ozonolysis of β-caryophyllene (C15H24). Part I: an experimental study, Physical Chemistry Chemical Physics, 11, 4152-4172, 10.1039/B817824K, 2009.

Yan, C., Nie, W., Äijälä, M., Rissanen, M. P., Canagaratna, M. R., Massoli, P., Junninen, H., Jokinen, T., Sarnela, N., Häme, S. A. K., Schobesberger, S., Canonaco, F., Yao, L., Prévôt, A. S. H., Petäjä, T., Kulmala, M., Sipilä, M., Worsnop, D. R., and Ehn, M.: Source characterization of highly oxidized multifunctional compounds in a boreal forest environment using positive matrix factorization, Atmos. Chem. Phys., 16, 12715-12731, 10.5194/acp-16-12715-2016, 2016.

Yee, L. D., Isaacman-VanWertz, G., Wernis, R. A., Meng, M., Rivera, V., Kreisberg, N. M., Hering, S. V., Bering, M. S., Glasius, M., Upshur, M. A., Gray Bé, A., Thomson, R. J., Geiger, F. M., Offenberg, J. H., Lewandowski, M., Kourtchev, I., Kalberer, M., de Sá, S., Martin, S. T., Alexander, M. L., Palm, B. B., Hu, W., Campuzano-Jost, P., Day, D. A., Jimenez, J. L., Liu, Y., McKinney, K. A., Artaxo, P., Viegas, J., Manzi, A., Oliveira, M. B., de Souza, R., Machado, L. A. T., Longo, K., and Goldstein, A. H.: Observations of sesquiterpenes and their oxidation products in central Amazonia during the wet and dry seasons, Atmos. Chem. Phys., 18, 10433–10457, https://doi.org/10.5194/acp-18-10433-2018, 2018.

Yuan, B., Koss, A. R., Warneke, C., Coggon, M., Sekimoto, K., and de Gouw, J. A.: Proton-Transfer-Reaction Mass Spectrometry: Applications in Atmospheric Sciences, Chem Rev, 117, 13187-13229, 2017.

Yucuis, R. A., Stanier, C. O., and Hornbuckle, K. C.: Cyclic siloxanes in air, including identification of high levels in Chicago and distinct diurnal variation, Chemosphere, 92, 905-910, https://doi.org/10.1016/j.chemosphere.2013.02.051, 2013.

Zaytsev, A., Koss, A. R., Breitenlechner, M., Krechmer, J. E., Nihill, K. J., Lim, C. Y., Rowe, J. C., Cox, J. L., Moss, J., Roscioli, J. R., Canagaratna, M. R., Worsnop, D. R., Kroll, J. H., and Keutsch, F. N.: Mechanistic study of the formation of ring-retaining and ring-opening products from the oxidation of aromatic compounds under urban atmospheric conditions, Atmos. Chem. Phys., 19, 15117–15129, https://doi.org/10.5194/acp-19-15117-2019, 2019.

Zha, Q., Yan, C., Junninen, H., Riva, M., Sarnela, N., Aalto, J., Quéléver, L., Schallhart, S., Dada, L., Heikkinen, L., Peräkylä, O., Zou, J., Rose, C., Wang, Y., Mammarella, I., Katul, G., Vesala, T., Worsnop, D. R., Kulmala, M., Petäjä, T., Bianchi, F., and Ehn, M.: Vertical characterization of highly oxygenated molecules (HOMs) below and above a boreal forest canopy, Atmos. Chem. Phys., 18, 17437–17450, https://doi.org/10.5194/acp-18-17437-2018, 2018.

Zhang, H., Yee, L. D., Lee, B. H., Curtis, M. P., Worton, D. R., Isaacman-VanWertz, G., Offenberg, J. H., Lewandowski, M., Kleindienst, T. E., Beaver, M. R., Holder, A. L., Lonneman, W. A., Docherty, K. S., Jaoui, M., Pye, H. O. T., Hu, W., Day, D. A., Campuzano-Jost, P., Jimenez, J. L., Guo, H., Weber, R. J., de Gouw, J., Koss, A. R., Edgerton, E. S., Brune, W., Mohr, C., Lopez-Hilfiker, F. D., Lutz, A., Kreisberg, N. M., Spielman, S. R., Hering, S. V., Wilson, K. R., Thornton, J. A., and Goldstein, A. H.: Monoterpenes are the largest source of summertime organic aerosol in the southeastern United States, Proceedings of the National Academy of Sciences, 115, 2038-2043, 10.1073/pnas.1717513115, 2018.

Zhang, Q., Jimenez, J. L., Canagaratna, M. R., Ulbrich, I. M., Ng, N. L., Worsnop, D. R., and Sun, Y.: Understanding atmospheric organic aerosols via factor analysis of aerosol mass spectrometry: a review, Anal Bioanal Chem, 401, 3045-3067, 10.1007/s00216-011-5355-y, 2011.

Zhang, X., Schwantes, R. H., Coggon, M. M., Loza, C. L., Schilling, K. A., Flagan, R. C., and Seinfeld, J. H.: Role of ozone in SOA formation from alkane photooxidation, Atmos. Chem. Phys., 14, 1733–1753, https://doi.org/10.5194/acp-14-1733-2014, 2014.

Zhang, Y., Peräkylä, O., Yan, C., Heikkinen, L., Äijälä, M., Daellenbach, K. R., Zha, Q., Riva, M., Garmash, O., Junninen, H., Paatero, P., Worsnop, D., and Ehn, M.: A novel approach for simple statistical analysis of high-resolution mass spectra, Atmos. Meas. Tech., 12, 3761-3776, 10.5194/amt-12-3761-2019, 2019a.

Zhang, Y., Peräkylä, O., Yan, C., Heikkinen, L., Äijälä, M., Daellenbach, K. R., Zha, Q., Riva, M., Garmash, O., Junninen, H., Paatero, P., Worsnop, D., and Ehn, M.: Insights on Atmospheric Oxidation Processes by Performing Factor Analyses on Sub-ranges of Mass Spectra, Atmos. Chem. Phys. Discuss., https://doi.org/10.5194/acp-2019-838, in review, 2019b.

Zhu, Y., Yang, L., Kawamura, K., Chen, J., Ono, K., Wang, X., Xue, L., and Wang, W.: Contributions and source identification of biogenic and anthropogenic hydrocarbons to secondary organic aerosols at Mt. Tai in 2014, Environ Pollut, 220, 863-872, https://doi.org/10.1016/j.envpol.2016.10.070, 2017.

Table 1. Summary of source identification results for the two forest sites (L, Landes; S, SMEAR II).

	Factor name	Possible source/chemistry	Fingerprint molecules
Landes forest			
	Factor L1	$C_4H_8H^+$ ion-related	$C_4H_8H^+$, $C_4H_{10}O_2H^+$
	Factor L2	A plume event	$C_6H_6H^+$, $C_7H_6H^+$, $C_6H_6OH^+$, unidentified peaks
	Factor L3	C_6 and C_7 lightly oxidized products	$C_6H_{10}OH^+$, $C_7H_{10}OH^+$, $C_6H_{10}O_2H^+$, $C_7H_{12}O_2H^+$,
	Factor L4	Monoterpenes	$C_6H_8H^+$, $C_7H_{10}H^+$, $C_{10}H_{16}H^+$
	Factor L5	Isoprene and its oxidation products	$C_5H_8H^+$, $C_4H_6OH^+$, $C_4H_6O_3H^+$
	Factor L6	Unknown source	$C_6H_4O_2H^+$, $C_6H_6O_3H^+$, unidentified peaks with negative mass defect
	Factor L7	Monoterpene lightly oxidized products	$C_9H_{14}OH^+$, $C_{10}H_{14}OH^+$, $C_{10}H_{16}O_2H^+$, $C_{10}H_{16}O_3H^+$
	Factor L8	C_{13} lightly oxidized products	$C_{13}H_{18}O_2H^+$, $C_{13}H_{20}O_3H^+$
	Factor L9	A plume event	Unidentified peaks
	Factor L10	Sesquiterpene lightly oxidized products	$C_{15}H_{22}OH^+$, $C_{15}H_{24}OH^+$, $C_{15}H_{22}O_2H^+$, $C_{15}H_{24}O_2H^+$, $C_{15}H_{24}O_3H^+$
	Factor L11	Monoterpene more oxidized products	$C_{10}H_{16}O_4H^+$, $C_{10}H_{14}O_5H^+$, $C_{10}H_{16}O_5H^+$, $C_{10}H_{16}O_6H^+$
	Factor L12	Sesquiterpenes	$C_{15}H_{24}H^+$
	Factor L13	Monoterpene-derived organic nitrates	$C_{10}H_{15}NO_4H^+$, $C_{10}H_{15}NO_5H^+$, $C_9H_{13}NO_6H^+$, $C_{10}H_{15}NO_6H^+$
	Factor L14	C_{12}, C_{14} or C_{16} lightly oxidized products	$C_{12}H_{26}O_3H^+$, $C_{14}H_{26}O_2H^+$, $C_{16}H_{30}O_2H^+$
	Factor L15	Unknown source	D3 siloxane, D4 siloxane, unidentified peaks
SMEAR II			
	Factor S1	$C_4H_8H^+$ ion-related	$C_4H_8H^+$, $C_4H_{12}O_2H^+$, $C_4H_{14}O_3H^+$
	Factor S2	Monoterpenes	$C_6H_8H^+$, $C_7H_{10}H^+$, $C_{10}H_{16}H^+$
	Factor S3	C_6-C_9 lightly oxygenated compounds	$C_6H_{10}OH^+$, $C_6H_{12}OH^+$, $C_7H_{10}OH^+$, $C_8H_{14}OH^+$, $C_9H_{12}O_2H^+$
	Factor S4	Isoprene and its oxidation products	$C_5H_8H^+$, $C_4H_6OH^+$
	Factor S5	Monoterpene lightly oxidized products	$C_9H_{14}OH^+$, $C_{10}H_{14}OH^+$, $C_{10}H_{16}OH^+$, $C_{10}H_{16}O_2H^+$, $C_{10}H_{16}O_3H^+$
	Factor S6	Sesquiterpene lightly oxidized products	$C_{14}H_{22}OH^+$, $C_{14}H_{24}OH^+$, $C_{15}H_{22}OH^+$, $C_{15}H_{24}OH^+$
	Factor S7	Sesquiterpenes	$C_{15}H_{24}H^+$
	Factor S8	Monoterpene more oxidized products including organic nitrates	$C_{10}H_{16}O_4H^+$, $C_{14}H_{22}O_3H^+$, $C_{15}H_{24}O_3H^+$, $C_{10}H_{17}NO_3H^+$, $C_9H_{13}NO_6H^+$
	Factor S9	Unknown source	D3 siloxane, D4 siloxane, unidentified peaks

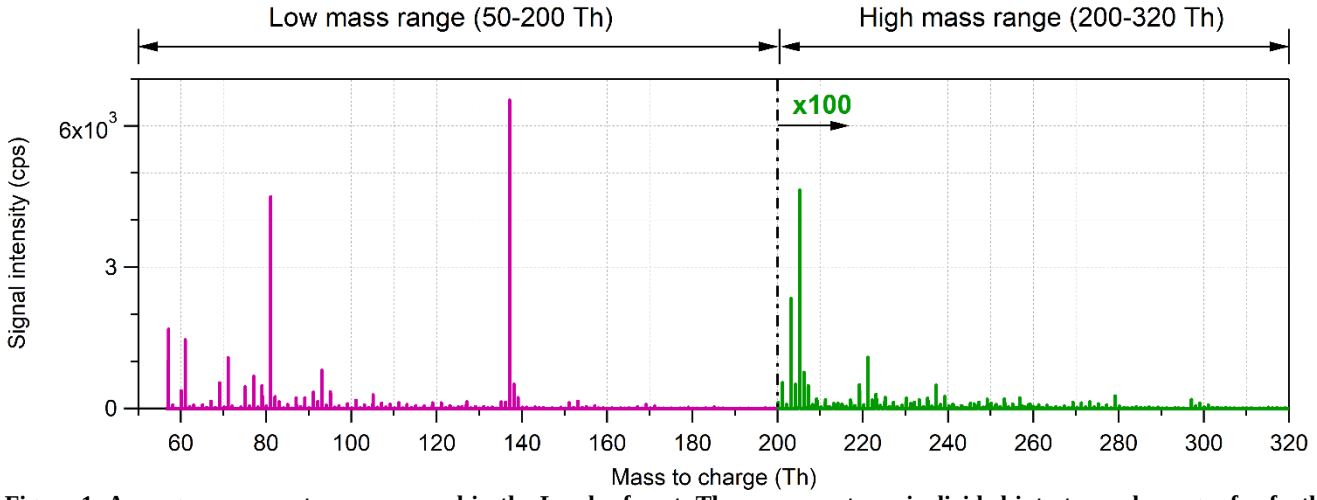

990 **Figure 1. Average mass spectrum measured in the Landes forest. The mass spectrum is divided into two sub-ranges for further source identification analysis. The intensity scale is shown 100-fold for the high mass range (201-320 Th).**

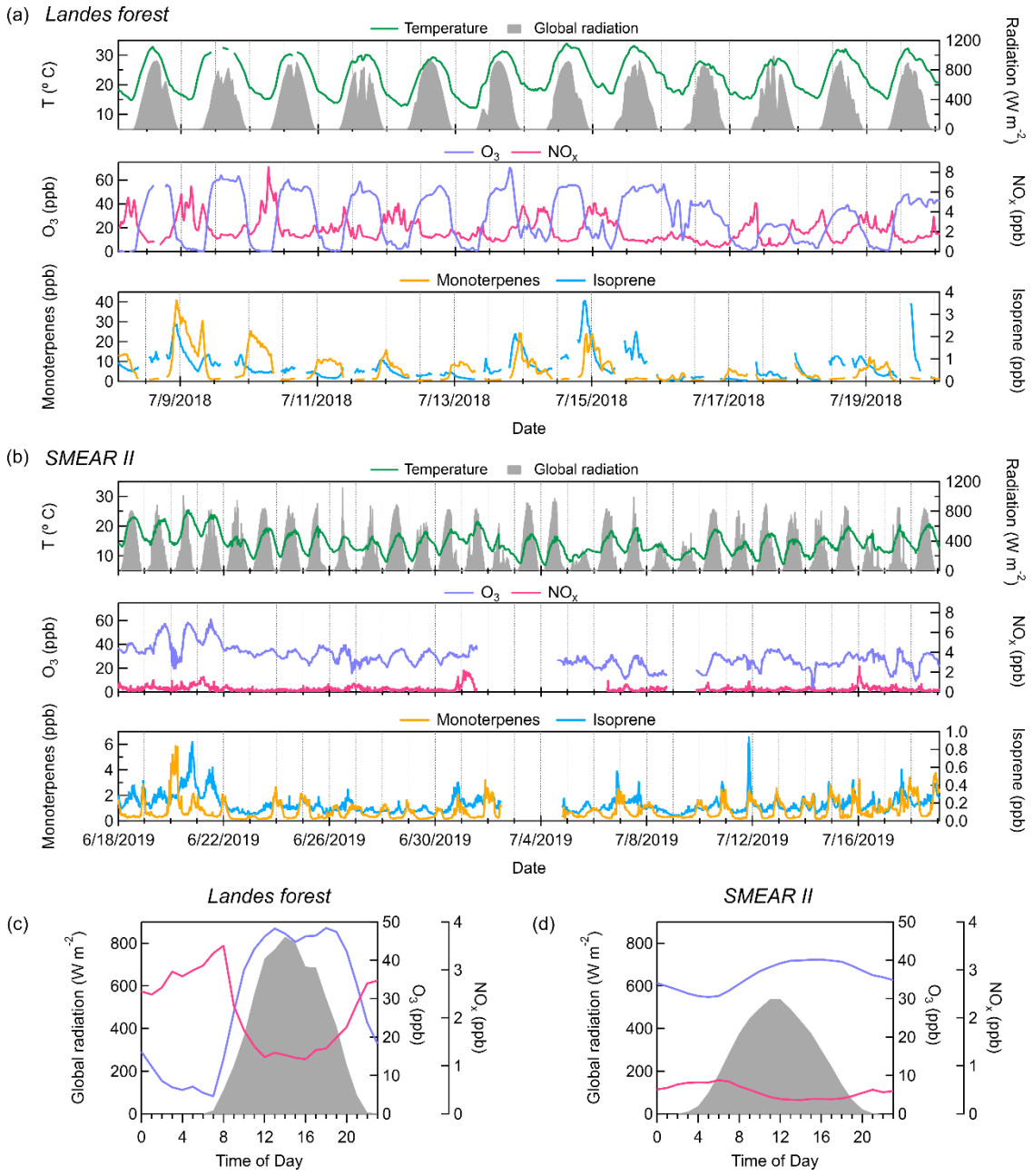

995 **Figure 2. Time series of temperature, global radiation, concentrations of O_3 and NO_x, and mixing ratios of monoterpenes and isoprene throughout the measurements (a) in the Landes forest and (b) at the SMEAR II station. Average diurnal cycles of global radiation, O_3 concentration (in blue), and NO_x concentration (in pink) (c) in the Landes forest and (d) at the SMEAR II station. All parameters, except monoterpenes and isoprene, are shown in the same y-axis scale for the two sites. Monoterpene and isoprene concentrations are much lower at the SMEAR II station than in the Landes forest.**

1000

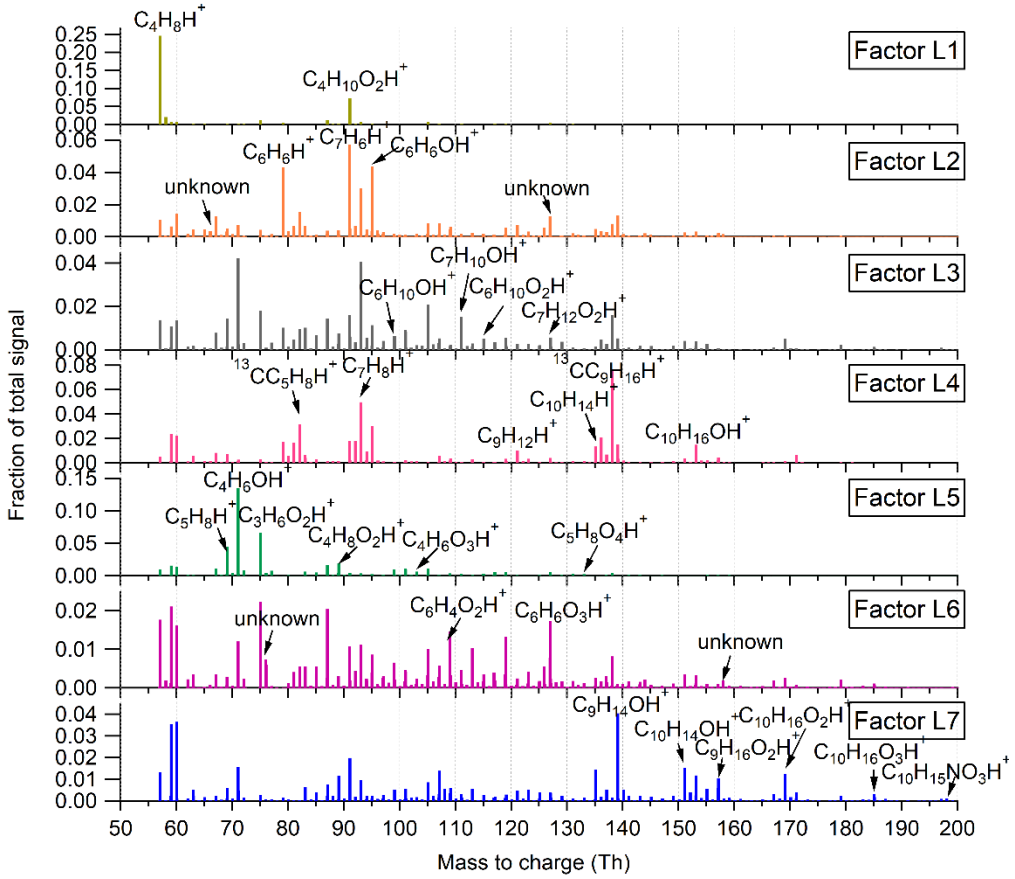

Figure 3. Mass profiles of the seven factors resolved in the low mass range in the Landes forest. Fingerprint peaks identified by high-resolution peak fitting are shown in the mass spectra.

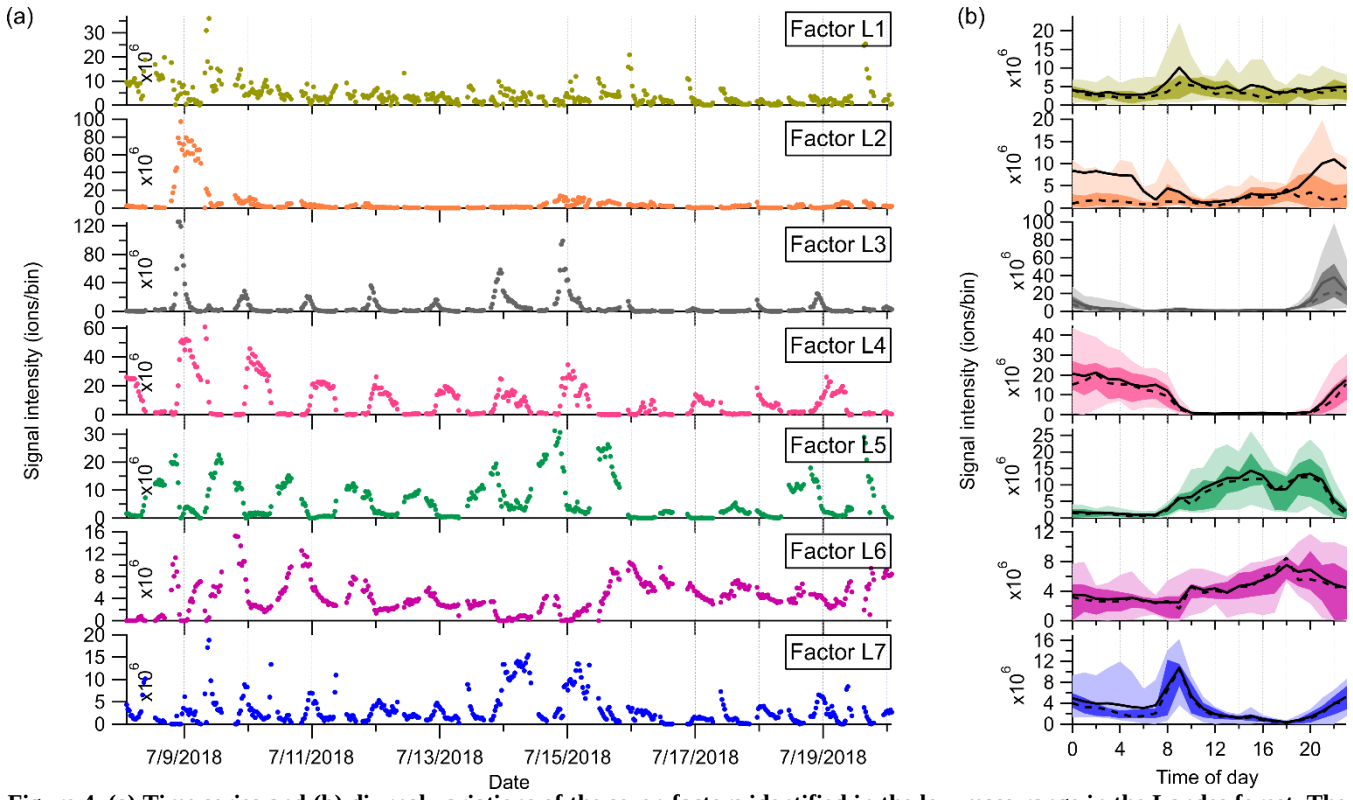

Figure 4. (a) Time series and (b) diurnal variations of the seven factors identified in the low mass range in the Landes forest. The solid and dashed lines in the diurnal plots show the mean and median values, respectively, and the shaded area shows 10th, 25th, 75th, and 90th percentiles.

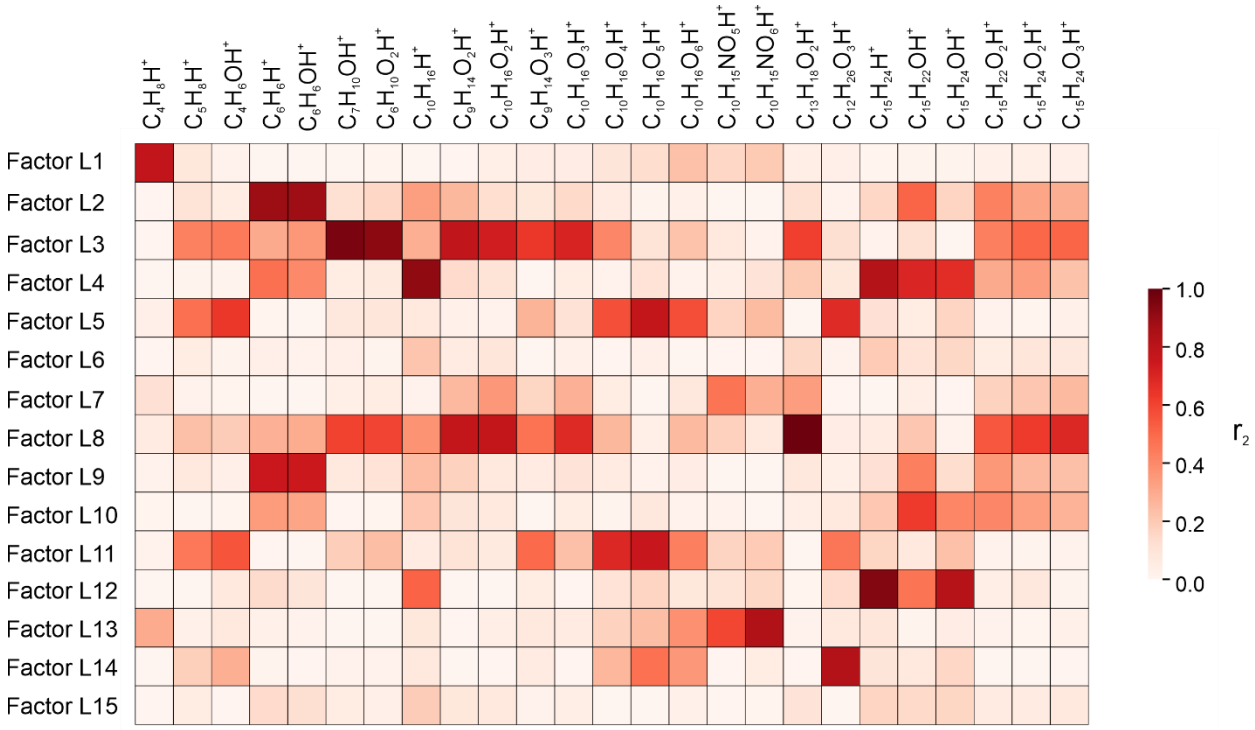

~~Figure 5. Correlations between PMF factors and marker molecules in the Landes forest, with the color representing the correlation coefficients (r^2).~~

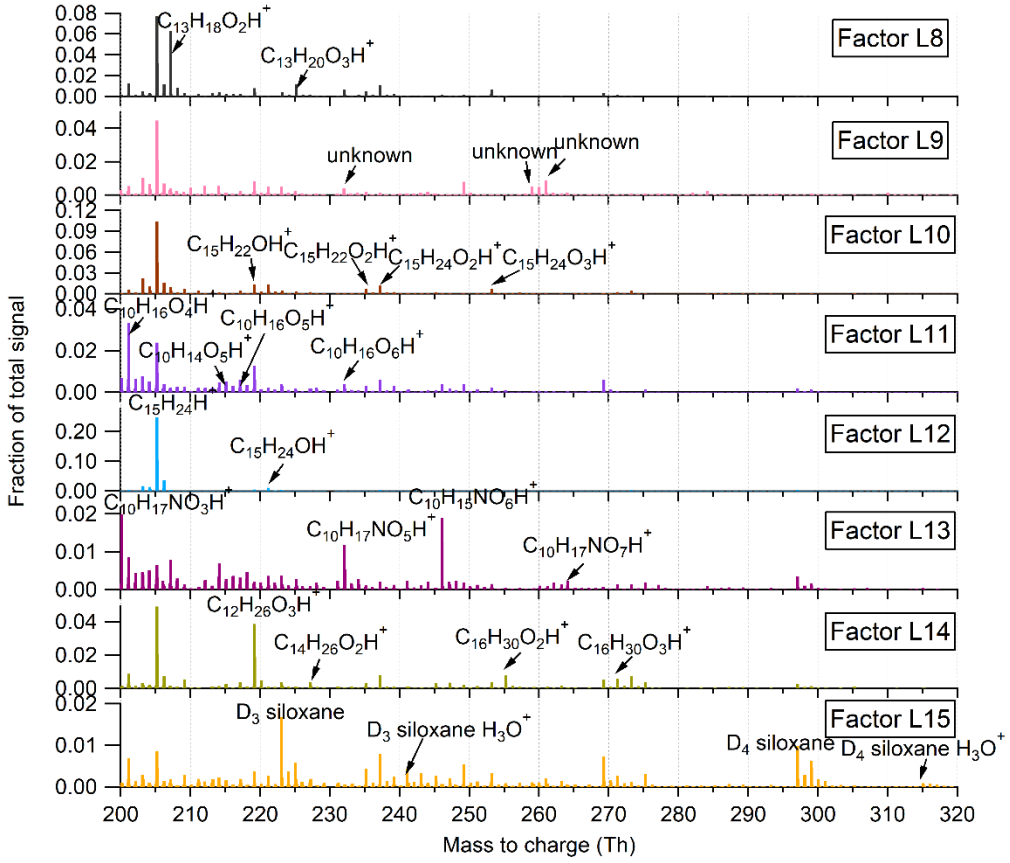

Figure 5~~6~~. Mass profiles of the eight factors resolved in the high mass range in the Landes forest, with major fingerprint peaks labeled in the mass spectra.

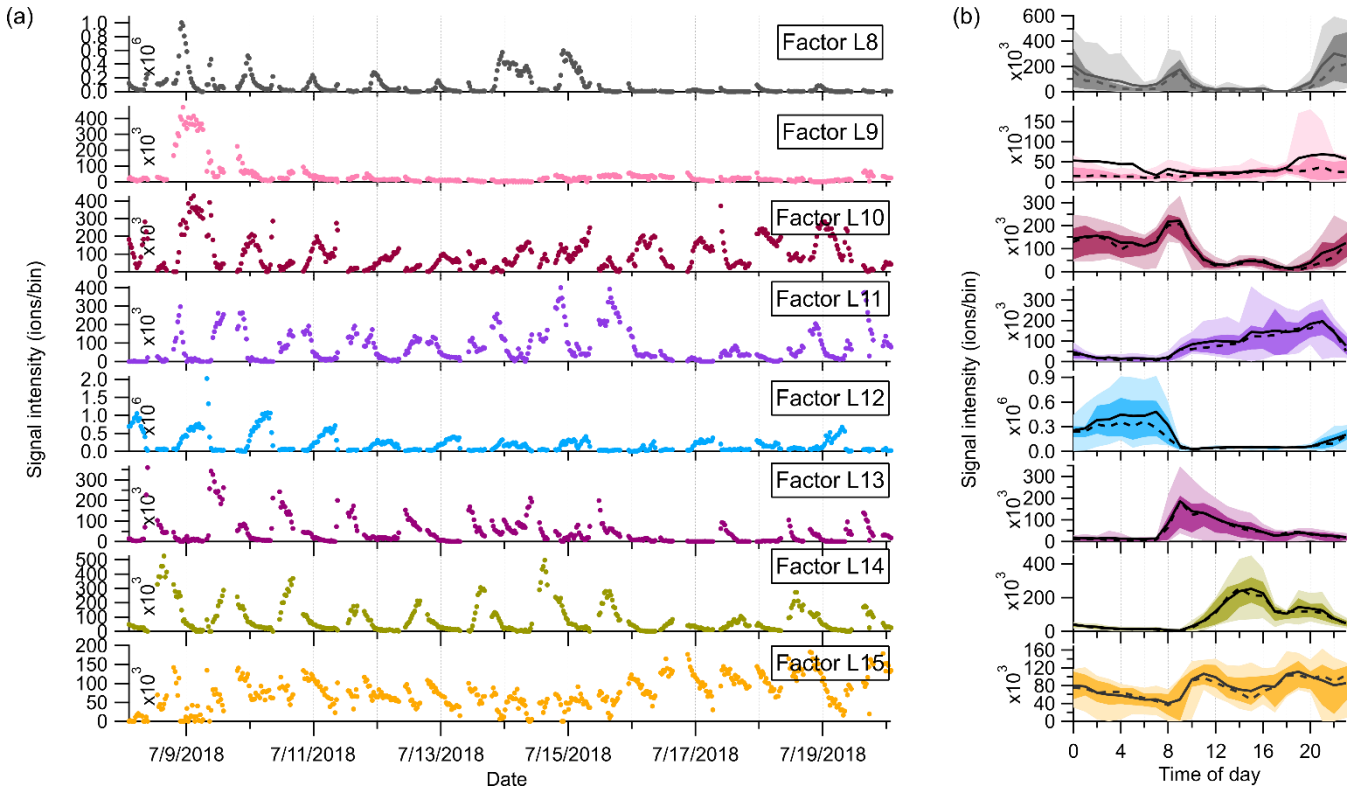

Figure 6~~7~~. (a) Time series and (b) diurnal trends of the eight factors resolved in the high mass range in the Landes forest. The solid and dashed lines in the diurnal plots show the mean and median values, respectively, and the shaded area shows 10th, 25th, 75th, and 90th percentiles.

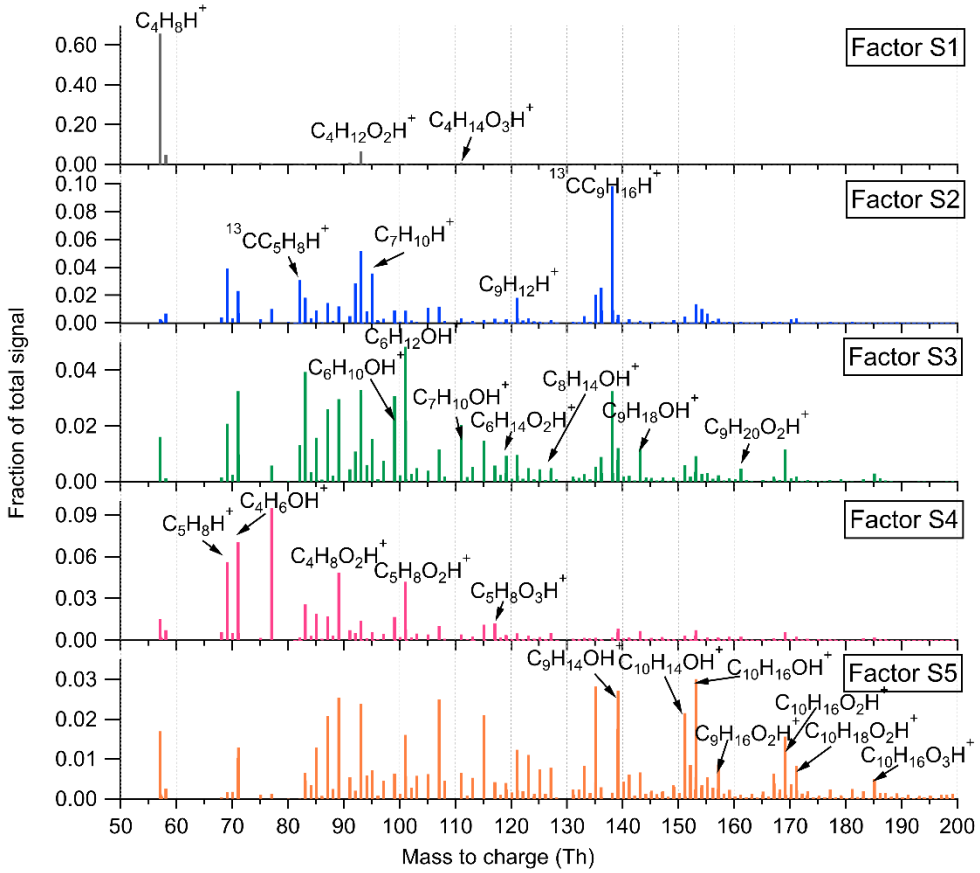

Figure 7~~8~~. Mass profiles of the five factors identified in the low mass range at the SMEAR II station, with fingerprint peaks shown in the mass spectra.

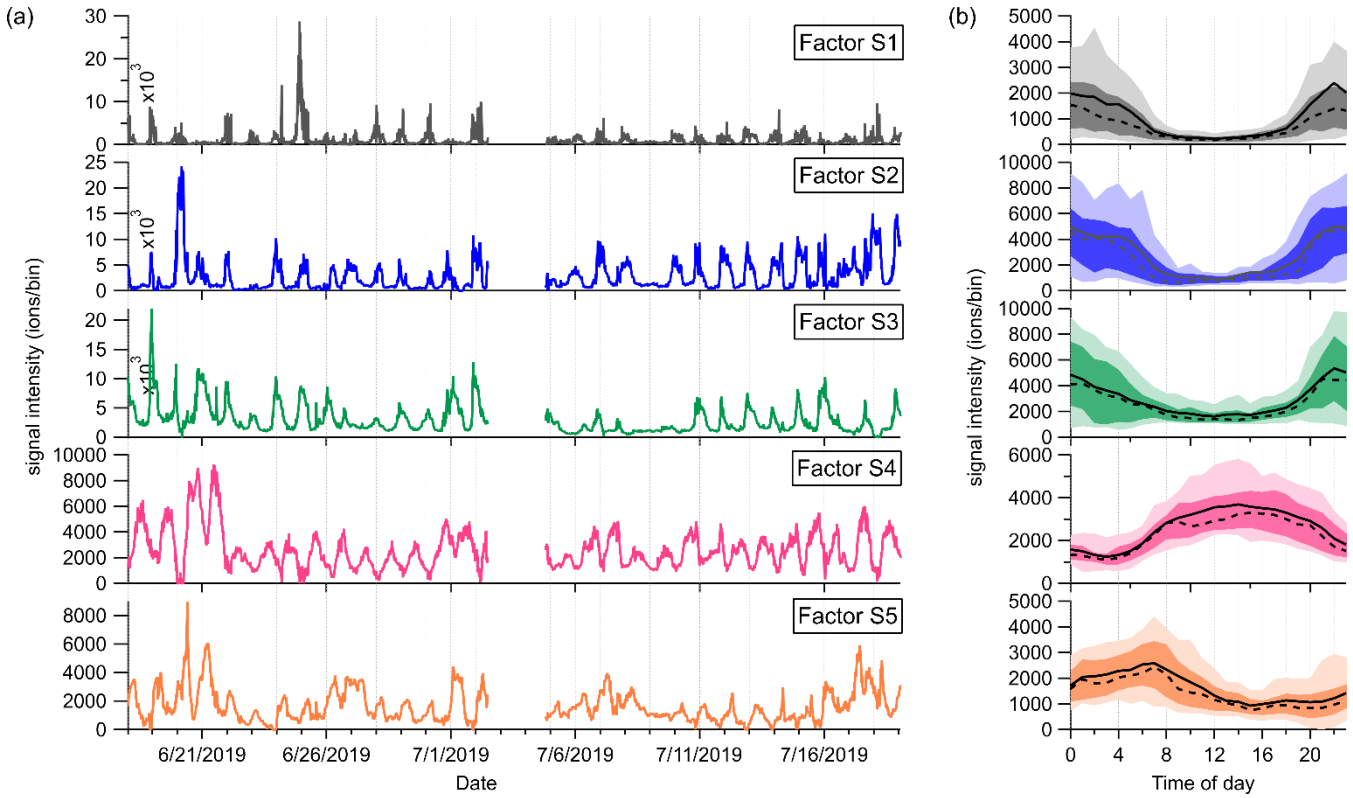

Figure 89. (a) Time series and (b) diurnal cycles of the five factors in the low mass range at the SMEAR II station. The solid and dashed lines in the diurnal plots show the mean and median values, respectively, and the shaded area shows 10th, 25th, 75th, and 90th percentiles.

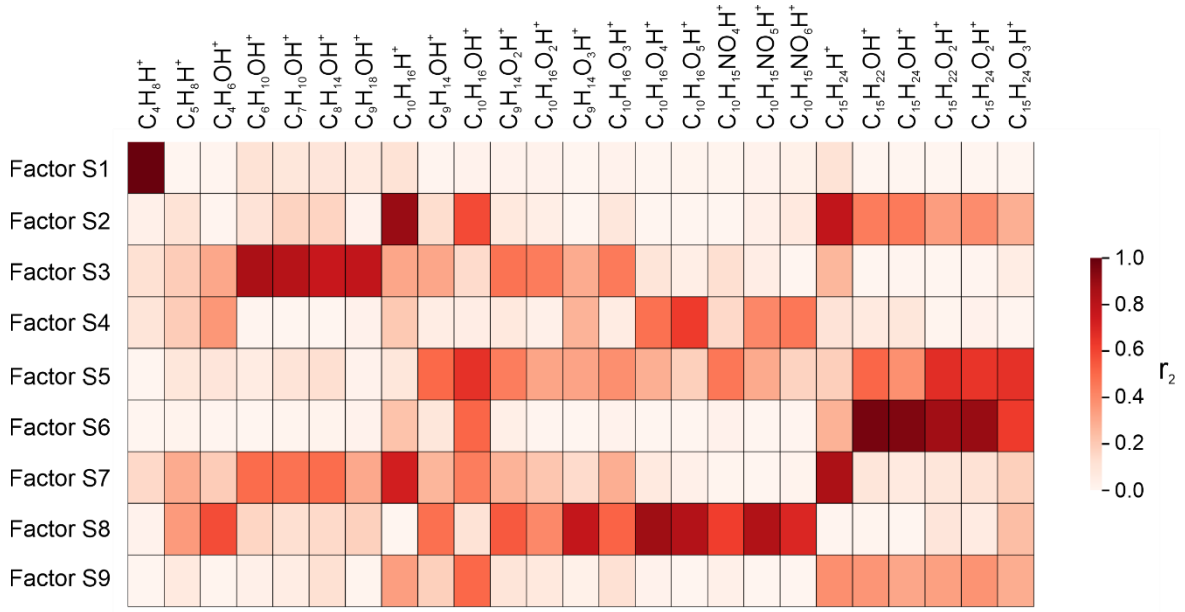

Figure 10. Correlations between PMF factors and marker molecules at the SMEAR II station, with the color indicating the correlation coefficients (r^2).

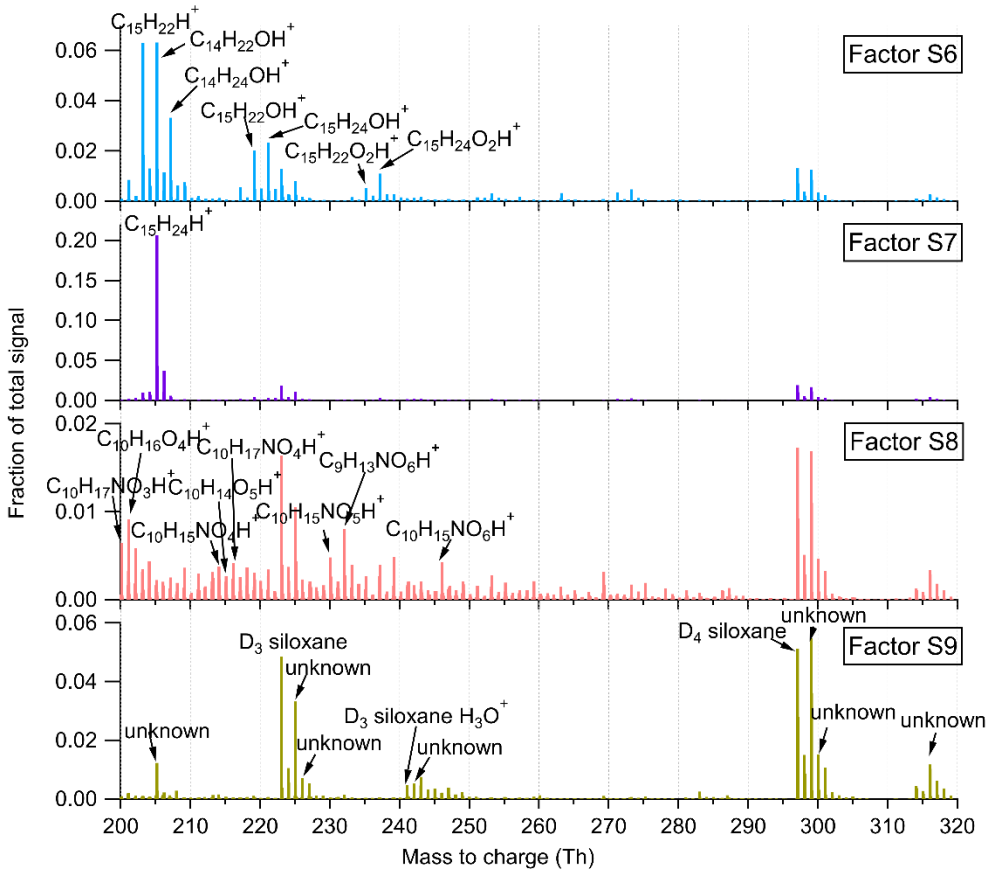
Factor S6
Factor S7
Factor S8
Factor S9
Fraction of total signal
Mass to charge (Th)
C15H22H+
C14H22OH+
C14H24OH+
C15H22OH+
C15H24OH+
C15H22O2H+
C15H24O2H+
C15H24H+
C10H16O4H+
C10H17NO4H+
C9H13NO6H+
C10H17NO3H+
C10H14O5H+
C10H15NO4H+
C10H15NO5H+
C10H15NO6H+
D3 siloxane
unknown
D3 siloxane H3O+
D4 siloxane

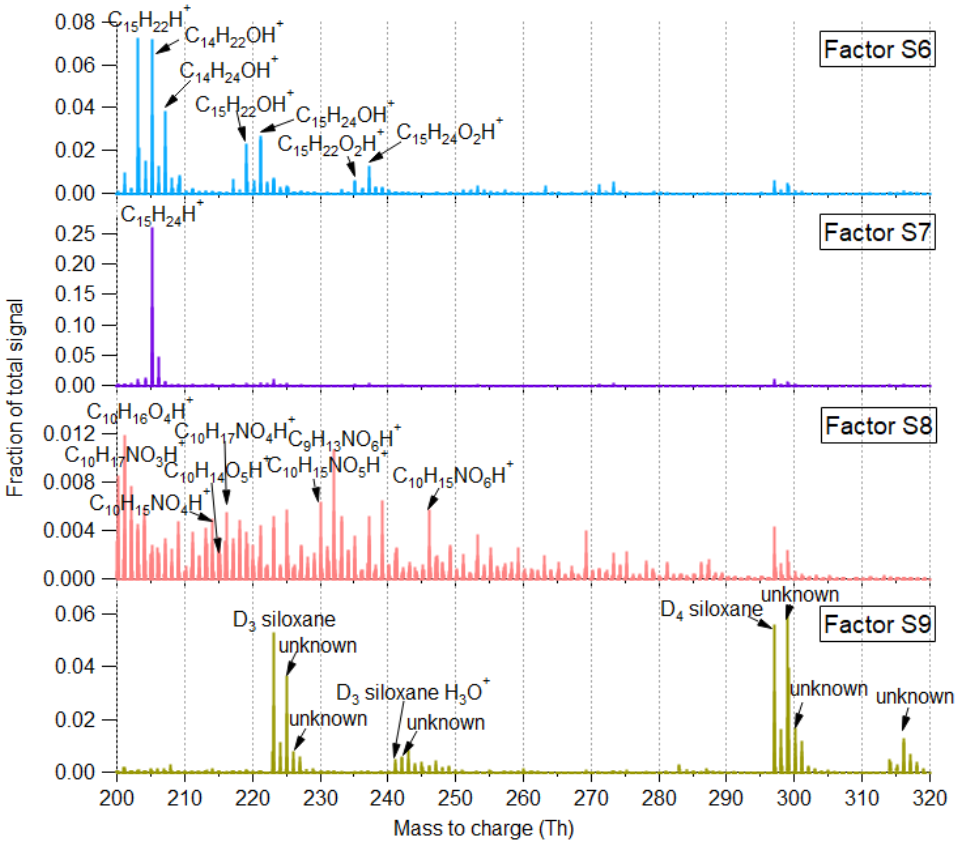

Figure 9~~11~~. Mass profiles of the four factors resolved in the high mass range at the SMEAR II station. The fingerprint peaks are labeled in the mass spectra.

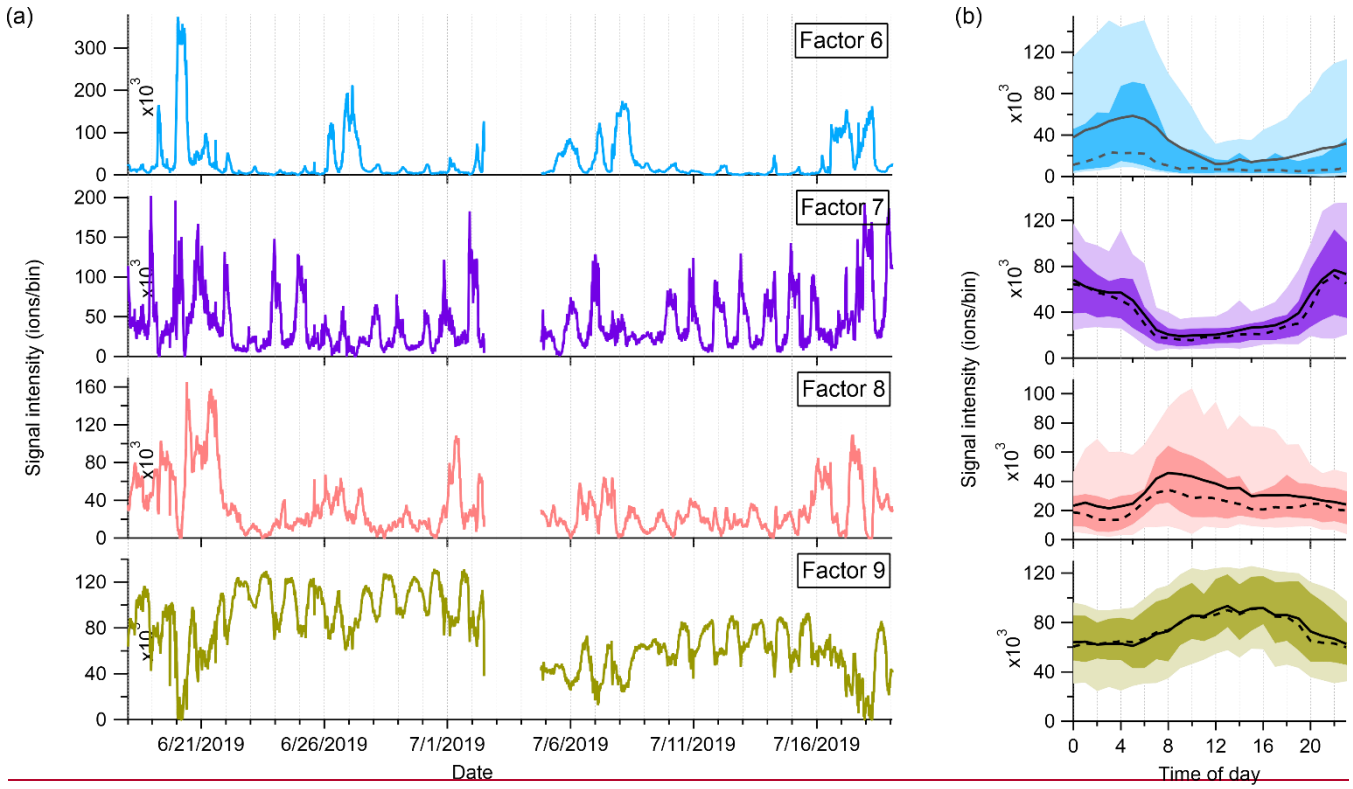
(a)
Factor 6
Factor 7
Factor 8
Factor 9
x10^3
Signal intensity (ions/bin)
6/21/2019
6/26/2019
7/1/2019
7/6/2019
7/11/2019
7/16/2019
Date
(b)
Signal intensity (ions/bin)
Time of day

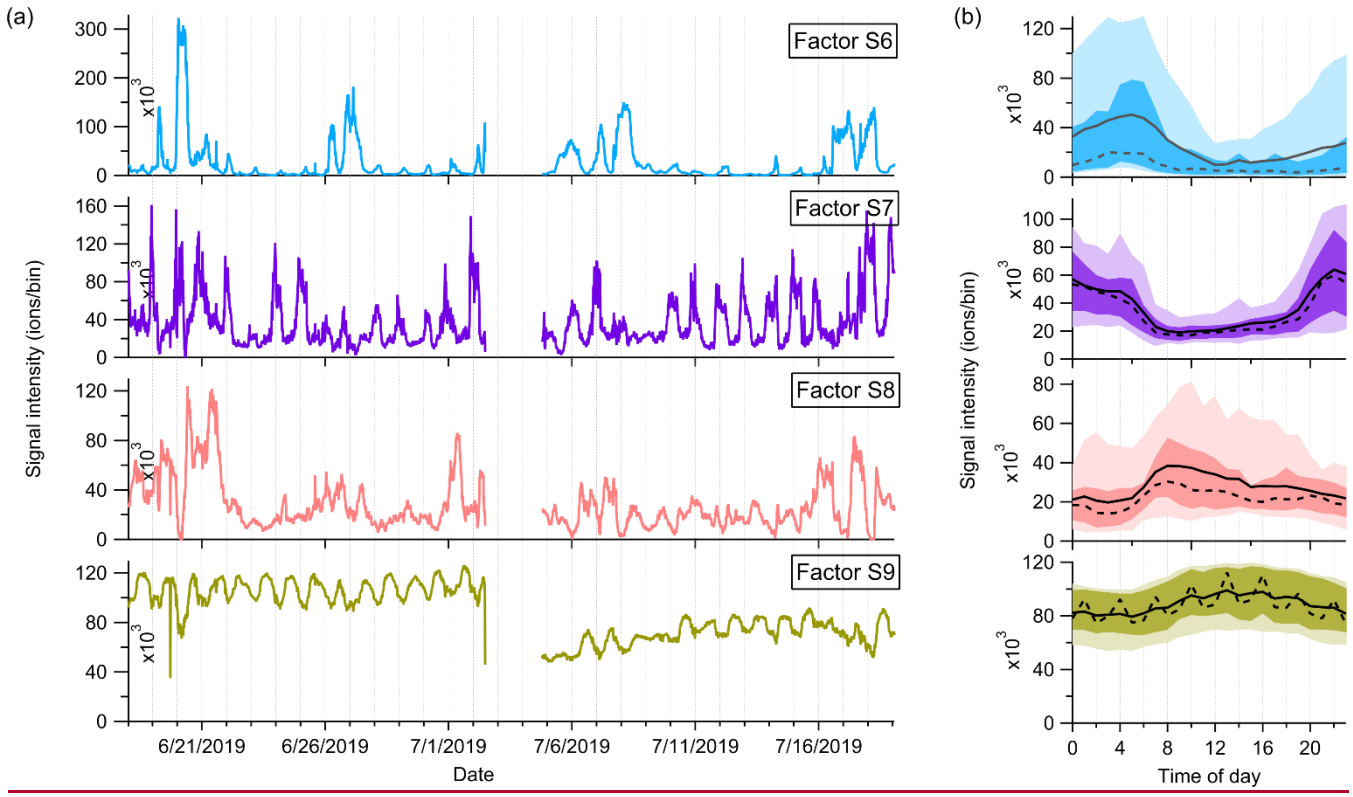

Figure 10~~2~~. (a) Time series and (b) daily trends of the four factors in the high mass range at the SMEAR II station. The solid and dashed lines in the diurnal plots show the mean and median values, respectively, and the shaded area shows 10th, 25th, 75th, and 90th percentiles.

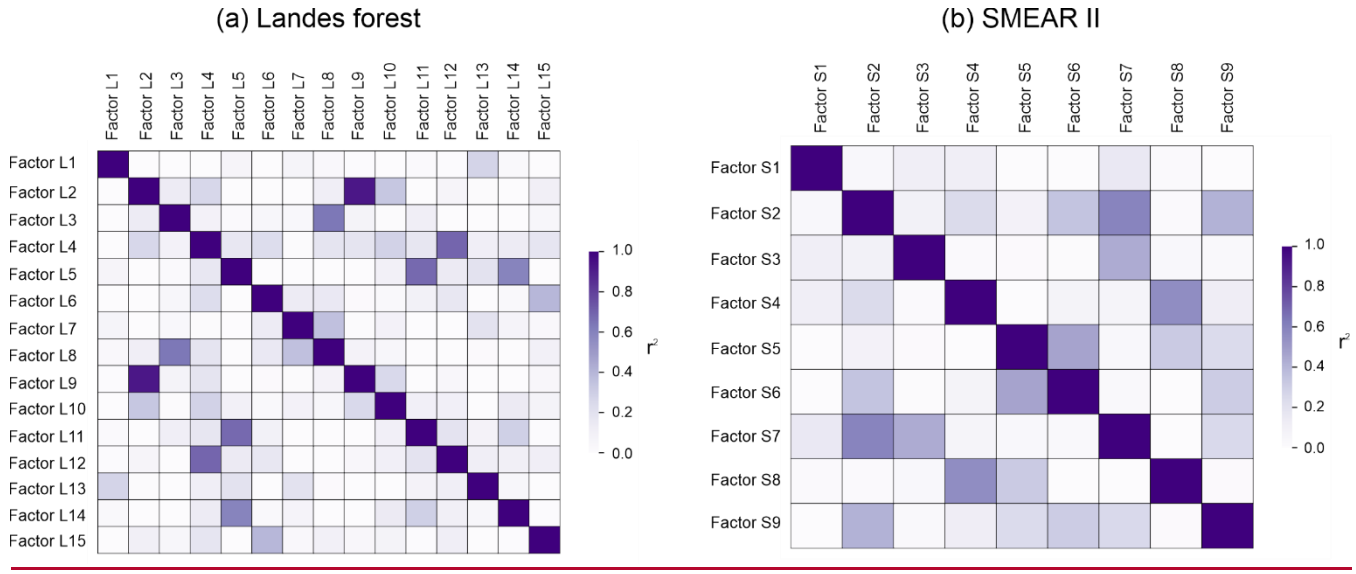

Figure 11. The correlations among various factors identified (a) in the Landes forest and (b) at the SMEAR II station, with the color representing the correlation coefficients (r^2).

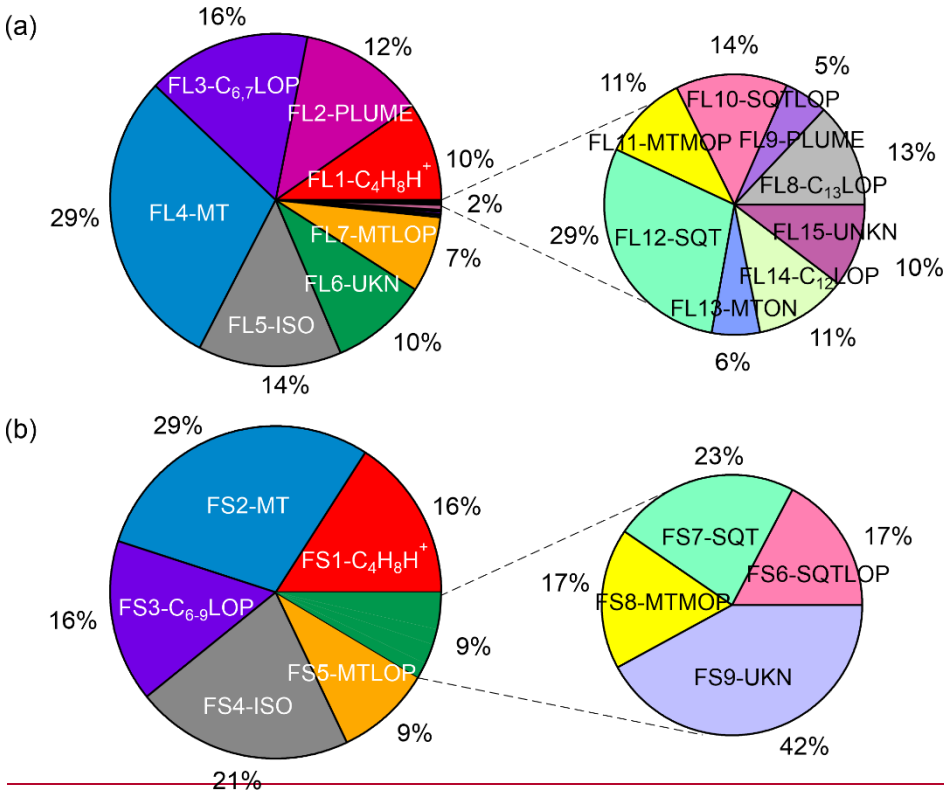
(a)
16%
12%
FL3-C6,7LOP
FL2-PLUME
FL1-C4H8H+
10%
2%
29%
FL4-MT
FL7-MTLOP
7%
FL6-UKN
FL5-ISO
10%
14%
14%
5%
11%
FL10-SQTLOP
FL11-MTMOP
FL9-PLUME
13%
FL8-C13LOP
29%
FL12-SQT
FL15-UNKN
FL14-C12LOP
10%
FL13-MTON
11%
6%
(b)
29%
FS2-MT
16%
FS1-C4H8H+
16%
FS3-C6-9LOP
9%
FS5-MTLOP
FS4-ISO
9%
21%
23%
FS7-SQT
17%
FS6-SQTLOP
17%
FS8-MTMOP
FS9-UKN
42%

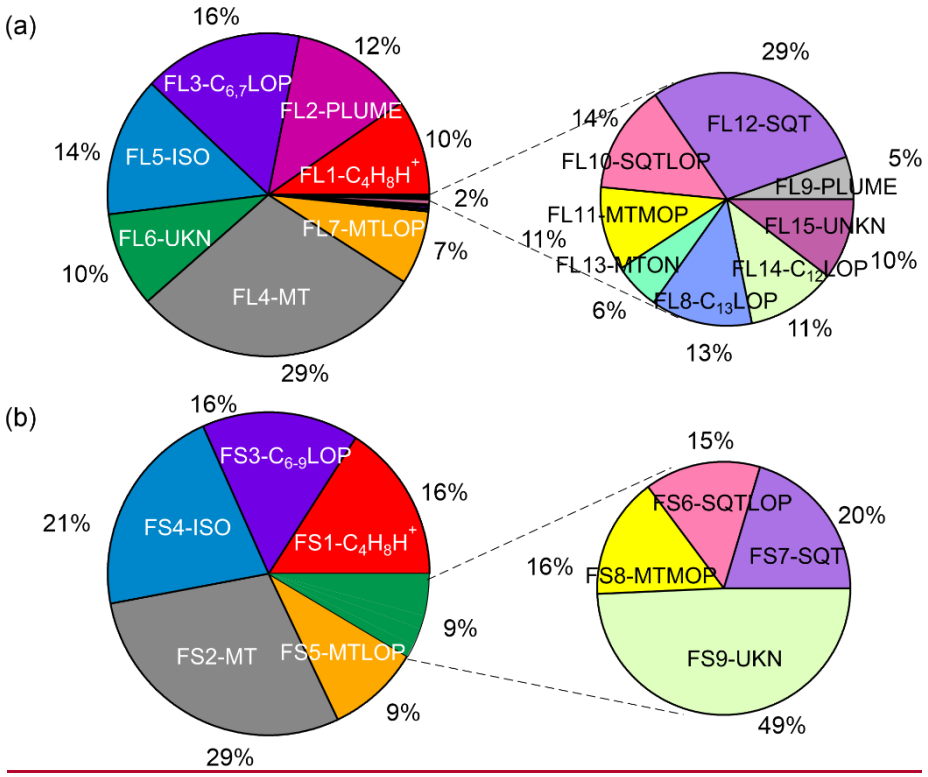

Figure 1~~2~~3. Average mass contributions of various identified factors in total measured organic vapors (a) in the Landes forest and (b) at the SMEAR II station. The common sources apportioned at both sites are presented in the same color in (a) and (b). FL: factors in the Landes forest; FS: factors at the SMEAR II station; $C_4H_8H^+$, $C_4H_8H^+$ ion-related; PLUME: a plume event; $C_{6,7}$LOP: C_6 and C_7 lightly oxidized products; $C_{6\text{-}9}$LOP: C_6-C_9 lightly oxygenated compounds; MT: monoterpenes; ISO: isoprene and its oxidation products; UKN: unknown source; MTLOP: monoterpene lightly oxidized products; C_{12}LOP: C_{12}, C_{14}, or C_{16} lightly oxidized products; C_{13}LOP: C_{13} lightly oxidized products; SQT: sesquiterpenes; MTON: monoterpene-derived organic nitrates; SQTLOP: sesquiterpene lightly oxidized products; MTMOP: monoterpene more oxidized products.

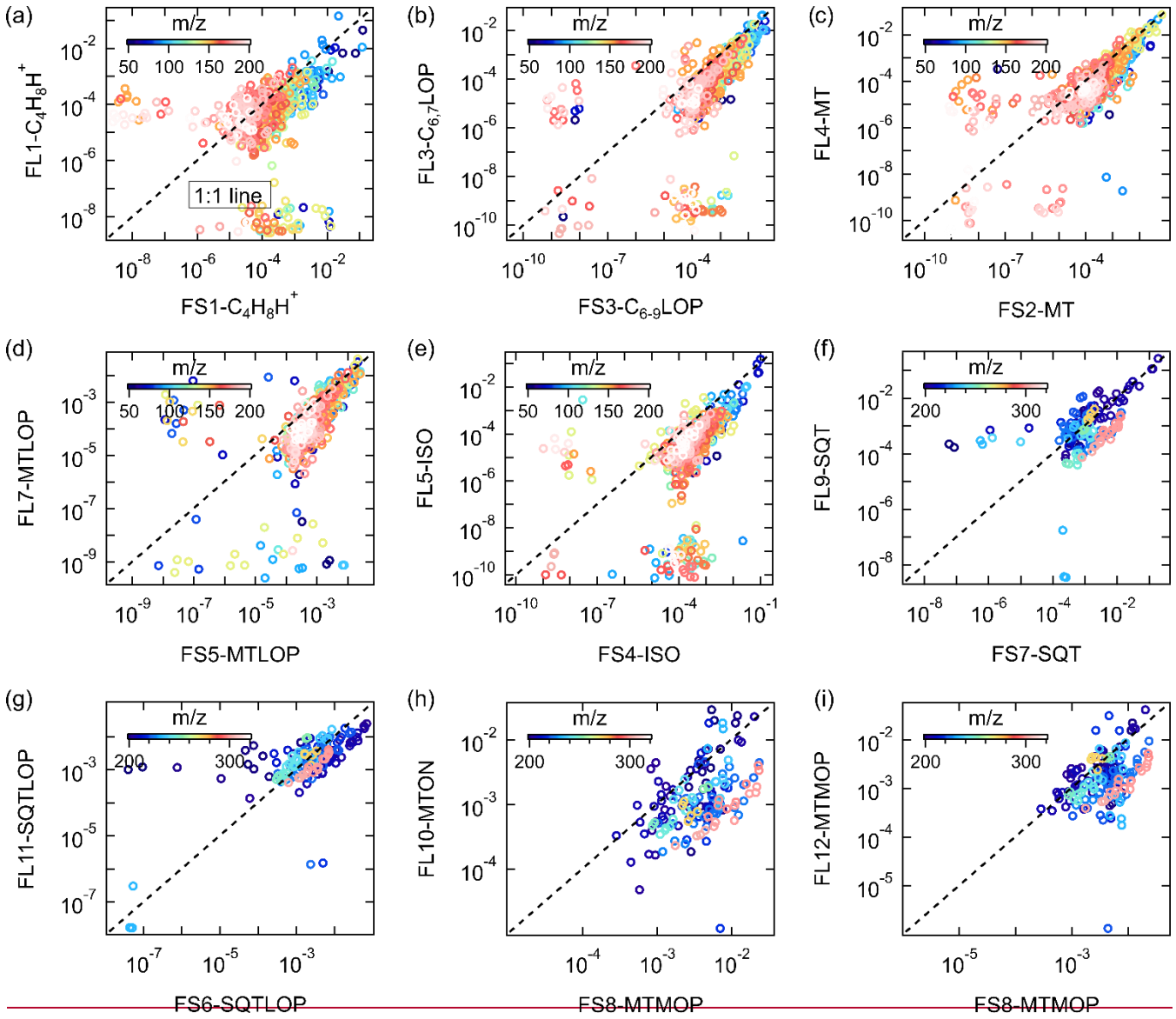
(a)
FL1-C4H8H+
FS1-C4H8H+
m/z
50 100 150 200
1:1 line
(b)
FL3-C6,7LOP
FS3-C6-9LOP
(c)
FL4-MT
FS2-MT
(d)
FL7-MTLOP
FS5-MTLOP
(e)
FL5-ISO
FS4-ISO
(f)
FL9-SQT
FS7-SQT
200 300
(g)
FL11-SQTLOP
FS6-SQTLOP
(h)
FL10-MTON
FS8-MTMOP
(i)
FL12-MTMOP
FS8-MTMOP

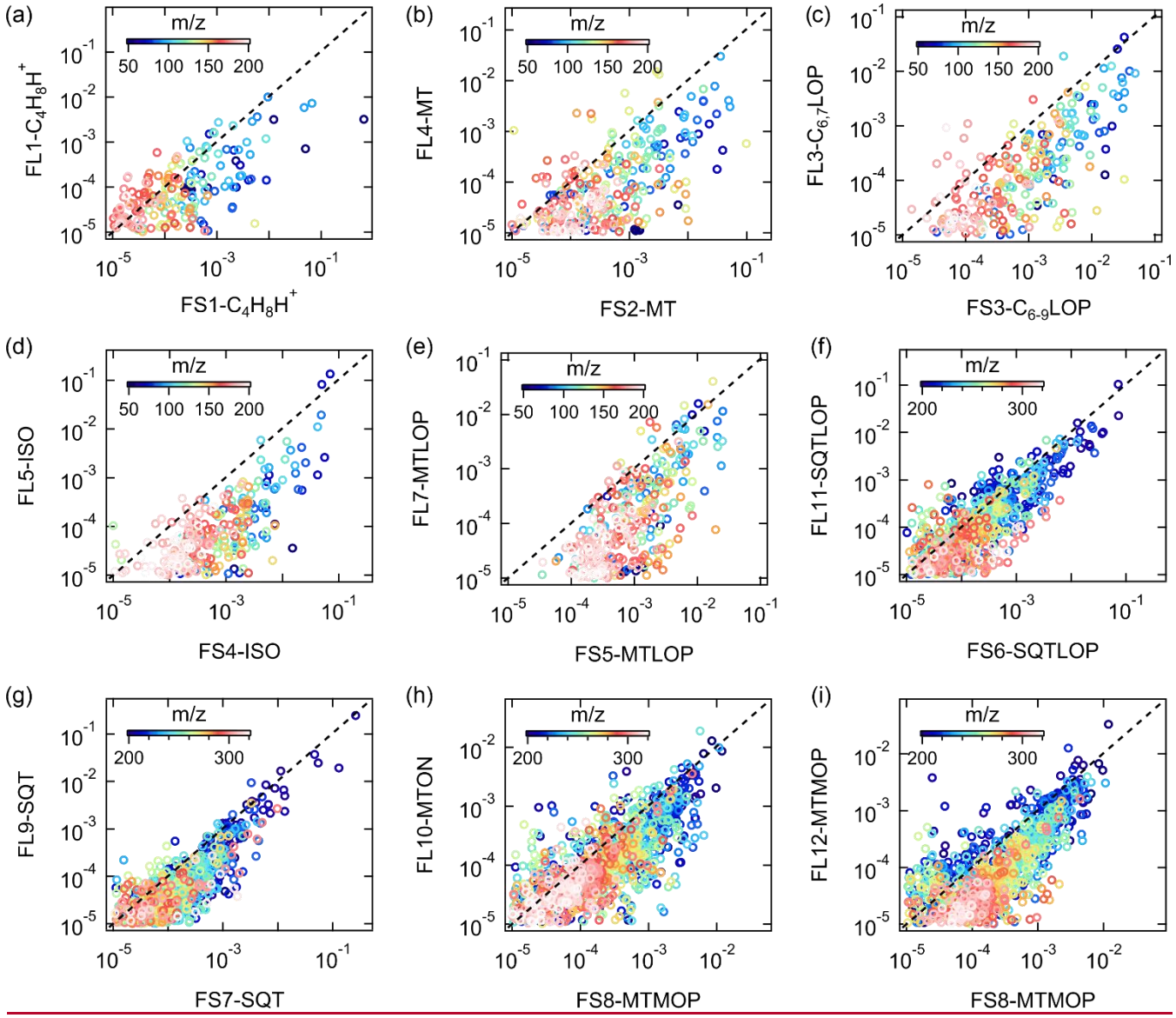

Figure 134. Comparison between factor profiles of the common sources apportioned in the Landes forest and at the SMEAR II station. The x- and y-axis show the fraction of each bin in the mass spectra of the factors. FL: factors in the Landes forest; FS: factors at the SMEAR II station; $C_4H_8H^+$, $C_4H_8H^+$ ion-related; $C_{6,7}$LOP: MT: monoterpenes; C_6 and C_7 lightly oxidized products; $C_{6\text{-}9}$LOP: C_6-C_9 lightly oxygenated compounds; ISO: isoprene and its oxidation products; MTLOP: monoterpene lightly oxidized products; C_{13}LOP: SQTLOP: sesquiterpene lightly oxidized products; SQT: sesquiterpenes; MTON: monoterpene-derived organic nitrates; MTMOP: monoterpene more oxidized products.

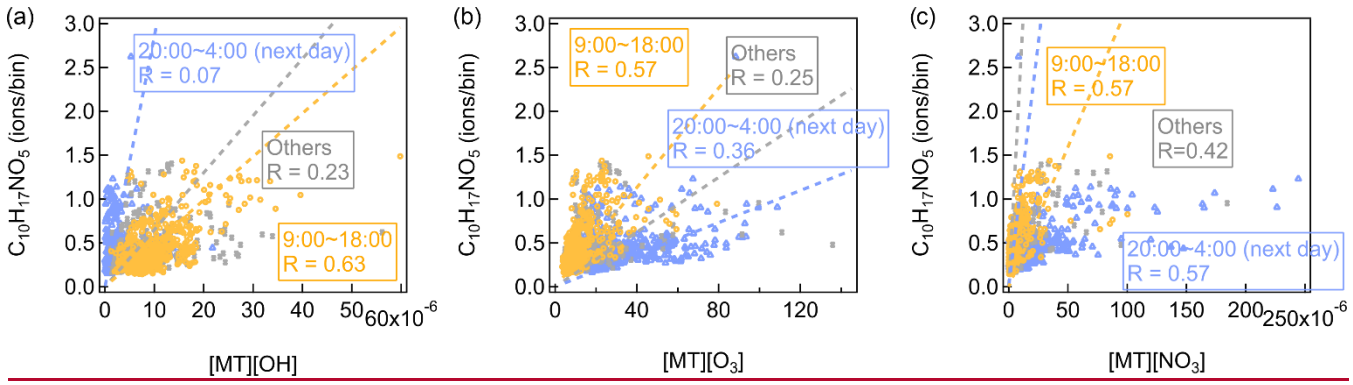

Figure 14. Scatter plots of $C_{10}H_{17}NO_5$ versus the product of (a) [OH] × [monoterpenes], (b) [O_3] × [monoterpenes], and (c) [NO_3] × [monoterpenes]. Different colours represent different periods of the day.

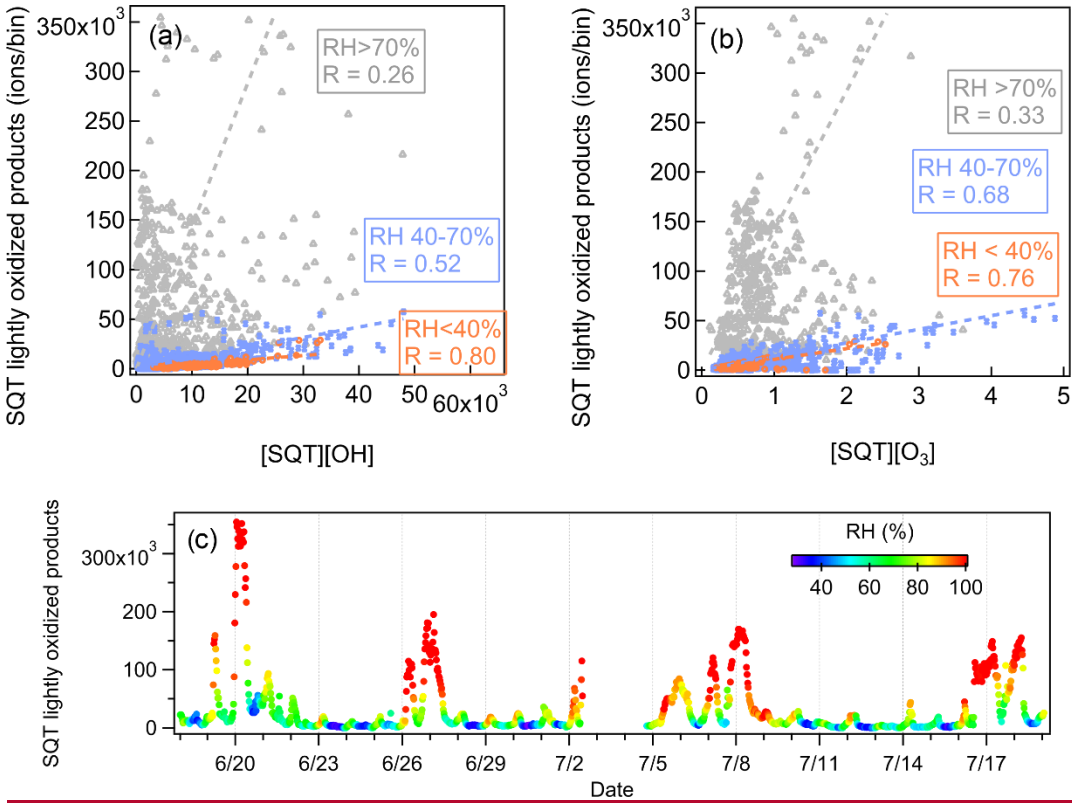

Figure 15. Scatter plots of sesquiterpene lightly oxidized products versus the product of (a) [OH] × [sesquiterpenes], and (b) [O_3] × [sesquiterpenes]. Different colours indicate different ranges of RH. (c) Time series of sesquiterpene lightly oxidized products colored by RH.

Supplementary Information

~~Source identification of a~~Atmospheric organic vapors in two European pine forests measured by a~~: Results from~~ Vocus PTR-TOF ~~observations~~: insights into monoterpene and sesquiterpene oxidation processes

Haiyan Li[1], Manjula R. Canagaratna[2], Matthieu Riva[3], Pekka Rantala[1], Yanjun Zhang[1], Steven Thomas[1], Liine Heikkinen[1], Pierre-Marie Flaud[4,5], Eric Villenave[4,5], Emilie Perraudin[4,5], Douglas Worsnop[2], Markku Kulmala[1], Mikael Ehn[1], Federico Bianchi[1]

[1] Institute for Atmospheric and Earth System Research/Physics, Faculty of Science, University of Helsinki, Helsinki, 00014, Finland
[2] Aerodyne Research Inc., Billerica, Massachusetts 01821, USA
[3] Univ. Lyon, Université Claude Bernard Lyon 1, CNRS, IRCELYON, 69626, Villeurbanne, France
[4] University of Bordeaux, EPOC, UMR 5805 CNRS, 33405 Talence Cedex, France
[5] CNRS, EPOC, UMR 5805 CNRS, 33405 Talence Cedex, France

Correspondence: Haiyan Li (haiyan.li@helsinki.fi)

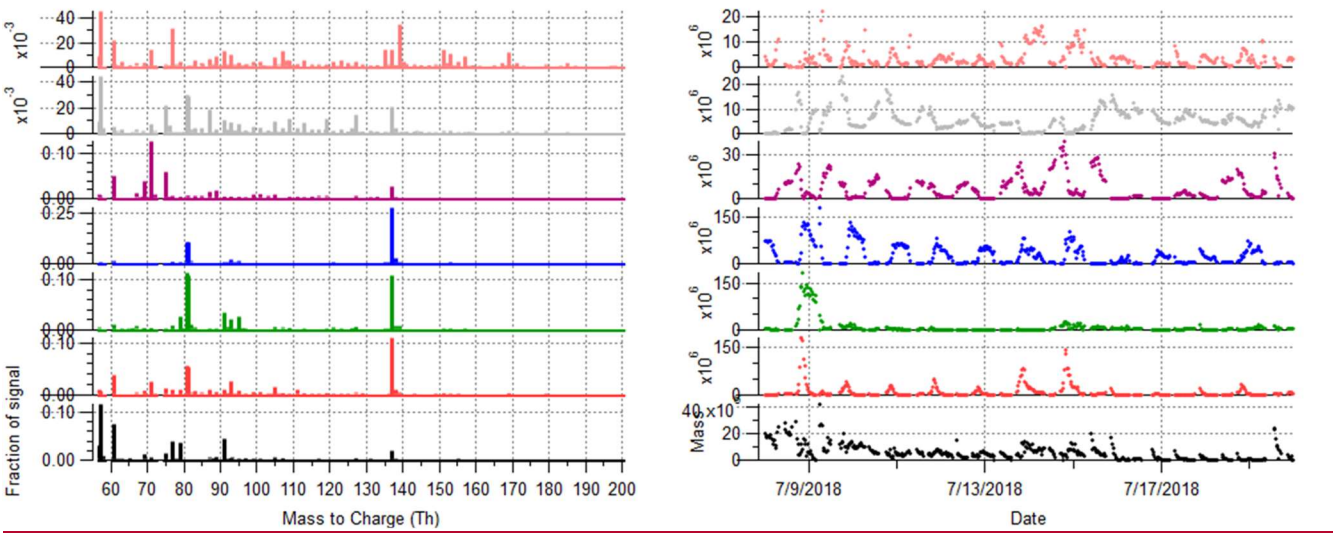

Figure S1. The mass profiles and time series of the seven-factor solution for the low mass range in the Landes forest with the inclusion of the signals at *m/z* 81 Th and *m/z* 137 Th.

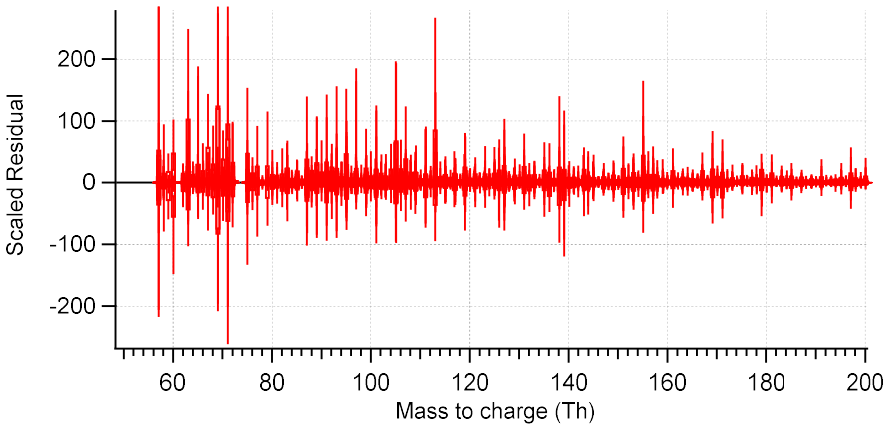

Figure S2~~1~~. The distribution of scaled residuals as a function of *m/z* of the seven-factor solution for the low mass range in the Landes forest.

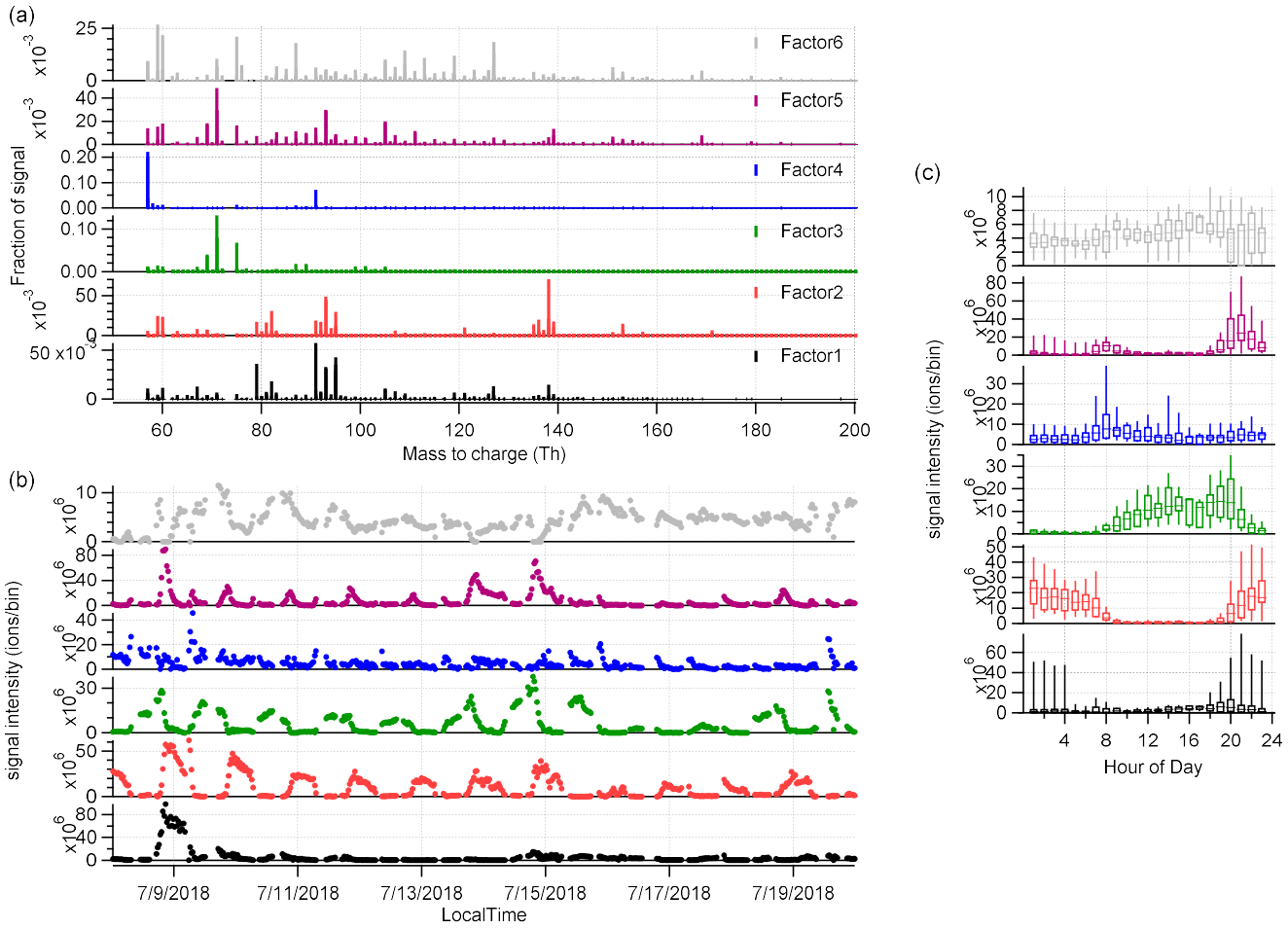

Figure S3~~2~~. The six-factor solution for the low mass range in the Landes forest, showing (a) factor mass profiles, (b) factor time series, and (c) diurnal cycles of different factors.

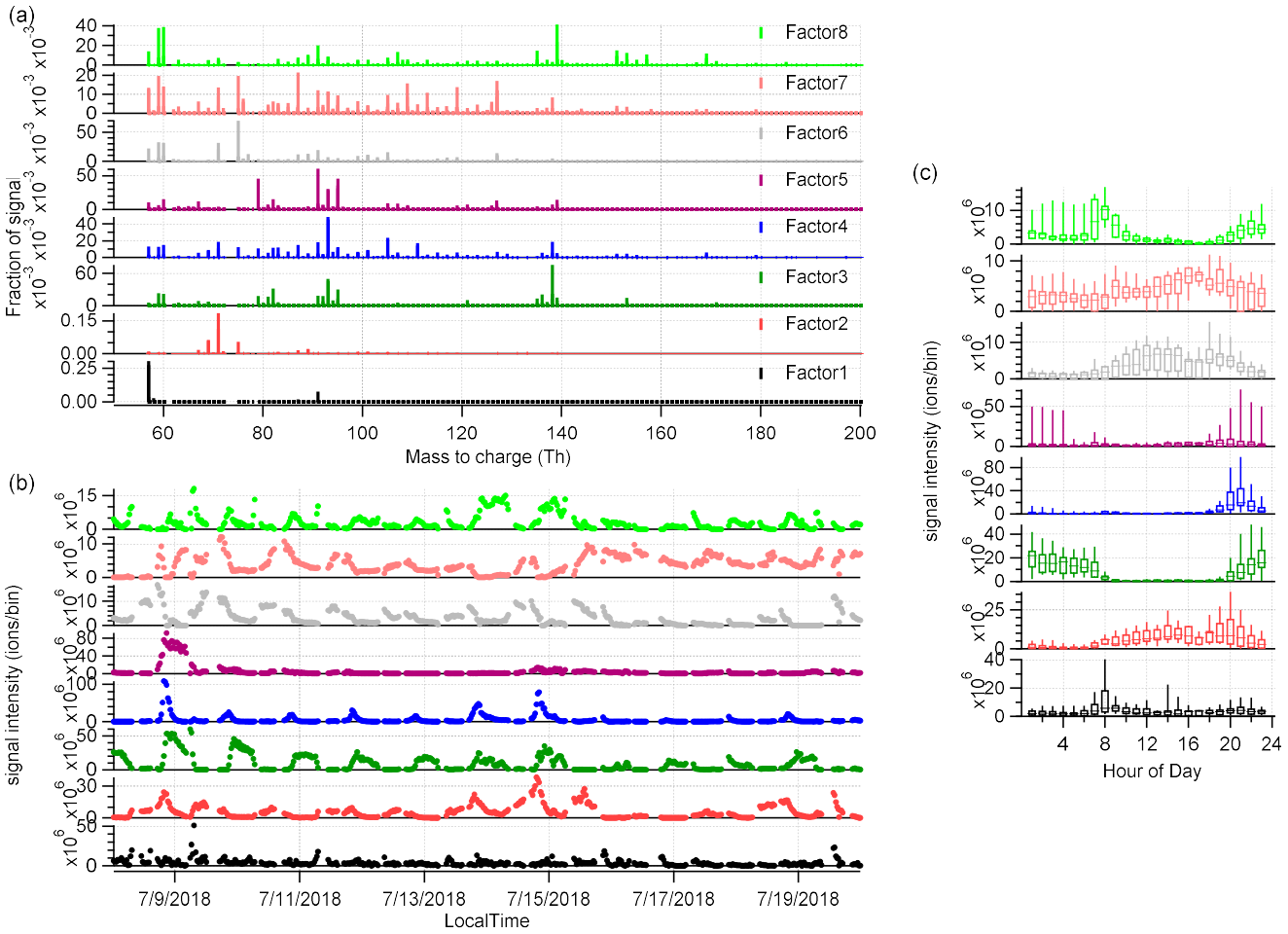

Figure S43. The eight-factor solution for the low mass range in the Landes forest, showing (a) factor mass profiles, (b) factor time series, and (c) diurnal cycles of different factors.

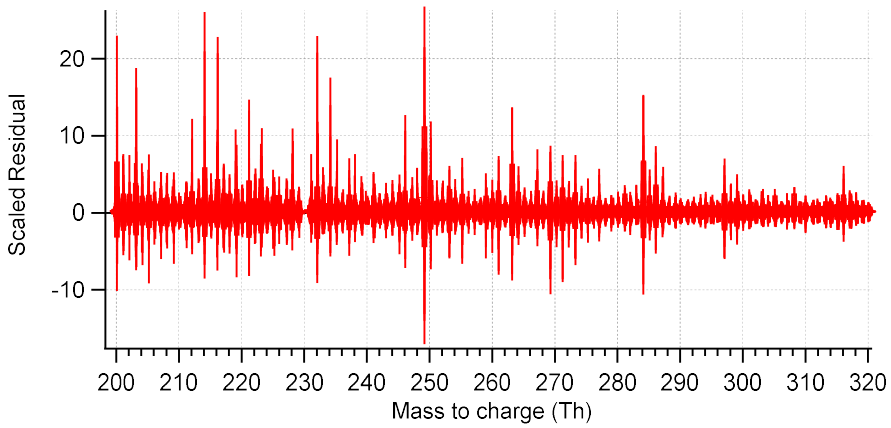

Figure S54. The distribution of scaled residuals as a function of *m/z* of the eight-factor solution for the high mass range in the Landes forest.

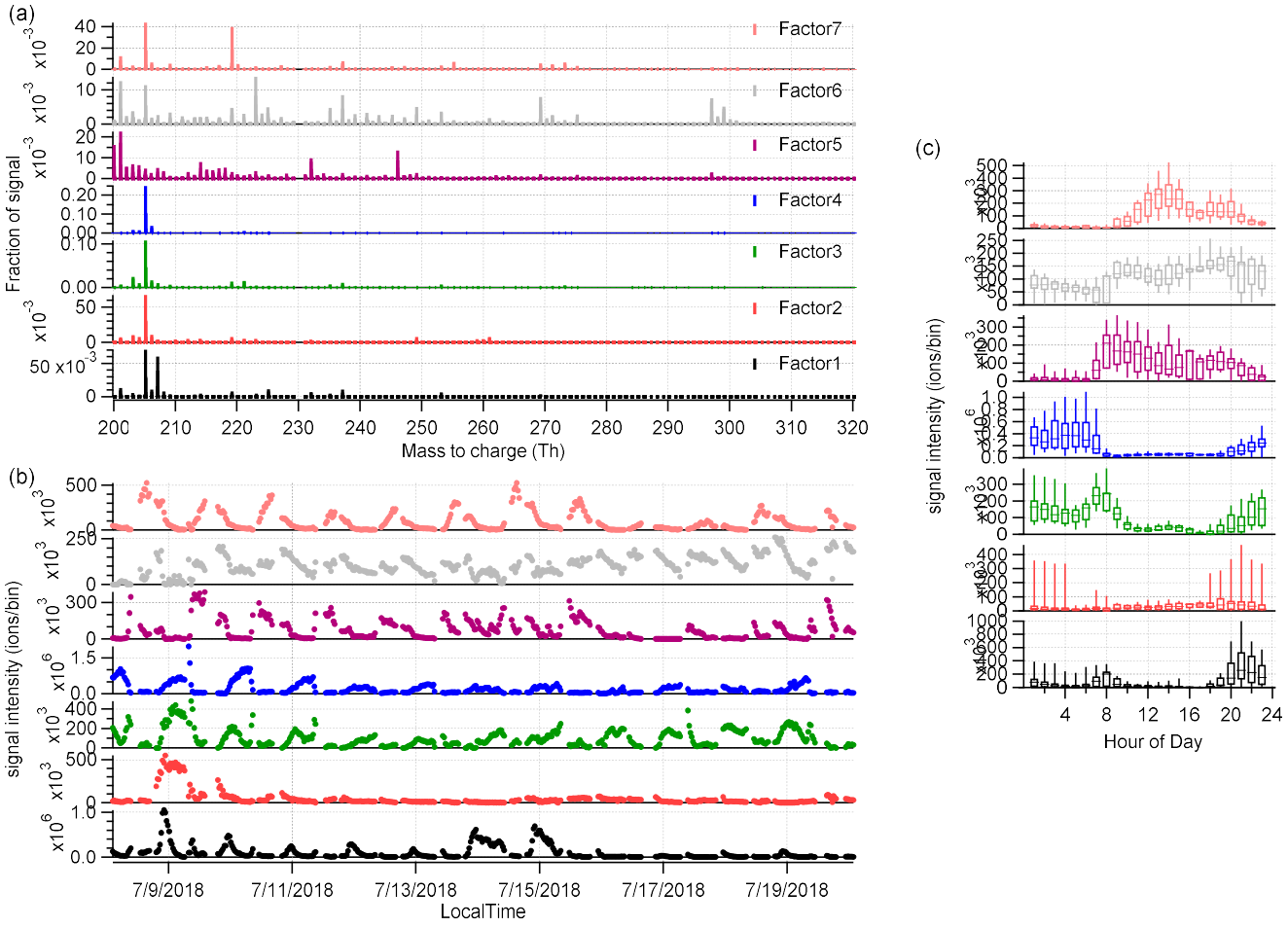

Figure S6~~5~~. The seven-factor solution for the high mass range in the Landes forest, showing (a) factor mass profiles, (b) factor time series, and (c) diurnal trends of different factors.

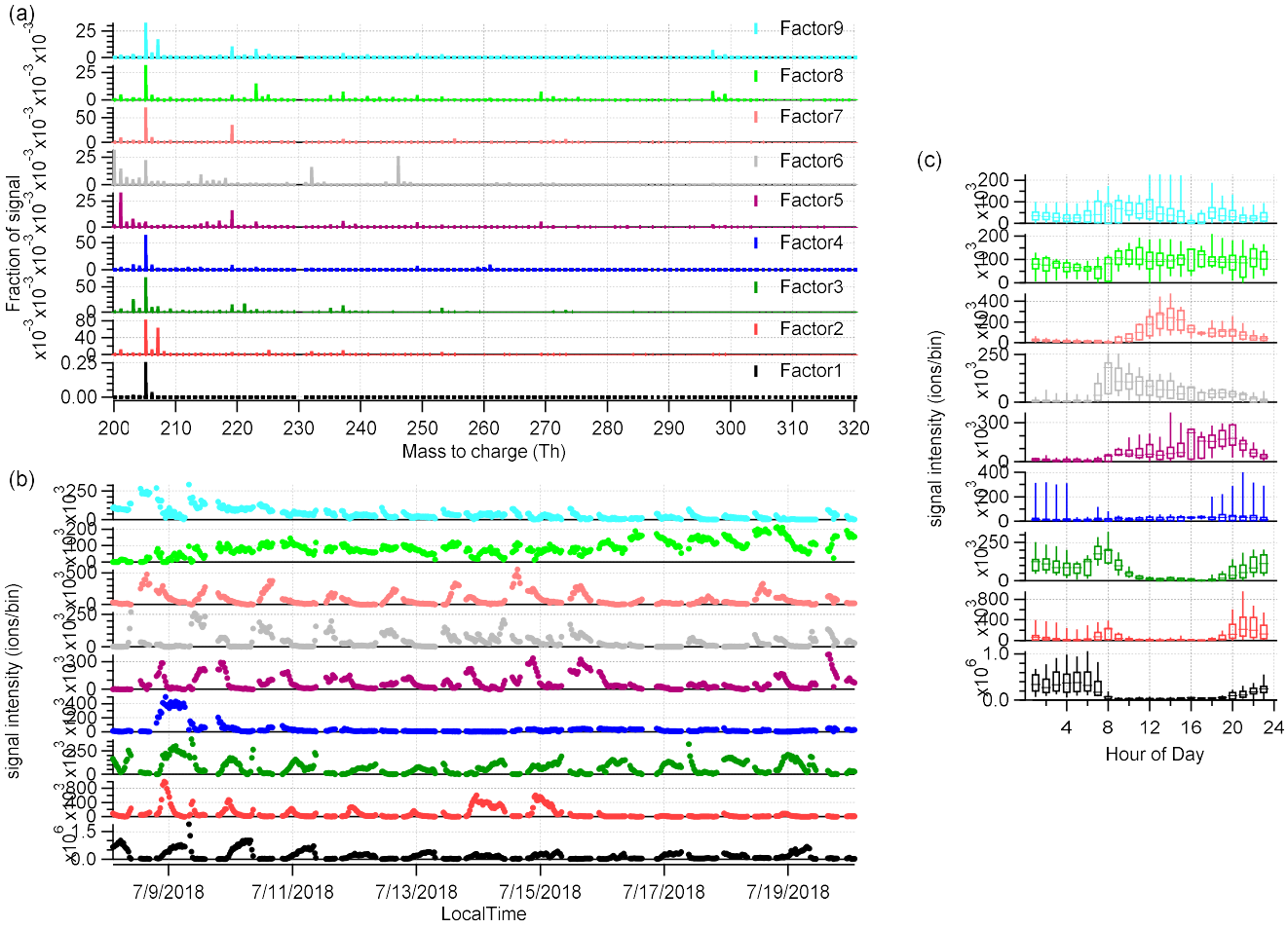

Figure S76. The nine-factor solution for the high mass range in the Landes forest, showing (a) factor mass profiles, (b) factor time series, and (c) diurnal trends of different factors.

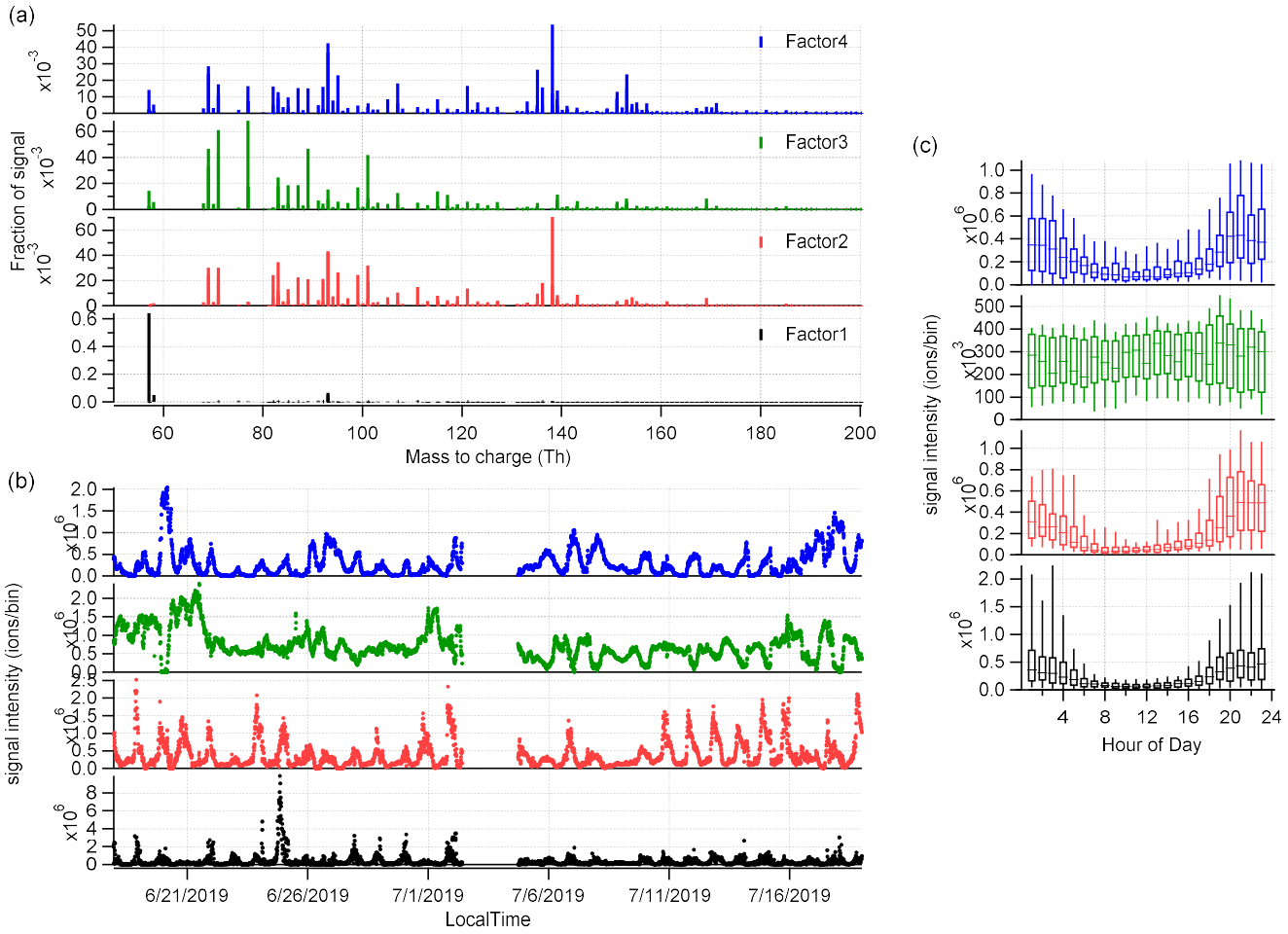

Figure S87. The four-factor solution for the low mass range at SMEAR II station, showing (a) factor mass profiles, (b) factor time series, and (c) diurnal trends of different factors.

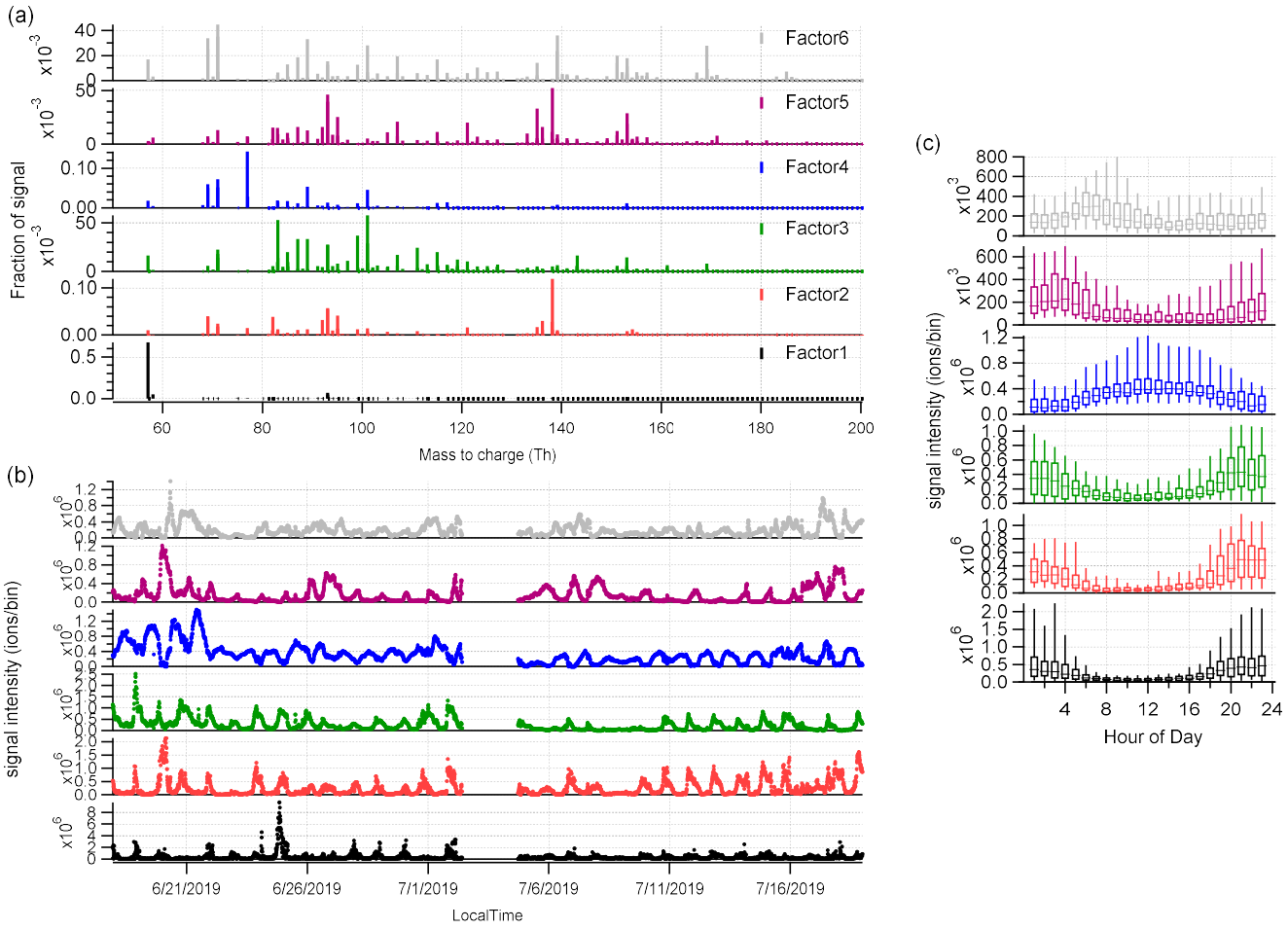

Figure S98. The six-factor solution for the low mass range at SMEAR II station, showing (a) factor mass profiles, (b) factor time series, and (c) diurnal trends of different factors.

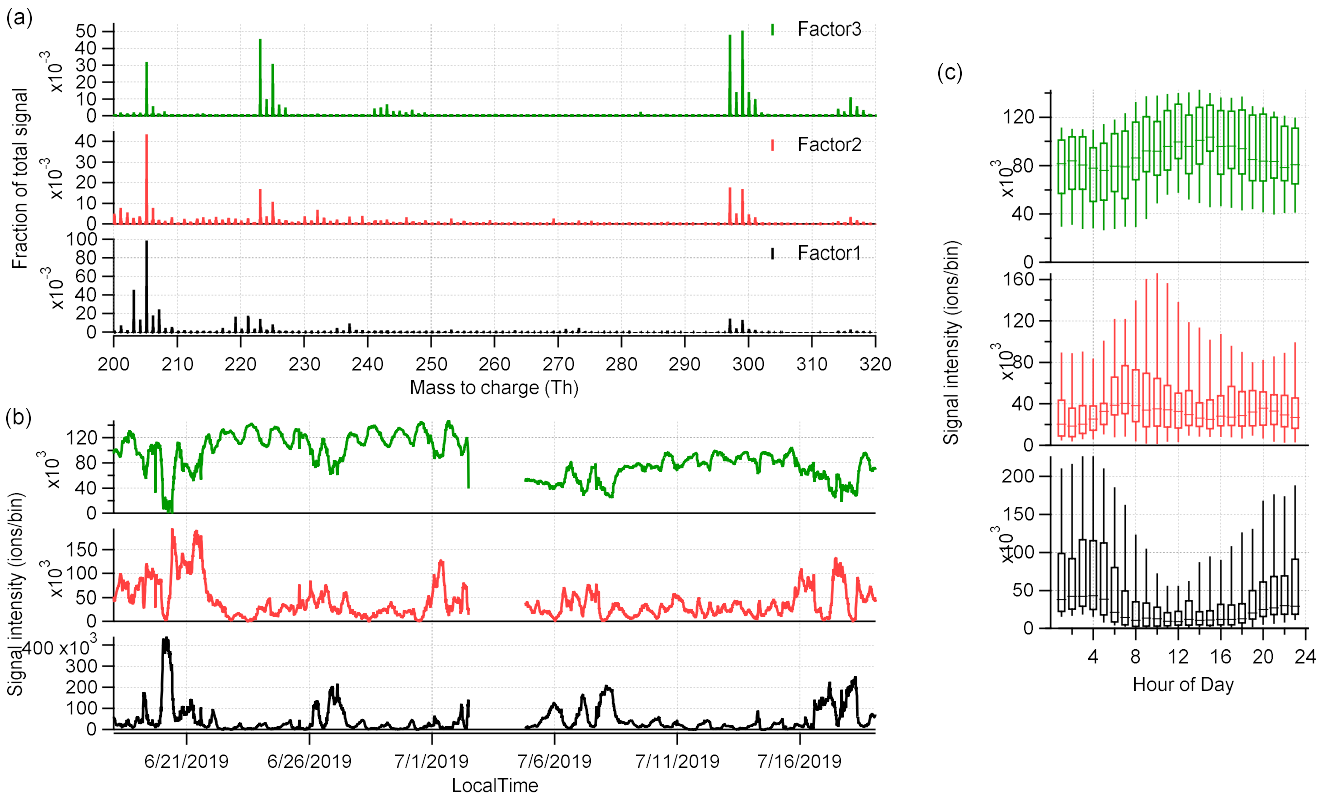

Figure S109. The three-factor solution for the high mass range at SMEAR II station, showing (a) factor mass profiles, (b) factor time series, and (c) diurnal cycles of different factors.

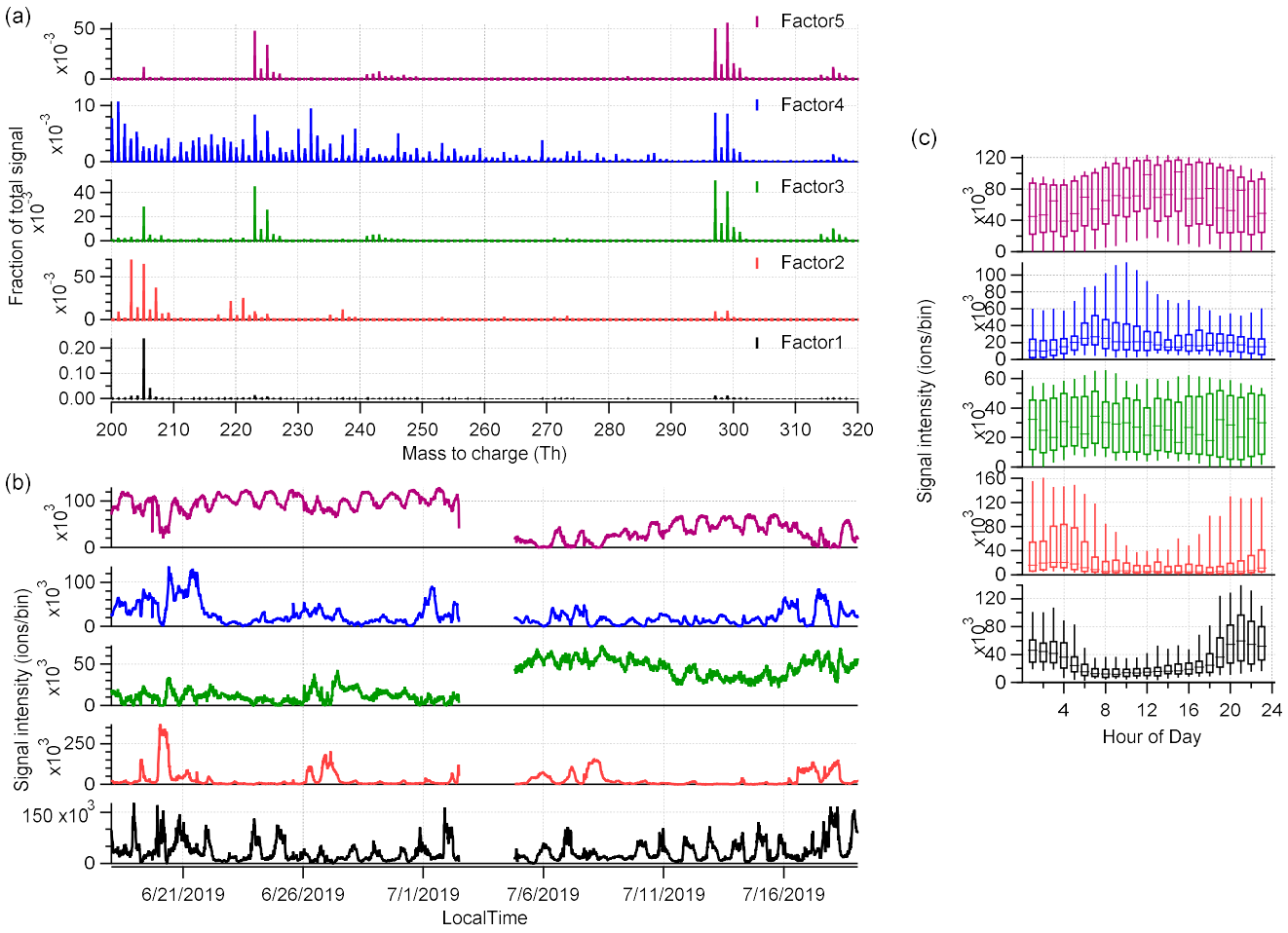

Figure S1~~0~~1. The five-factor solution for the high mass range at SMEAR II station, showing (a) factor mass profiles, (b) factor time series, and (c) diurnal cycles of different factors.

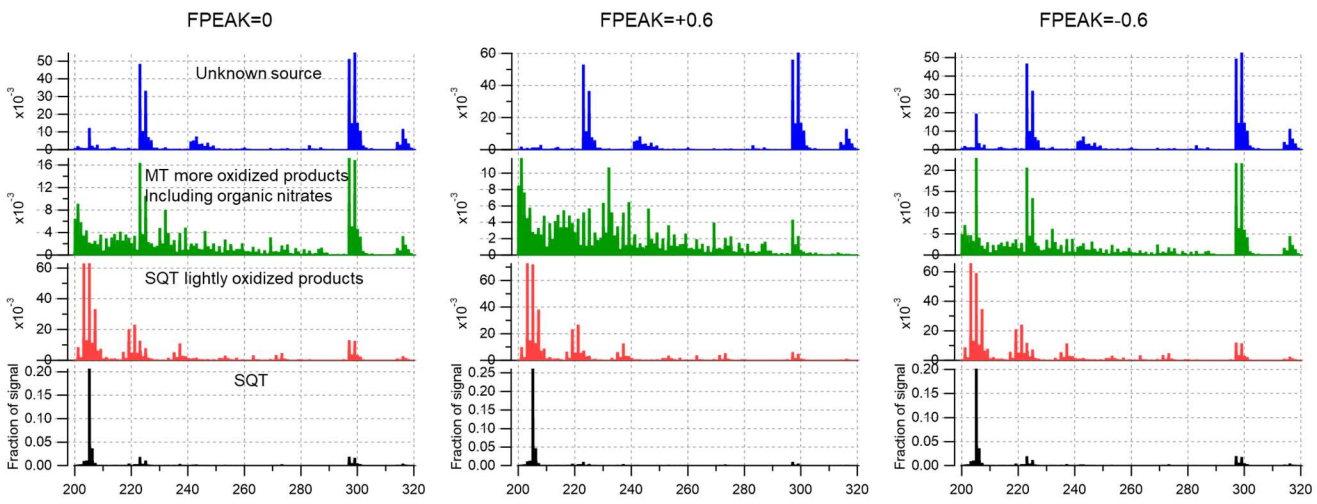

Figure S12. The factor profiles of the four-factor solution for the high mass range of the SMEAR Ⅱ measurements with FPEAK = 0, +0.6, and -0.6.

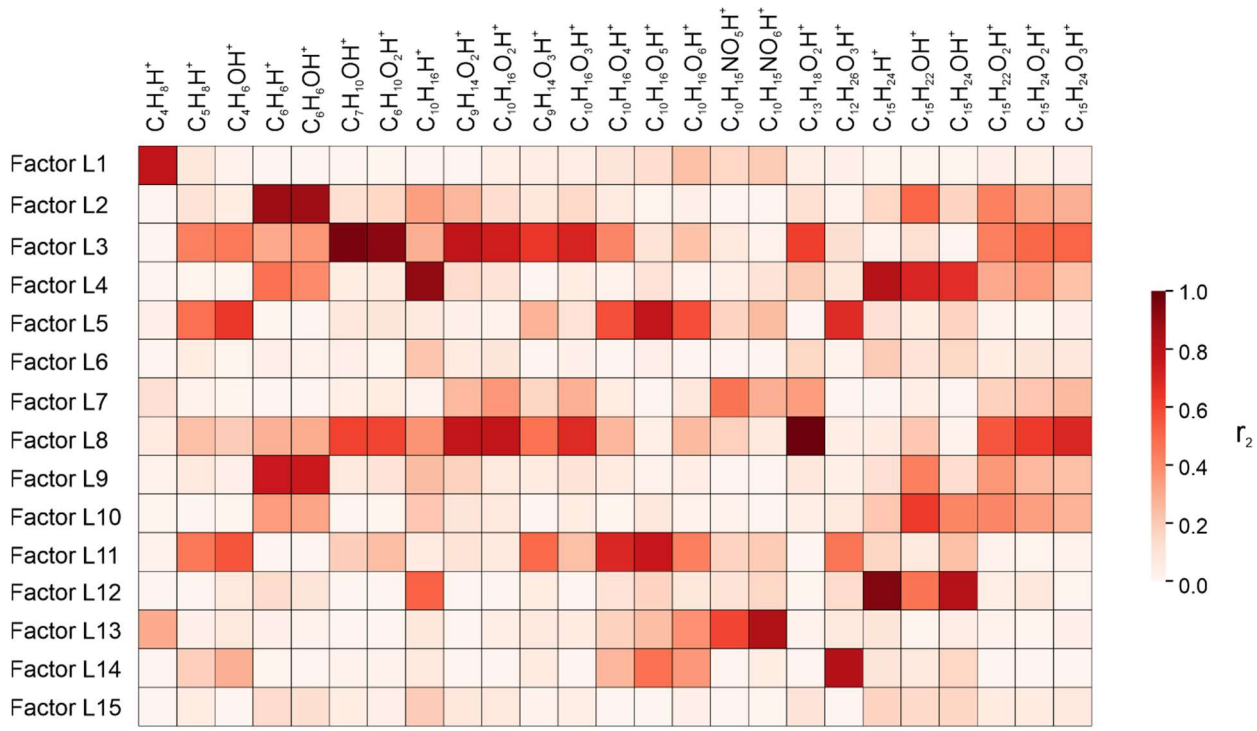

Figure S13. Correlations between PMF factors and marker molecules in the Landes forest, with the color representing the correlation coefficients (r^2).

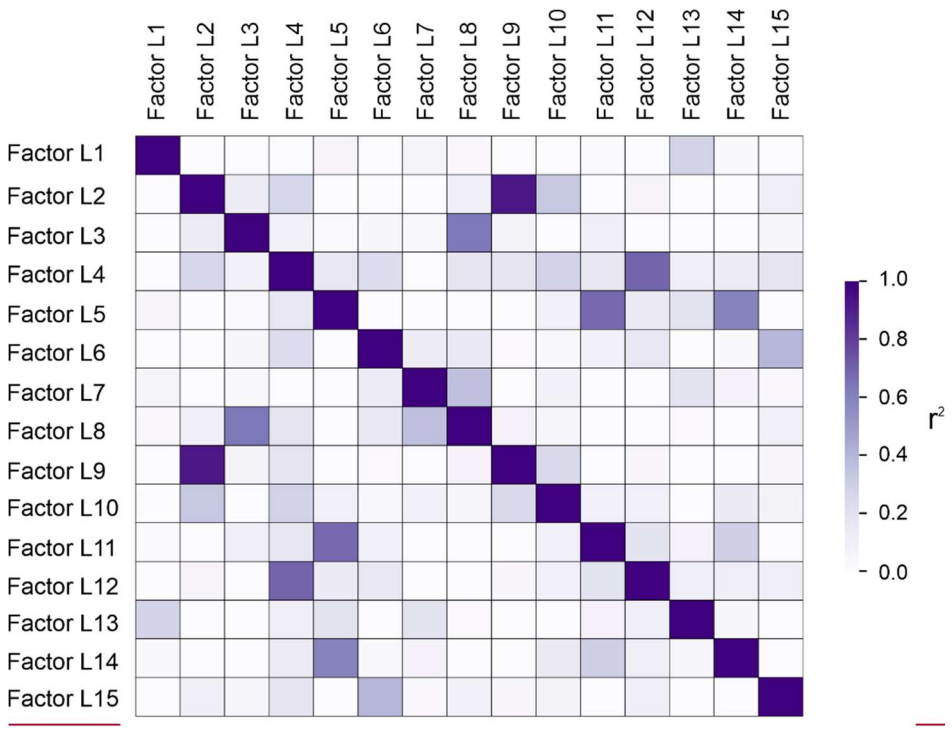

~~Figure S11. The correlations among various factors identified in the Landes forest, with the color representing the correlation coefficients (r^2).~~

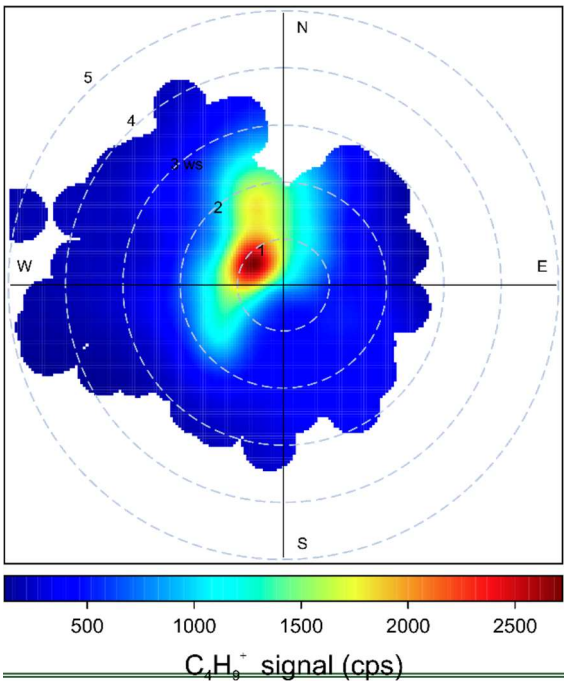

~~Figure S12. Bivariate polar plot of $C_4H_9^+$ signal measured at SMEAR II station as a function of wind speed and wind direction using the OpenAir software (Carslaw and Ropkins, 2012).~~

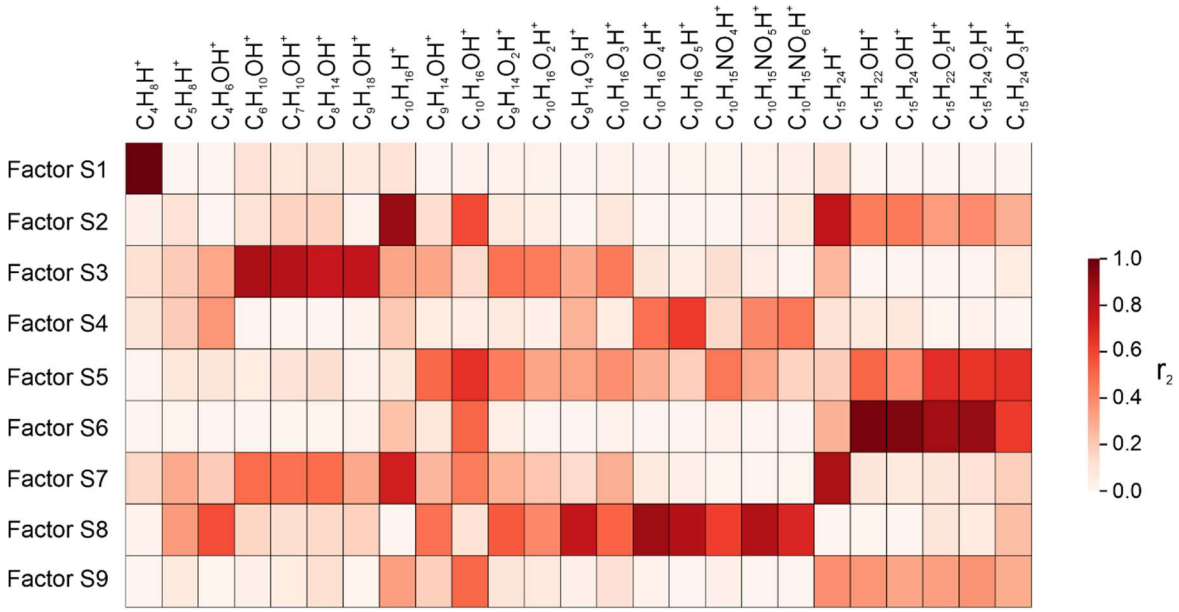

Figure S14. Correlations between PMF factors and marker molecules at the SMEAR II station, with the color indicating the correlation coefficients (r^2).

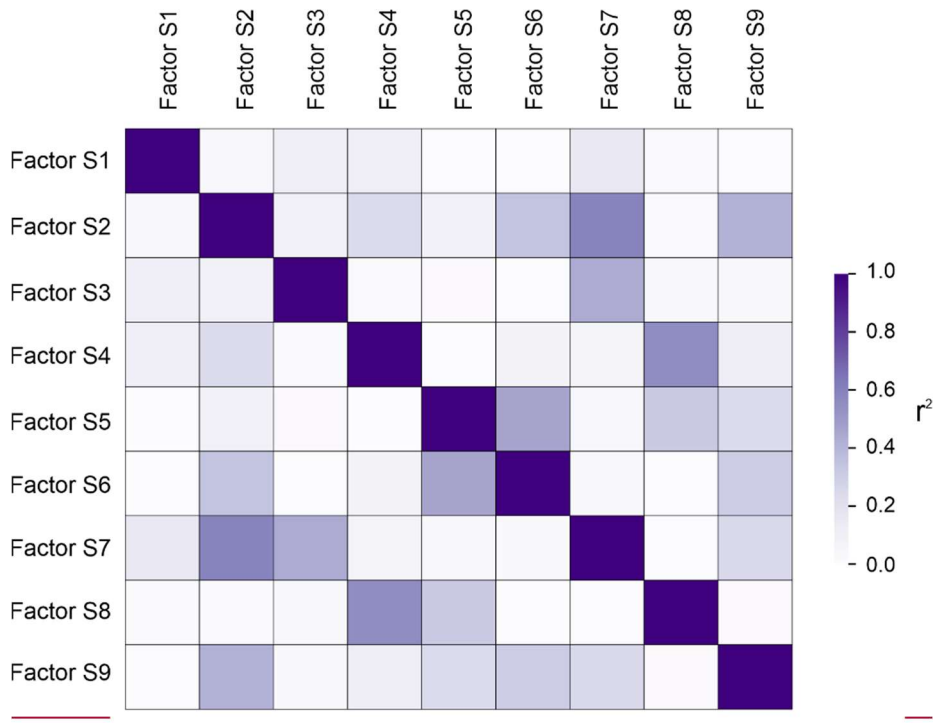

~~Figure S13. The correlations among various factors identified at SMEAR II station, with the color representing the correlation coefficients (r^2).~~

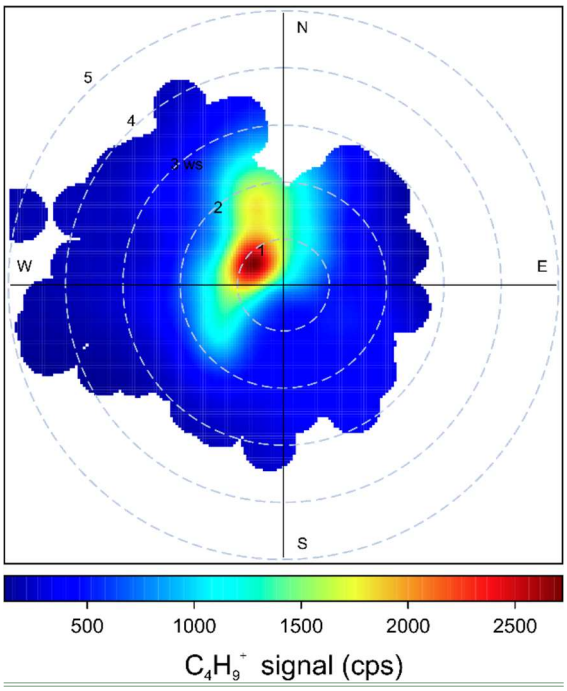

Figure S152. Bivariate polar plot of $C_4H_9^+$ signal measured at SMEAR II station as a function of wind speed and wind direction using the OpenAir software (Carslaw and Ropkins, 2012).

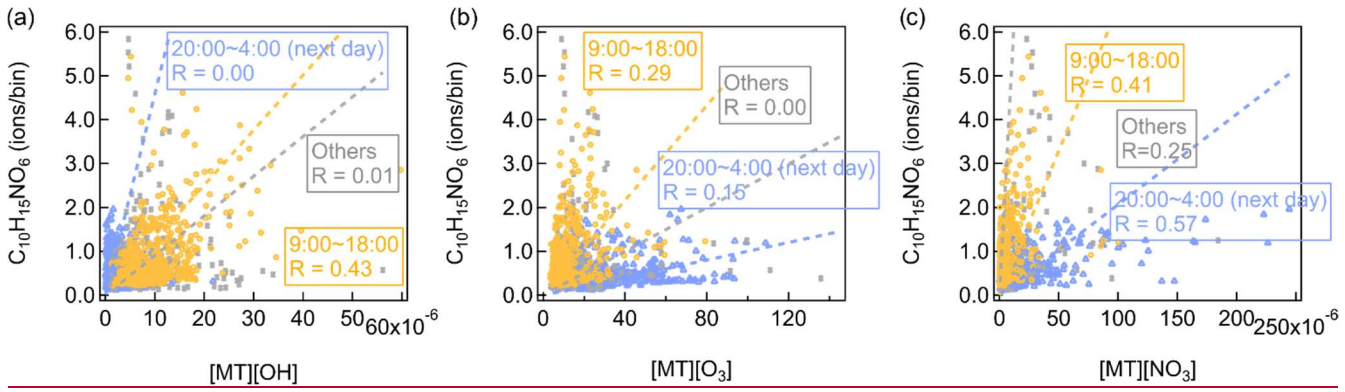

Figure S16. Scatter plots of $C_{10}H_{15}NO_6$ versus the product of (a) [OH] × [monoterpenes], (b) [O_3] × [monoterpenes], and (c) [NO_3] × [monoterpenes]. Different colours represent different periods of the day.

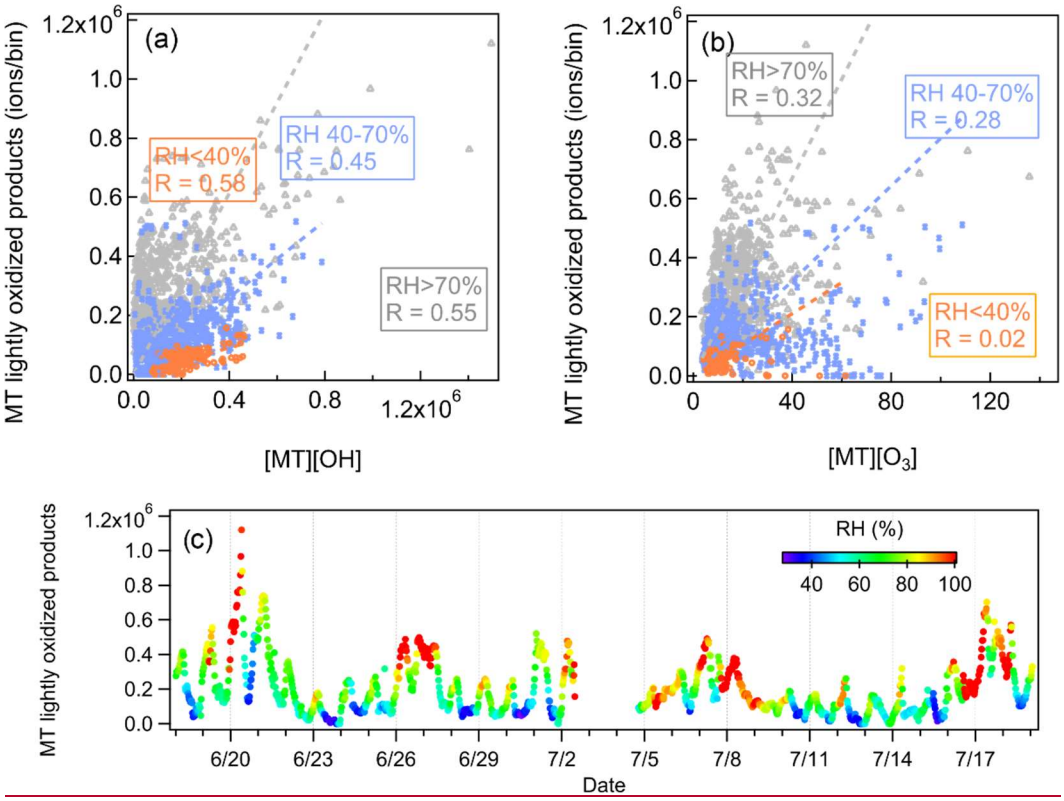

Figure S17. Scatter plots of monoterpene lightly oxidized products versus the product of (a) [OH] × [monoterpenes], and (b) [O_3] × [monoterpenes]. Different colours indicate different ranges of RH. (c) Time series of monoterpene lightly oxidized products colored by RH.

References

Carslaw, D. C. and Ropkins, K.: openair – An R package for air quality data analysis, Environ. Modell. Softw., 27–28, 52–61, 2012.